การสังเคราะห์และสมบัติของไทโอเลเทดไคโทซานยึดติดเยื่อเมือกสำหรับระบบ
นำส่งยาซิมวาสแตติน

นางสาวมัลลิกา คงสง

วิทยานิพนธ์นี้เป็นส่วนหนึ่งของการศึกษาตามหลักสูตรปริญญาวิทยาศาสตรมหาบัณฑิต
สาขาวิชาปิโตรเคมีและวิทยาศาสตร์พอลิเมอร์
คณะวิทยาศาสตร์ จุฬาลงกรณ์มหาวิทยาลัย
ปีการศึกษา 2555
ลิขสิทธิ์ของจุฬาลงกรณ์มหาวิทยาลัย

SYNTHESIS AND PROPERTIES OF MUCOADHESIVE THIOLATED CHITOSAN
FOR SIMVASTATIN DELIVERY SYSTEM

Miss Mullika Kongsong

A Thesis Submitted in Partial Fulfillment of the Requirements
for the Degree of Master of Science Program in Petrochemistry and Polymer Science
Faculty of Science
Chulalongkorn University
Academic Year 2012
Copyright of Chulalongkorn University

Thesis Title	SYNTHESIS AND PROPERTIES OF MUCOADHESIVE THIOLATED CHITOSAN FOR SIMVASTATIN DELIVERY SYSTEM
By	Miss Mullika Kongsong
Field of Study	Petrochemistry and Polymer Science
Thesis Advisor	Associate Professor Polkit Sangvanich, Ph.D.

Accepted by the Faculty of Science, Chulalongkorn University in Partial Fulfillment of the Requirements for the Master's Degree

………………………………….Dean of the Faculty of Science

(Professor Supot Hannongbua, Dr.rer.nat.)

THESIS COMMITTEE

……………………………….Chairman

(Assistant Professor Warinthorn Chavasiri, Ph.D.)

……………………………….Thesis Advisor

(Associate Professor Polkit Sangvanich, Ph.D.)

……………………………….Examiner

(Associate Professor Voravee Hoven, Ph.D.)

……………………………….External Examiner

(Assistant Professor Nalena Praphairaksit, D.V.M., Ph.D.)

มัลลิกา คงสง : การสังเคราะห์และสมบัติของไทโอเลเทดไคโทซานยึดติดเยื่อเมือกสำหรับ
ระบบนำส่งยาซิมวาสแตติน (SYNTHESIS AND PROPERTIESOFMUCOADHESIVE
THIOLATED CHITOSAN FOR SIMVASTATIN DELIVERY SYSTEM)
อ.ที่ปรึกษาวิทยานิพนธ์หลัก: รศ.ดร.พลกฤษณ์ แสงวาณิช, 111หน้า.

วัตถุประสงค์ของงานวิจัยนี้คือการสังเคราะห์ไทโอเลตเตดไคโทซานยึดติดเยื่อเมือกให้มี
สมบัติที่เหมาะสมสำหรับการนำส่งยาประเภทไฮโครโฟบิก ซึ่งทำได้สำเร็จโดยการดัดแปรไคโท
ซานด้วย 5-amino-2-mercaptobenzimidazole (MBI) โดยใช้เมทิลแอคริเลต (MA) เป็นตัวเชื่อม
การแทนที่ของ MA มีค่าประมาณ 14.38% คำนวณโดยเทคนิค ^{1}H NMR ปริมาณหมู่ไทออลและ
พันธะไดซัลไฟด์ ที่ติดบน MA-CS หาด้วยวิธีของเอลแมน มีค่าประมาณ 11.86±0.01 และ 6.54
ไมโครโมลต่อกรัมของพอลิเมอร์ ตามลำดับ ศึกษาความสามารถในการยึดติดเยื่อเมือกของพอลิ
เมอร์ ที่ทดสอบด้วย Periodic acid: Schiff (PAS) ในของเหลวจำลองระบบทางเดินอาหาร (pH
1.2, 4.0 และ 6.4) พบว่า MA-CS และ MBI-MA-CS ให้ความสามารถในการยึดติดเยื่อเมือก 10.28
และ 11 เท่า ที่ pH 1.2 ตามลำดับ เมื่อเทียบกับไคโทซานที่ไม่ได้ดัดแปร นอกจากนี้ ได้ศึกษาการ
ประยุกต์ใช้ไคโทซานและไคโทซานดัดแปรเพื่อเป็นตัวนำส่งยาประเภทไฮโครโฟบิก โดยใช้ซิม
วาสแตตินเป็นยาจำลอง ขึ้นรูปอนุภาคไคโทซานและไคโทซานดัดแปรด้วยเทคนิค อิเล็กโทรสเปรย์
ได้อนุภาคขณะบวมตัวอยู่ในช่วง 1-5 ไมโครเมตร ซึ่งวัดโดยเครื่องวัดขนาดอนุภาค มีประสิทธิภาพ
ในการควบคุมการกักเก็บยามากกว่า 80 เปอร์เซ็นต์ อีกทั้งความสามารถยึดติดเยื่อเมือกของอนุภาค
SV-MA-CS และ SV-MBI-MA-CS มีค่าประมาณ 7 และ 7.33 เท่า ตามลำดับ เทียบกับ SV-CS ใน
สภาวะ pH 1.2 นอกจากนั้นอนุภาคดังกล่าวไม่เพียงแต่จะลด burst effect แต่ยังสามารถปลดปล่อย
ซิมวาสแตตินนานถึง 12 ชั่วโมง

สาขาวิชา   ปิโตรเคมี และวิทยาศาสตร์พอลิเมอร์ ลายมือชื่อนิสิต...
ปีการศึกษา   2555   ลายมือชื่อ อ.ที่ปรึกษาวิทยานิพนธ์หลัก..................

5372460523:   MAJOR PETROCHEMISTRY AND POLYMER SCIENCE
KEYWORDS: CHITOSAN/ MUCOADHESIVE/ THIOLATED- CHITOSAN

MULLIKA KONGSONG: SYNTHESIS AND PROPERTIES OF MUCOADHESIVE THIOLATED CHITOSAN FOR SIMVASTATIN DELIVERY SYSTEM. ADVISOR: ASSOC. PROF. POLKIT SANGVANICH, Ph.D., 111 pp.

The objective of this research was to prepare a mucoadhesive thiolated chitosan suitable for delivery of hydrophobic drugs. This can be achieved by modification of chitosan with 5-amino-2-mercaptobenzimidazole (MBI) using methyl acrylate (MA) as a linker agent. The substitution of MA was about 14.38% calculated by ^{1}H NMR. The amounts of thiol groups (MBI) and disulfide bonds coupled on MA-CS determined by Ellman's method were 11.86 and 6.54 μmol per gram of polymer, respectively. Periodic acid: schiff (PAS) colorimetric method was used to study mucin-conjugated polymer bioadhesive strength in the simulated gastrointestinal fluid (pH 1.2, 4.0 and 6.4). The MA-CS and MBI-MA-CS showed stronger mucoadhesive property 10.28 and 11-fold, respectively than that of unmodified chitosan at pH 1.2. Additionally, the applications of CS and modified CS as hydrophobic drug delivery carriers were investigated using simvastatin (SV) as a model drug. The microspheres of CS and modified CS were fabricated using electrospray ionization technique. The swollen particle sizes of microspheres were in the range of 1-5 μm measured by particle sizer. The SV loaded microspheres exhibited over 80% drug entrapment efficiency. The mucoadhesiveness of SV-MA-CS and SV-MBI-MA-CS microspheres displayed 7- and 7.33-fold at pH 1.2, respectively compared to SV-CS. The obtained microspheres not only reduced the burst effect but also prolonged release of SV as long as 12 h.

Field of Study: Petrochemistry and polymer Science Student's Signature: ⸾

Academic Year: 2012   Advisor's Signature:

ACKNOWLEDGEMENTS

CONTENTS

LIST OF TABLES

LIST OF FIGURES

Figure **Page**

Figure **Page**

LIST OFABBREVIATIONS

%	percentage
μg	microgram
μL	microliter
μmol	micromole
APDs	avalanche photodiode array
aq	aqueous
cm	centimeter
cm^{-1}	unit of wave number
conc.	concentration
MBI	5-amino-2-mercaptobenzimidazole
MA	methylacrylate
CS	chitosan
°C	degree Celsius (centrigrade)
SV	simvastation
TGA	thermogravimetric analysis
%DD	degree of deacetylation
EE	entrapment efficiency
FTIR	Fourier Transform Infrared Spectrophotometer
g	gram
h	hour
kDa	kilodalton
kV	kilovolt
M	concentration in molar
mCS	modifiedchitosan
mg	milligram
min	minute
mL	milliliter
mL/h	milliliter per hour

MW	molecular weight
nm	nanometer
PDI	polydispersity index
pH	power of hydrogen ion or the negative logarithm (base ten)
ppm	part per million
KBr	potassium bromide disk
r^2	correlation coefficient
rpm	round per minute
S.D.	standard deviation
SEM	Scanning Electron Microscope
t	time
Tm	melting temperature
UV	ultraviolet
v/v	volume/volume
w/w	weight/weight
XRD	X-ray diffraction
PAS	periodic acid schiff

CHAPTER I

INTRODUCTION

1.1 Introduction

Simvastatin (SV) is a synthetic derivate of a fermentation product of *Aspergillus terreus*, and marketed under the trade name of Zocor. It is widely used for the treatment of primary hypercholesterolemia and coronary heart disease. After oral administration, Simvastatin (a lactone) (Figure 1.1) undergoes hydrolysis and is converted to its β, δ-dihydroxy acid form (simvastatin acid) by the cytochrome-3A system in liver, where it is a potent competitive inhibitor of 3-hydroxyglutaryl-CoA reductase the enzyme that catalyzes the rate-limiting step of cholesterol biosynthesis [1]. This leads to up-regulation of low-density lipoprotein (LDL) receptors and an increase in catabolism of LDL cholesterol.

Simvastatin is practically insoluble in water with solubility of 30 μg/mL [2], short biological half-life (3 hours), high first-pass metabolism and poorly absorbed from the gastrointestinal (GI) tract (*<5%*) [3]. The past years, developement mucoadhesive buccal tablets of SV using mucoadhesive polymers found that the polymer retarded the release of simvastatin and the absorbtion of SV improved [4].
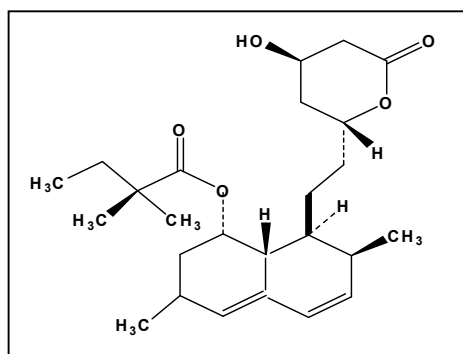
Figure 1.1 Chemical structure of simvastatin.

Mucoadhesive polymers are synthetic or natural macromolecules which are capable of attaching to mucosal surfaces. The concept of mucoadhesive polymers has been introduced into the pharmaceutical application [5]. Over the past few years, mucoadhesive polymers have received attention as excipients for various drug delivery systems due to the possibility of drug localization at the target site, a prolonged residence time at the site of drug absorption that shows sustained release of drug there. The drugs that are absorbed through the mucosal lining of tissues can enter directly into the blood stream and not be inactivated by enzymatic degradation in the gastrointestinal tract and an increase in drug concentration gradient on the mucosa, as a result, the bio-availability of drug can be improved [6-8]. Due to these advantages, many attempts have been made to improve the mucoadhesive properties of polymeric carriers.

The design and selection of polymers for drug delivery is partially based on the concept that mucoadhesive polymers should have functional groups, which can be summarized as follows:

1) Carboxyl (-COOH) and hydroxyl (-OH), hydrogen-bonding group
2) Hydroxyl (-OH) and amide ($-NH_2$) groups, or strong anionic or positive charges
3) Sufficient chain flexibility.
4) High molecular weight

These polymers would be able to interact more strongly to the mucus glycol-proteins [9, 10].

Chitosan or poly [β-(1–4)-2-amino-2-deoxy-d-glucopyronose] (Figure 1.2b) is a cationic natural linear polysaccharide consisting of copolymers of glucosamine and N-acetylglucosamine. It is obtained by deacetylation of chitin (Figure 1.2a), which present in outer structure in marine crustaceans such as crabs and shrimp. Chitosan is soluble in dilute acidic solutions below pH 6.0 due to the quaternisation of the amine groups that have a pKa value of 6.3 making chitosan promotes

solubility, wheraeas chitosan is insoluble at alkaline and neutral pH. The primary amino group accounts for the possibility of relatively easy chemical modification of chitosan and salt formation with acids.

Chitosan used for developing mucoadhesive polymer due to its non-toxic, high biocompatible and enzymatic biodegradable [11]. The presence of -OH and -NH_2 groups, together with cationic property of chitosan are considered to be responsible via non-covalent bonds e.g. hydrogen bonds and ionic interactions with sialic groups of the mucus layer, resulting in a good mucoadhesive property. Therefore, chitosan considered to be suitable for application in pharmaceutical technology such as drug delivery and gene delivery carriers [12], wound healing accelerators and tissue engineering scaffolds [13].
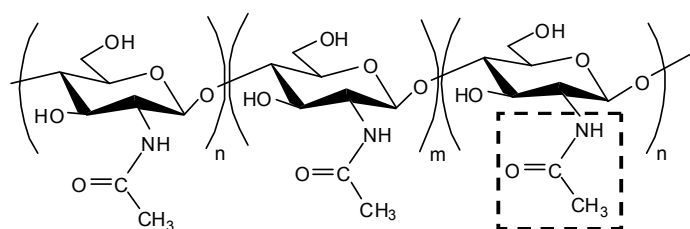
(a) Chitin
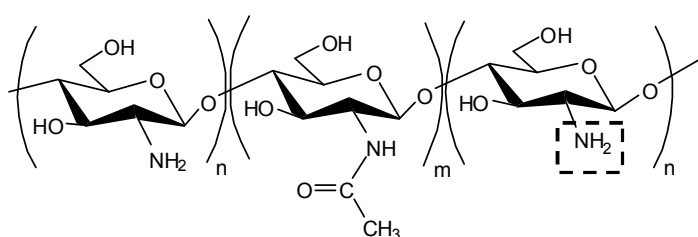
(b) Chitosan

Figure 1.2 Structures of a) chitin and b) chitosan

Recently, these mucoadhesive properties can be enhanced with introducing thiol groups on chitosan so called for thiomer/thiolated chitosan (Figure 1.3a) [14]. Some research, such as chitosan–thioglycolic acid conjugates (chitosan-TGA) [15],

chitosan-N-acetyl cysteine [16] and chitosan-homocysteine thiolactone (HT-chitosan) [17] are strongly improved in comparison to the unmodified chitosan. Mucoadhesive properties of thiolated chitosans are explained by the formation of covalent bonds between thiol groups of the polymer and cysteine rich sub-domains of mucus glycoproteins layer via thio/disulfide exchange reaction and an oxidation process (Figure 1.3b) [18]. These covalent bonds are stronger than the non-covalent bonds.

Chitosan chain

(a)   (b)
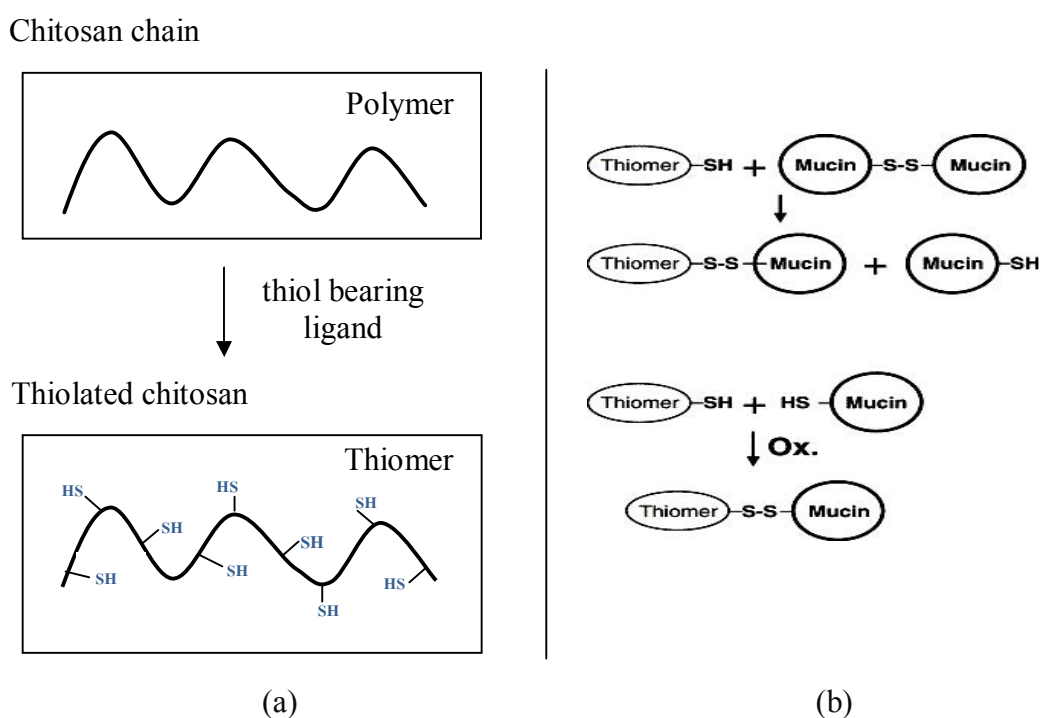
Figure 1.3 Structures of (a) thiolated chitosan and (b) mechanism of disulfide bond formation between thiomer and mucus glycoproteins (mucin)

However, the poor interaction of these thiolated polymers with hydrophobic drug molecules often resulted in a faster drug release, which will affect their potential applications in pharmaceutical fields [19].

The aim of this study was to attempt synthesize a mucoadhesive thiolated chitosan suitable for delivery of simvastatin (as a model hydrophobic drugs). These mucoadhesive thiolated chitosan designed in order to increase hydrophobicity. This

can be perform by (i) increase the length of the grafted chain, (ii) coupling an aromatic system into the chitosan backbone to increase the stacking with the hydrophobic drugs and finally, (iii) introducing the thiol group to form chemical bond with thiol group in mucus membrane. This can be achieved by modification of chitosan with 5-amino-2-mercaptobenzimidazole (MBI) using methyl acrylate (MA) as a linker agent (Figure 1.4). The amount of thiol groups immobilized on chitosan was determined by Ellman's method, Periodic acid: Schiff (PAS) colorimetric method was used to qualify mucin-conjugated polymer bioadhesived strength in the simulated gastrointestinal fluid (pH 1.2, 4.0 and 6.4).
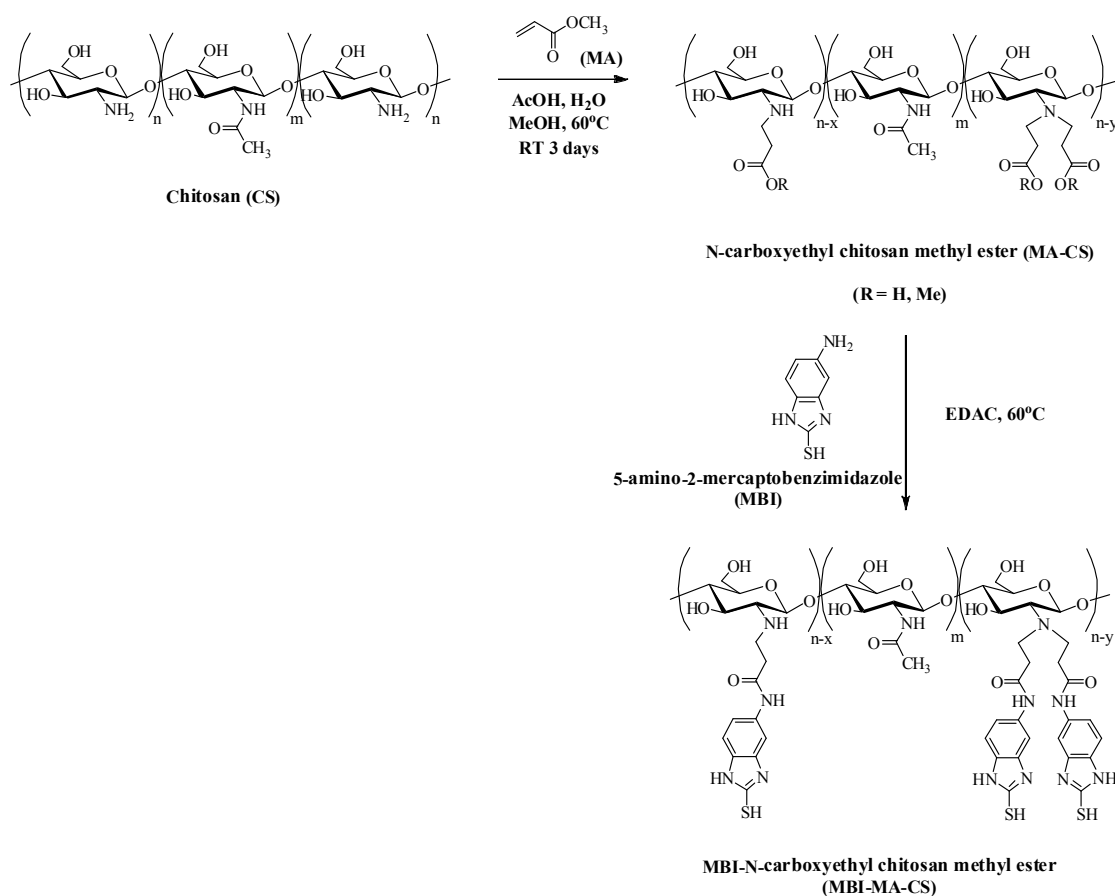
Figure 1.4 Sythesis scheme of *N*-carboxyethyl chitosan methyl ester (MA-CS) and MBI-*N*-carboxyethyl chitosan methyl ester (MBI-MA-CS)

Various methods have been used to prepare chitosan particulate systems such as ionic gelation, coacervation/precipitation, emulsion cross-linking [12] and ultra-sonification [20] are summarized in Table 1.1. The disadvantages of microspheres is difficult to control the particle sizes and widely size distribution, the droplet easily agglomerate. This disadvantage will bring some limitations in application: (1) the reproducibility of microspheres is poor among batches, which will result in poor repeatability of the release behavior and efficacy of drug among doses; (2) the bioavailability of drug will be low if the size distribution of microsphere is broad. And, the side-effects of the drug will be increased. Therefore, it is necessary to prepare uniform-sized microspheres and control the size of microspheres for their applications in drug delivery system.

Table 1.1 Chitosan- based drug delivery systems prepared by different methods [12]

Type of system	Method of preparation
Microspheres	Emulsion cross-linking,
	Coacervation/precipitation
	Spray-drying, Ionic gelation
Nanoparticles	Emulsion-droplet coalescence
	Coacervation/precipitation

One of the novel an attractive technique has been applied to generate nanoparticles is known as electrospraying ionization technique (Figure 1.5) is a method of liquid atomization using electrostatic forces. The polymer flowing out of the nozzle in the form of droplet when applied high voltage potential forces. The advantages of this technique are simplicity and unique one-step technique [21]. It's able to obtain uniform particle size, narrow size distribution can be produced under easily controlled conditions [22], such as the flow rate, voltage applied to the nozzle and working distance. Electrospraying technicque suitable for use in drug delivery systems as well as many other applications such as encapsulate various materials (biomacromolecules, microparticles and living cells) within the microcapsules [23].
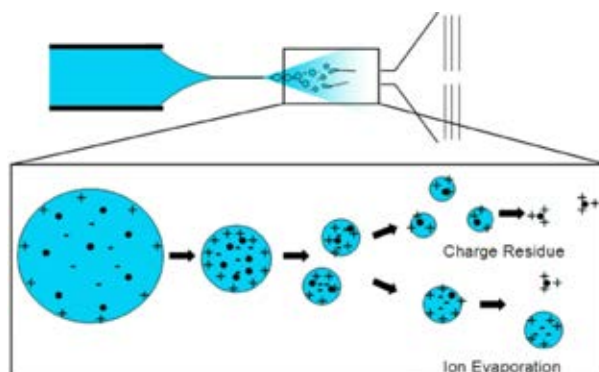
Figure 1.5 The droplet is generated by electrical force

Therefore, the present work was to prepare controlled release microsphere of SV, using CS and modified chitosan (MA-CS and MBI-MA-CS) as the retarding material, by application of electrospray ionization technique (Figure 1.6) and study the *In vitro* release behavior of the spheres in simulated gastrointestinal fluid pH 1.2, 4.0 and 6.4
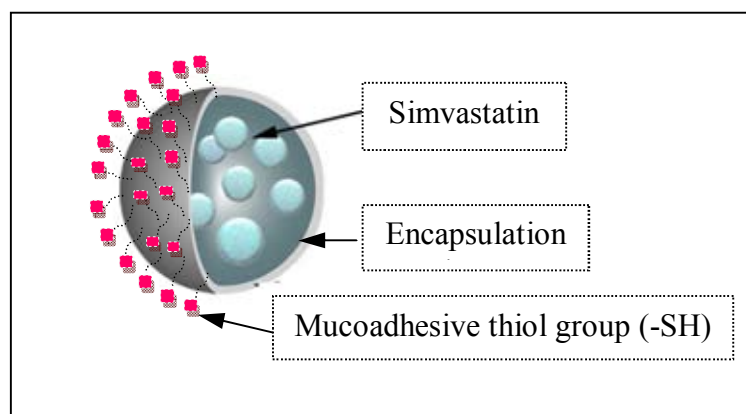
Figure 1.6 Scheme of drugs loaded mucoadhesive microspheres

1.2 The objectives of this research

1) Modify chitosan to improve mucoadhesive properties suitable for hydrophobic drugs delivery.

2) Preparation of chitosan and modified chitosan solid micro/nanoparticles with electrospray technique.

1.3 The scope of research

The scope of this research was carried out by stepwise methodology as follows:

1) Review literature for related research work.

2) **Part I** : Modifying chitosan

    a.   Preparation of thiolated chitosan (MA-CS, MBI-MA-CS)

    b.   Characterization of the physical and chemical properties of chitosan and modified chitosan using FTIR, ^{1}H-NMR, ^{13}C-NMR, TGA.

    c.   Determination degree of MA substitution.

    d.   Determination degree of thiol and disulfide substitution.

    e.   *In vitro* investigation of mucoadhesive property in simulated gastric fluid (SGF) pH 1.2 and 4.0 and the simulated intestinal fluid (SIF) pH 6.4 by using UV-Vis method

    f.   swelling properties in pH 1.2, 4.0 and 6.4.

    g.   Toxicity study of chitosan and modified chitosan.

    Part II : Fabrication and evaluation of the modified chitosan and chitosan as a drug delivery carrier

    a.   Preparation of the microspheres with and without drug

    b.   Characterization of the obtained microspheres in terms of morphology , size and size distribution, zeta potential, chemical analysis and thermal behavior.

    c.   Determination of the drug encapsulation efficiency

    d.   Study the *In vitro* release behavior of the spheres in simulated gastrointestinal fluid pH 1.2, 4.0 and 6.4 using UV-Vis method.

3) Report, Discussion and Writing up thesis.

Part I: Flow chart for synthesis and characteristic

```
                    ┌─────────────────────────────────┐
                    │  Preparation of thiolated polymer│
                    │     -    MA-CS (3 days)          │
                    │     -    MBI-MA-CS               │
                    └─────────────────────────────────┘
```

Preparation of thiolated polymer
- MA-CS (3 days)
- MBI-MA-CS

Characterization of MBI-MA-CS
- ^{1}H NMR, ^{13}C NMR
- FT-IR
- TGA

- Degree of substitution of MA (^{1}H NMR)
- Determination degree of thiol and disulfide substitution. (UV-Vis method)

Mucoadhesive properties
(In pH 1.2, 4.0 and 6.4)

Swelling properties
(In pH 1.2, 4.0 and 6.4)

Contact angle
Anti-bacterial

Part II: Pharmaceutical application
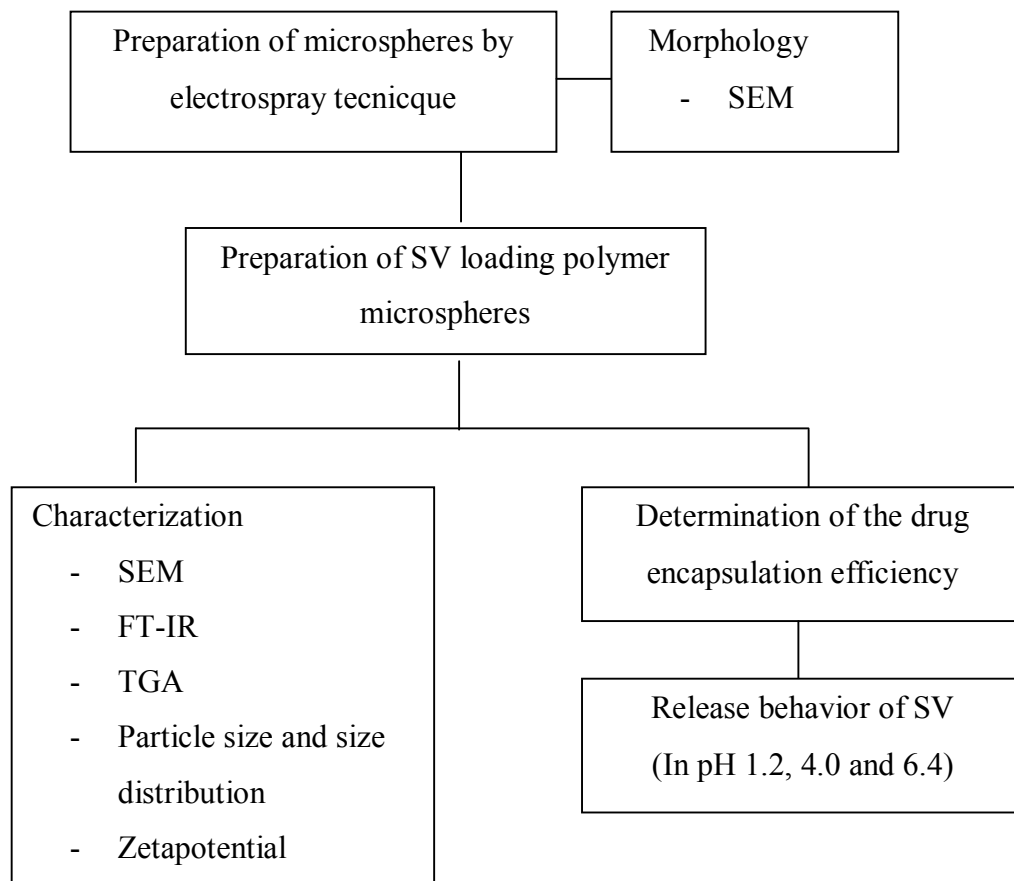
Figure 1.5 Flow chart of research

CHAPTER II

THEORY AND LITERATURE REVIEWS

2.1   Hypercholesterolemia and coronary heart disease

Hypercholesterolemia is a condition characterized by very high levels of cholesterol in the blood that result from a combination of genetic (*the APOB*, *LDLR*, *LDLRAP1*, and *PCSK9* genes) and environmental risk factors. Lifestyle choices including diet, exercise, and tobacco smoking strongly influence the amount of cholesterol in the blood. Additional factors that impact cholesterol levels include a person's gender and age. People with hypercholesterolemia have a high risk of developing a form of coronary artery disease. This condition occurs when excess cholesterol in the bloodstream is deposited in the walls of blood vessels (Figure 2.1), particularly in the arteries that supply blood to the heart (coronary arteries).
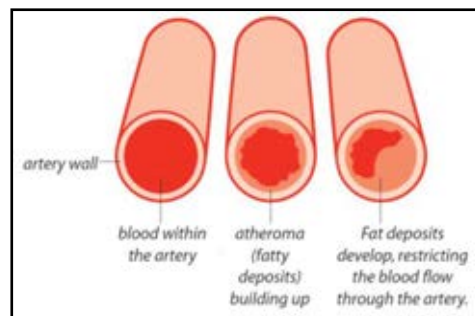
Figure 2.1 A gradual build-up of fatty material (called atheroma) within their walls

2.2   Simvastatin

Simvastatin (SV) is a synthetic derivate of a fermentation product of *Aspergillus terreus*, and marketed under the trade name of Zocor. It is a member of the statin class of pharmaceuticals that widely used for Lowering cholesterol and other lipids (fats) in the blood to reduce the risk of heart disease problems but

practically insoluble in water, short biological half-life, high first-pass metabolism and poorly absorbed from the gastrointestinal (GI) tract.

2.2.1 Structure

Simvastatin is a nonhygroscopic white crystalline powder, insoluble in water but quite soluble in chloroform, methanol and alcohol with pKa of 4.68 [24]. The molecular weight of this compound $C_{25}H_{38}O_5$ is 418.57. Simvastatin is the pharmacologically inactive lactone form of simvastatin acid, butanoic acid, 2,2-dimethyl-1,2,3,7,8,8a-hexahydro-3,7-   dimethyl-8-[2-(tetrahydro-4-hydroxy-6-oxo-2H-pyran-2-yl) ethyl]-1-naphthalenylbester. Simvastatin is a lactone which needs the opening of the ring for it to become active. Figure 2.1 shows the chemical structure of simvastatin [24, 25].

Figure 2.2 Chemical structure of simvastatin

2.2.2 Physical and chemical properties

Simvastatin (a lactone) (Figure 2.2) undergoes hydrolysis and is converted to its β, δ-dihydroxy acid form (simvastatin acid) by the cytochrome-3A system in liver, where it is a potent competitive inhibitor of 3-hydroxyglutaryl-CoA reductase the enzyme that catalyzes the rate-limiting step of cholesterol biosynthesis. This leads to up-regulation of low-density lipoprotein (LDL) receptors and an increase in catabolism of LDL cholesterol shown in figure 2.3.

Figure 2.3 Pathway of simvastatin

2.3   Controlled released system

In recent years, the study of controlled release of drugs and other bioactive agents from polymeric devices has attracted many researchers from around the world. Controlled drug delivery include both sustained delivery over days/weeks/ months/ years and targeted (e.g., to a tumor, diseased blood vessel, etc.) delivery on a one-time or sustained basis. Controlled release formulations can be used to reduce the amount of drug necessary to cause the same therapeutic effect in patients. The convenience of fewer and more effective doses also increases patient compliance [26].

Controlled release over an extended duration is highly beneficial for drugs that are rapidly metabolized and eliminated from the body after administration [27]. An example of this benefit is shown schematically in Figure 2.4 in which the concentration of drug at the site of activity within the body is compared after

immediate release from 4 injections administered at 6 hourly intervals and after extended release from a controlled release system. Drug concentrations may fluctuate widely during the 24 h period when the drug is administered via bolus injection, and for only a portion of the treatment period is the drug concentration in the therapeutic window (i.e., the drug concentration that produces beneficial effects without harmful side effects). With the controlled release system, the rate of drug release matches the rate of drug elimination and, therefore, the drug concentration is within the therapeutic window for the vast majority of the 24 h period.
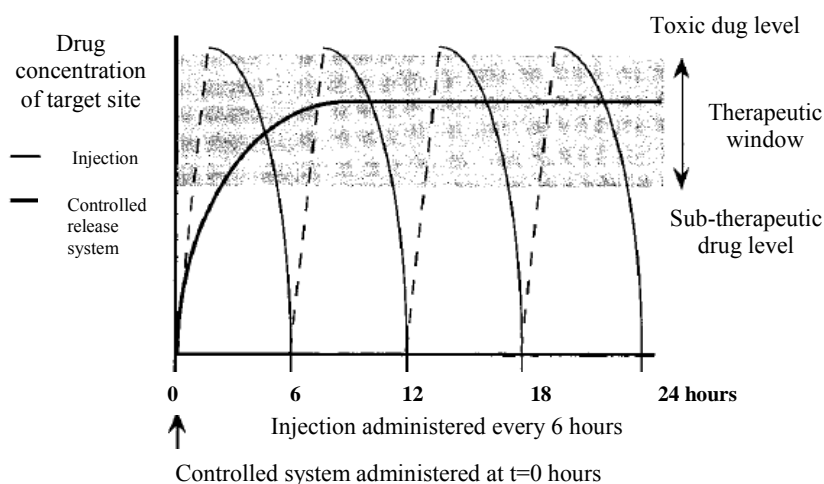
Figure 2.4 Drug concentrations at site of therapeutic action after delivery as a conventional injection (thin line) and as a temporal controlled release system (bold line) [27].

Controlled drug delivery occurs when a polymer is combined with the drug or other active agent in such a way that the active agent is released from the material in a predesigned manner [28].

a)

Polymeric
membrance

Drug
core

Drug
core

t = 0   t > 0

b)

Polymer

drug

t = 0   t > 0
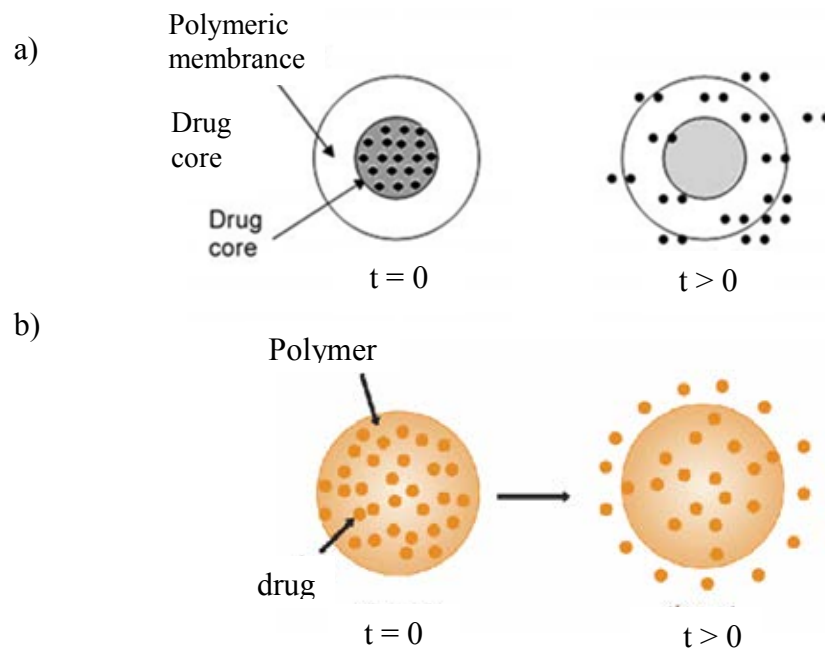
Figure 2.5 Representation of controlled release systems

a)   reservir and b) matrix devices [28].

2.3.1   Controlled-release mechanisms

There are three primary mechanisms by which active agents can be released
from a delivery system [29].

1. Diffusion-controlled delivery systems
2. Swelling-controlled delivery systems
3. Degradation-controlled delivery systems

Any or all of these mechanisms may occur in a given release system.
Diffusion occurs when a drug or other active agent passes through the polymer that
forms the controlled-release device. *The diffusion* can occur through pores in the
polymer matrix, by passing between polymer chains. Examples of diffusion-release
systems are shown in Figures 2.5
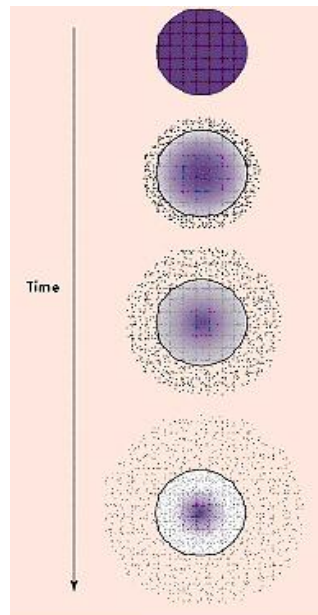
Figure 2.6 Drug delivery from a typical matrix drug delivery system

In Figure 2.5, a polymer and active agent have been mixed to form a homogeneous system, also referred to as a matrix system. Diffusion occurs when the drug passes from the polymer matrix into the external environment. As the release continues, its rate normally decreases with this type of system, since the active agent has a progressively longer distance to travel and therefore requires a longer diffusion time to release. For *the swelling* of the carrier increases the aqueous solvent content within the polymer matrix, enabling the drug to diffuse through the swollen network into the external environment. Most of materials used are based on hydrogel. The swelling can be triggered by a change in the environment surrounding such as pH, temperature, ionic strength, etc.

There are two major types of *degradation-controlled release systems*;
- Erodible systems, drug release occurs due to degradation or dissolution of the hydrogel.
- Pendant chain systems, the drug is affixed to the polymer backbone through degradable linkages. As these linkages degrade, the drug is released.

2.4   Mucoadhesion/bioadhesive

In the early 1980s, the concept of mucoadhesives, was introduced into the controlled drug delivery area. Mucoadhesives are synthetic or natural polymers that will attach to related tissue or to the surface coating of the tissue for targeting various absorptive mucosa such as ocular, nasal, pulmonary, buccal, vaginal etc [7]. The system of drug delivery is called as mucoadhesive drug delivery system.   This system has advantage like [30];

1. Prolongs the residence time of the dosage form at the site of absorption.
2. Due to an increased residence tine it enhances absorption and hence the therapeutic efficacy of the drug.
3. Increase in drug bioavailability due to first pass metabolism avoidance.
4. Drug is protected from degradation in the acidic environment in the gastrointestinal tract.
5. Improved patient compliance-ease of drug administration.

2.4.1   Mucoadhesive mechanism

Mucus is a complex viscous adherent secretion which is synthesized by specialized goblet cells. Mucus is composed mainly of water (>95%) and mucins, which are glycoproteins of exceptionally high molecular weight. Furthermore, pendant sialic acid and sulphate groups located on the glycoprotein molecules result in mucin behaving as an anionic polyelectrolyte at neutral pH [31]. Other non mucin components of mucus include secretory lysozyme, lactoferrin, lipids, polysaccharides, and various other ionic species [31].

Development of novel mucoadhesive delivery systems are being undertaken so as to understand the various mechanism of mucoadhesion (Figure 2.7) and improved permeation of active agents.
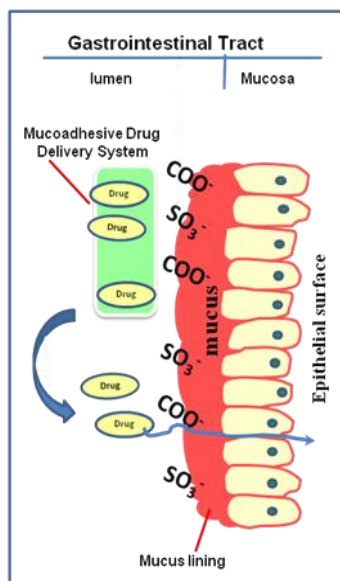
Figure 2.7 Mechanism of Mucoadhesion

The mechanism of mucoadhesion is generally divided into two steps are shown in Figure 2.8 [30]

The first stage (also known as contact stage), the contact between the mucoadhesive polymer and mucous membrane, with spreading and swelling of the formulation, intiating its deep contact with the mucus layer.

The second stage (the consolidation stage), the mucoadhesive materials are activated by the presence of moisture. Moisture plasticizes the system, allowing the mucoadhesive molecules to break free and to link up by weak vander Waals and hydrogen bond
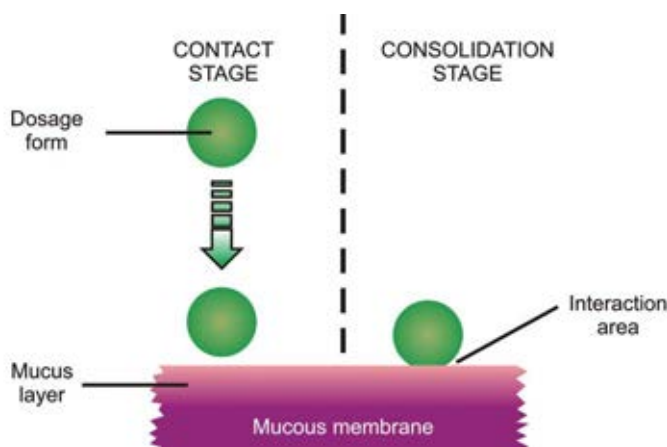
Figure 2.8 The two stages of the mucoadhesion process [32]

2.4.2 Mucoadhesion theories

There are six general theories have been proposed which can improve understanding for the phenomena of adhesion and can also be extended to explain the mechanism of bioadhesion. The theories include [30, 33]:

2.4.2.1 Electronic Theory

Electronic theory is based on the premise that both mucoadhesive and biological materials possess opposing electrical charges. Thus, when both materials come into contact, they transfer electrons leading to the building of a double electronic layer at the interface, where the attractive forces within this electronic double layer determines the mucoadhesive strength.

2.4.2.2 Wetting Theory

The wetting theory applies to liquid systems which present affinity to the surface in order to spread over it. This affinity can be found by using measuring techniques such as the contact angle. The general rule states that the lower the contact angle then the greater the affinity (Figure 2.9).
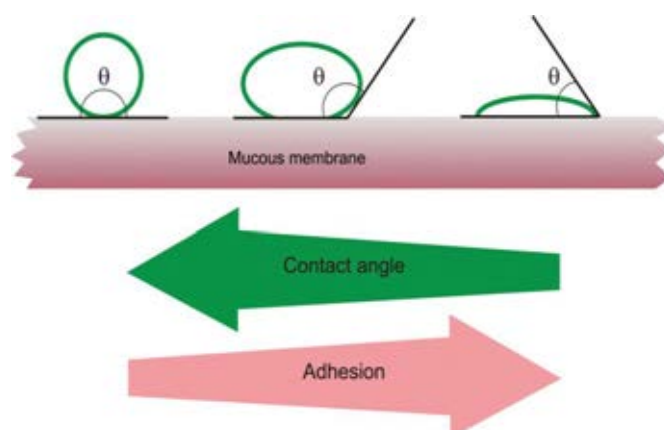
Figure 2.9 Schematic diagram showing influence of contact angle between device and mucous membrane on bioadhesion.

2.4.2.3. Adsorption Theory

According to the adsorption theory, the mucoadhesive device adheres to the mucus by secondary chemical interactions, such as in van der Waals and hydrogen bonds, electrostatic attraction or hydrophobic interactions. For example, hydrogen bonds are the prevalent interfacial forces in polymers containing carboxyl groups. Such forces have been considered the most important in the adhesive interaction phenomenon because, although they are individually weak, a great number of interactions can result in an intense global adhesion

2.4.2.4. Diffusion Theory

This theory assumes the diffusion of the polymer chains, present on the substrate surfaces shown in Figure 2.10, across the adhesive interface thereby forming a networked structure.
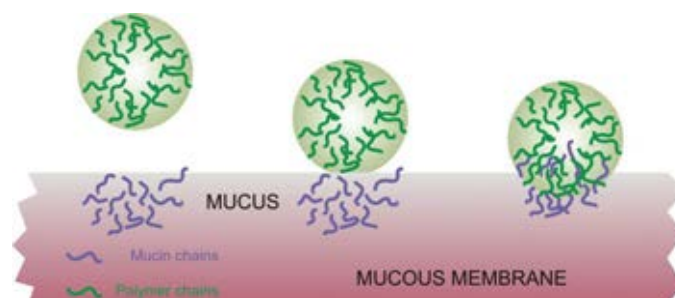
Figure 2.10 Secondary interactions resulting from interdiffusion of polymer chains of bioadhesive device and of mucus.

2.4.2.5. Mechanical Theory

Mechanical Theory explains the diffusion of the liquid adhesives into the micro-cracks and irregularities present on the substrate surface thereby forming an interlocked structure which gives rise to adhesion.

2.4.5.6. Cohesive Theory

This theory proposes that the phenomena of bioadhesion are mainly due to the intermolecular interactions amongst like-molecules. However, none of these mechanisms or theories alone can explain the mucoadhesion which occurs in an array of different situations.

2.4.3 The mucoadhesive/mucosa interaction

As mentioned above, bioadhesion may take place either by physical or by chemical interactions. For adhesion to occur, molecules must bond across the interface. These bonds can arise in the following way [32].

2.4.3.1. physical interactions

- Hydrogen bonds
A hydrogen atom, when covalently bonded to electronegative atoms such as oxygen, fluorine or nitrogen, carries a slight positively charge and is therefore is attracted to other electronegative atoms. The hydrogen can therefore be thought of as being shared, and the bond formed is generally weaker than ionic or covalent bonds.

- Van-der-Waals bonds
The Van – der – Waals bonds are some of the weakest forms of interaction that arise from dipole–dipole and dipole-induced dipole attractions in polar molecules, and dispersion forces with non-polar substances.

- Hydrophobic bonds
Hydrophobic bond that occur when non-polar groups are present in an aqueous solution. Water molecules adjacent to non-polar groups form hydrogen bonded structures, which lowers the system entropy. There is therefore an increase in the tendency of non-polar groups to associate with each other to minimise this effect.

2.4.3.2. chemical interactions

- Ionic bonds

The interaction between two oppositely charged ions via electro-static interactions (e.g. in a salt crystal).

- Covalent bonds

Electrons are shared, in pairs, between the bonded atoms in order to "fill" the orbitals in both. These are also strong bonds (*e.g.* thiomer).

2.4.4 Mucoadhesive polymers

Mucoadhesive polymers may provide an important tool to improve the bioavailability of the active agent by improving the residence time at the delivery site. Mucoadhesive polymer have been also used for coating medical devices. As an example a new generation of intestine inspection device has been recently developed in which mucoadhesive polymer coating make intestinal locomotion possible. These materials are natural or synthetic hydrophilic molecules (Table 2.1).

Table 2.1: List of Natural and Synthetic polymers [31]

Synthetic polymers	Natural polymers
Cellulose derivatives	Tragacanth
Polycarbophil	Sodium alginate
Poly acrylic acid	Karaya gum
Poly(vinyl pyrrolidone)	Guar gum
Poly(vinyl alcohol)	Gelatin
Poly(hydroxyethyl methylacrylate)	Chitosan

These polymers can be subdivided into three classes: cationic, anionic and nonionic.

- **Cationic polymers** such as chitosan can interact with the mucus surface, since it is negatively charged at physiological pH.
- **Aninonic polymers**, including carboxymethylcellulose and alginates. The alginates, negatively charged polysaccharides, are widely used in the production of microparticles and are frequently reported as polyanionic mucoadhesive polymers. Synthetic polymers derived from poly(acrylic acid)(carbomers) has been considered as a good mucoadhesive material with negatively charged and not water soluble but form viscous gels when hydrated such as polycarbophil.
- **Nonionic polymers**, including hydroxypropylmethylcellulose, hydroxy ethylcellulose and methylcellulose, present weaker mucoadhesion force compared to anionic polymers

The novel mucoadhesive systems such as thiolated polymers are obtained by the addition of conjugated sulfidryl groups increased mucoadhesive properties due to formation of disulfide bridges with cystein domains of glycoproteins of the mucus. An ideal polymer should exhibit the ability to incorporate both hydrophilic and lipophilic drugs. Moreover another study, carried out by Grabovac, Guggi, and Bernkop-Schnürch (2005) established a ranking of the most studied polymers, showing that both thiolated chitosan and polycarbophil are the most mucoadhesive polymer.

2.4.5 Mucoadhesive polymers dosage form

The primary objectives of mucoadhesive dosage forms are to provide intimate contact of the dosage form with the absorbing surface and to increase the residence time of the dosage form at the absorbing surface to prolong drug action. Mucoadhesive polymers have been utilised in many different dosage forms in efforts to achieve systemic delivery of drugs through the different mucosa in Figure 2.11. These dosage forms include tablets, patches, films, semisolids and powders. To serve as

mucoadhesive polymers, the polymers should possess some general physiochemical features such as predominantly anionic hydrophilicity with numerous hydrogen bond-forming groups, suitable surface property for wetting mucus/mucosal tissue surfaces and sufficient flexibility to penetrate the mucus network or tissue crevices [7]. The mucoadhesive drug delivery system may include the following [34].

1. Gastrointestinal delivery system.
2. Nasal delivery system.
3. Ocular delivery system.
4. Buccal delivery system.
5. Vaginal delivery System.
6. Rectal delivery system.
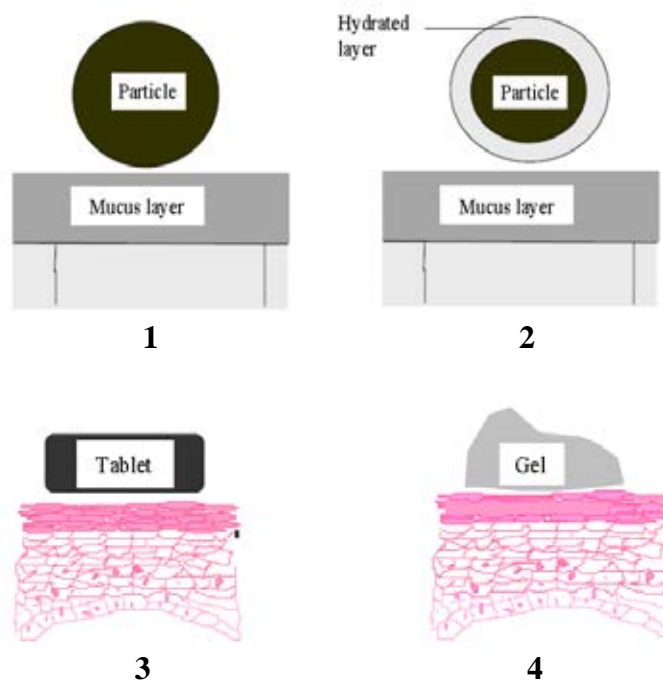
Figure 2.11 Some scenarios where mucoadhesion can occur [32].

1. Dry or partially hydrated dosage forms contacting surfaces with substantial mucus layers (e.g. aerosolised particles deposited in the nasal cavity).

2. Fully hydrated dosage forms contacting surfaces with substantial mucus layers (e.g. particle suspensions in the gastrointestinal tract).

3. Dry or partially hydrated dosage forms contacting surfaces with thin/ discontinuous mucus layers (e.g. a tablet placed onto the oral mucosa).

4. Fully hydrated dosage forms contacting surfaces with thin/discontinuous mucus layers (e.g. aqueous microparticles administered into the vagina).

2.5 Technique to prepare microparticle [12]

Various methods have been used to prepare microparticle such as thermal Cross-Linking, Spray Drying, Solvent Evaporation, Emulsification and Ionotropic Gelation Technique, Wet Inversion Technique, Complex Coacervation. These method have the disadvantages of microspheres is difficult to control the particle sizes and widely size distribution, the droplet easily agglomerate. This disadvantage will bring some limitations in application:

(1) The reproducibility of microspheres is poor among batches, which will result in poor repeatability of the release behavior and efficacy of drug among doses, and furthermore, it is difficult to investigate the relationship between doses and treatment effects

 (2) Because the accumulated location of the microspheres containing drug depends on the size of the particles, the bioavailability of drug will be low if the size distribution of microsphere is broad. And, the side-effects of the drug will be increased [35].

Therefore, it is necessary to prepare uniform-sized microspheres and control the size of microspheres for their applications in drug delivery system.

Electrospraying ionization technique

This technique is the novel an attractive technique has been applied to generate nanoparticles. The principle of electrospraying is based on the theory of charged droplets; stating that an electric field applied to a liquid droplet exiting a capillary is able to deform the interface of the droplet [36]. The electric charge generates an electrostatic force inside the droplet which competes with the surface tension of the droplet, forming the Taylor cone, characteristic of a charged droplet. Eventually, the electrostatic force generated by the use of high voltage on the

capillary that able to overcome the surface tension of the droplet. The excess charge then needs to be dissipated and smaller charged droplets on the micro to nano-scale are ejected from the primary droplet, thus reducing its charge without significantly reducing its mass. Due to Coulomb repulsion of the charges, the droplets disperse well and do not coalesce during their flight toward the collector.
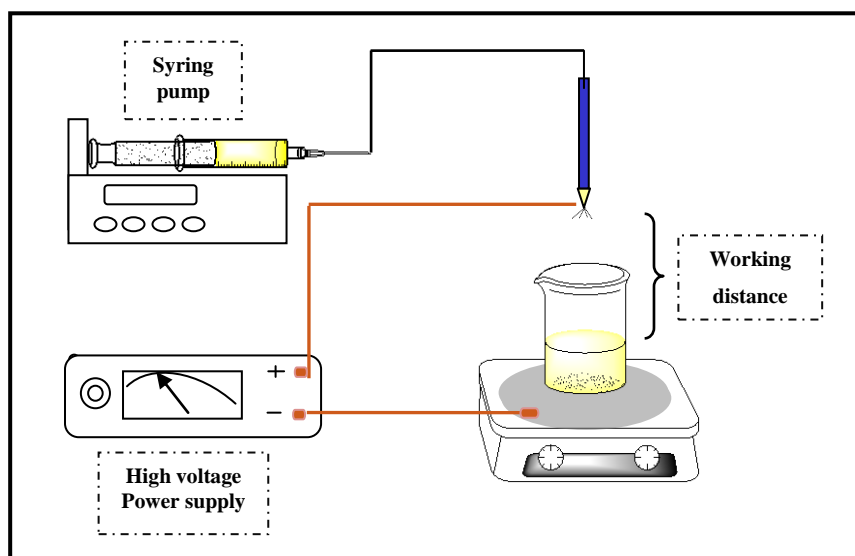
Figure 2.12 Schematic diagram of the instrumentation for electrospray technique

Several spraying modes [37] can occur during electrospraying that depending on setup geometry (e.g. distance between capillary and plate or capillary radius), volume feed rate, liquid properties (surface tension, electrical conductivity) and applied potential (Figure 2.12).

Firstly: The dripping mode

In the absence of an electric field the liquid flows drop by drop. Increasing the potential from zero increases the droplet dripping frequency and decreases the droplet size.

Secondly: The microdripping mode

The liquid droplet at the capillary exit is deformed by the electric field and takes the shape of a cone. A droplet is formed directly at the droplet apex.

Thirth: The cone jet mode

The cone is extended by a jet which is breaking up into droplets. The shape of the liquid at the capillary exit is alternating between the form of a cone (emitting a jet) and a rounded drop. The most desired being the single cone-jet mode, due to its stability and reproducibility

Fourth: The multi jet and ramified jet mode

At increased potential the cone jet becomes unstable and two or more jets appear. This is the multi jet. The number of jets increases with increasing potential. Simple jet, ramified jet and spindle mode are modes that appear at even higher electric potentials. Here the jets emitted by the capillary are highly charged and unstable.

Figure 2.13 Various mode of electrospraying
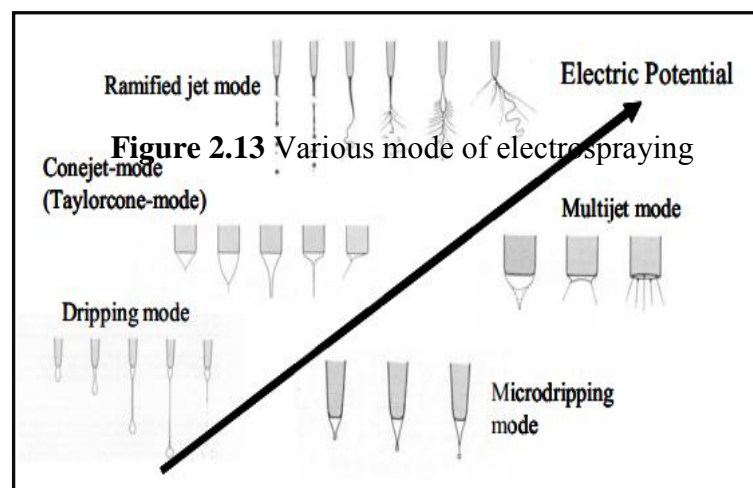
The advantages of this technique over conventional mechanical spraying systems with droplet charged by induction such as

1. simplicity and unique one-step technique.
2. It's able to obtain uniform particle size, narrow size distribution.

3. Droplet size is smaller than that available from conventional mechanical atomizers and can be smaller than 1 mm.

4. Particle size can be produced under easily controlled conditions such as the flow rate, voltage applied to the nozzle and working distance.

The applications of electrospraying such as, the ceramic coatings, as powder in the cosmetic or pharmaceutical industries, painting of automobiles, toner in electro-reprographic systems. Moreover used electrified masks to deposit silica nanoparticles in geometric micrometer-sized patterns on GaAs substrates. This makes electrosprays interesting for any kind of layer or film production [38].

CHAPTER III

EXPERIMENTAL

3.1 Materials

3.1.1 Model drug

Simvastatin (SV) was obtained as a gift sample from. Silommedical Co., Ltd. (Thailand)

3.1.2 Polymer

Chitosan, food grade, M_w 500 kDa., Deacetylation 85 %, Lot No. 497613, (Seafresh, Thailand)

3.1.3 Chemicals

1. Methyl acrylate: analytical grade; Sigma-Aldrich
2. 5-amino-2-mercaptobenzimidazole: analytical grade; Sigma-Aldrich
3. Basic fuchsin (pararosaniline): analytical grade; Sigma-Aldrich
4. Sodium metabisuphite: analytical grade; Sigma-Aldrich
5. Periodic acid: analytical grade; Sigma-Aldrich
6. 5, 5'-Dithio-bis(2-nitrobenzoic acid): analytical grade; Sigma-Aldrich
7. Hydrochloric acid fuming 37%: analytical grade; Merck
8. Acetic acid: AR grade; Union chemicals
9. Chloroform-D: NMR spectroscopy grade; Merck
10. Mucin from porcine stomach (type 2): analytical grade; Sigma-Aldrich
11. Potassium dihydrogen phosphate: analytical grade; Merck
12. Potassium bromide: analytical grade; Merck
13. Potassium iodide: analytical grade; Merck

14. Sodium chloride: analytical grade; Merck

15. Sodium hydrogen phosphate: analytical grade; Merck

16. Sodium hydroxide: analytical grade; Merck

17. Sodium tripolyphosphate: analytical grade; Sigma-Aldrich

18. Potassium hydroxide: analytical grade; Lab-Scan

19. Acetone, commercial grade; Merck

20. Ethanol 95 %: commercial grade; Merck

21. Methanol, commercial grade; Merck

22. Dialysis membrane with M_w cut off at 12,000 – 14,000 Da; Sigma-Aldrich

3.2 Instruments

Table 3.1 The Instruments used in this study

Instrument	Manufacture	Model
FTIR spectrometer	Nicolet	6700
NMR spectrometer	Varian	400 MHz
Freeze dryer	Labconco	Freeze 6
Vacuum pump	Bacthai	ME 2
Horizotal shaking water-bath	Lab-line instrument	3575-1
Micropipette	Mettler Toledo	Volumate
UV-VIS spectrometer	PerkinElmer	Lambda 80
TGA	PerkinElmer	Pyris Diamond
Scanning Electron Microscope	Philips	XL30CP
Syringe pump	Pennyful	kdScience
Small bench centrifuge	Hettich	EBA20
Particle sizer	Malvern Instruments	Zetasizer nanoseries
Ultrasonic bath	Ney Ultrasonik	28H

3.3 Methods

3.3.1   Synthesis of Thiolated chitosan

3.3.1.1 Synthesis of *N*-carboxyethyl chitosan methyl ester(MA-CS)

N-carboxyethyl chitosan methyl ester (MA-CS) was prepared from chitosan and methyl acrylate (MA) by Michael addition. 1 g of chitosan dissolved in 100 ml of 1% v/v acetic acid. To the solution added 0.50 ml of ME and 40.0 ml of methanol. The mixture was stirred at $60\,^{\circ}C$ for 3 days. The reaction mixture was concentrated under reduced pressure to remove excess amount of methyl acrylate and MeOH. The remaining mixture precipitated with excess acetone and harvested by centrifugation (12,000 rpm for 2 min). The pellet dialyzed (MW cut-off 12–14 kDa) against changes of 1 L of methanol for 1 days prior to being air dried to obtain MA-CS

3.3.1.2 Coupling of MBI on *N*-carboxyethyl chitosan methyl ester (MBI-MA-CS)

0.1 g of 5-amino-2-mercaptobenzimidazole (MBI) dissolved in 10 ml methanol were slowly added to 100 ml of *N*-carboxyethyl chitosan methyl ester under stirring.   1-Ethyl-3-(dimethylaminopropyl)carbodiimide (EDAc) used as activate was added to the mixture. The mixture was stirred at $60^{O}C$ in a nitrogen atmosphere for 2 days. The reaction mixture was precipitated with excess acetone and harvested by centrifugation (12,000 rpm for 2 min). The pellet was re-dissolved in water and dialyzed (MW cut-off 12–14 kDa) against changes of 1 L of methanol for 1 days prior to being lyophilized at $-30\,^{\circ}C$ and 0.01 mbar. The dry product was stored at $4^{o}C$ before use.
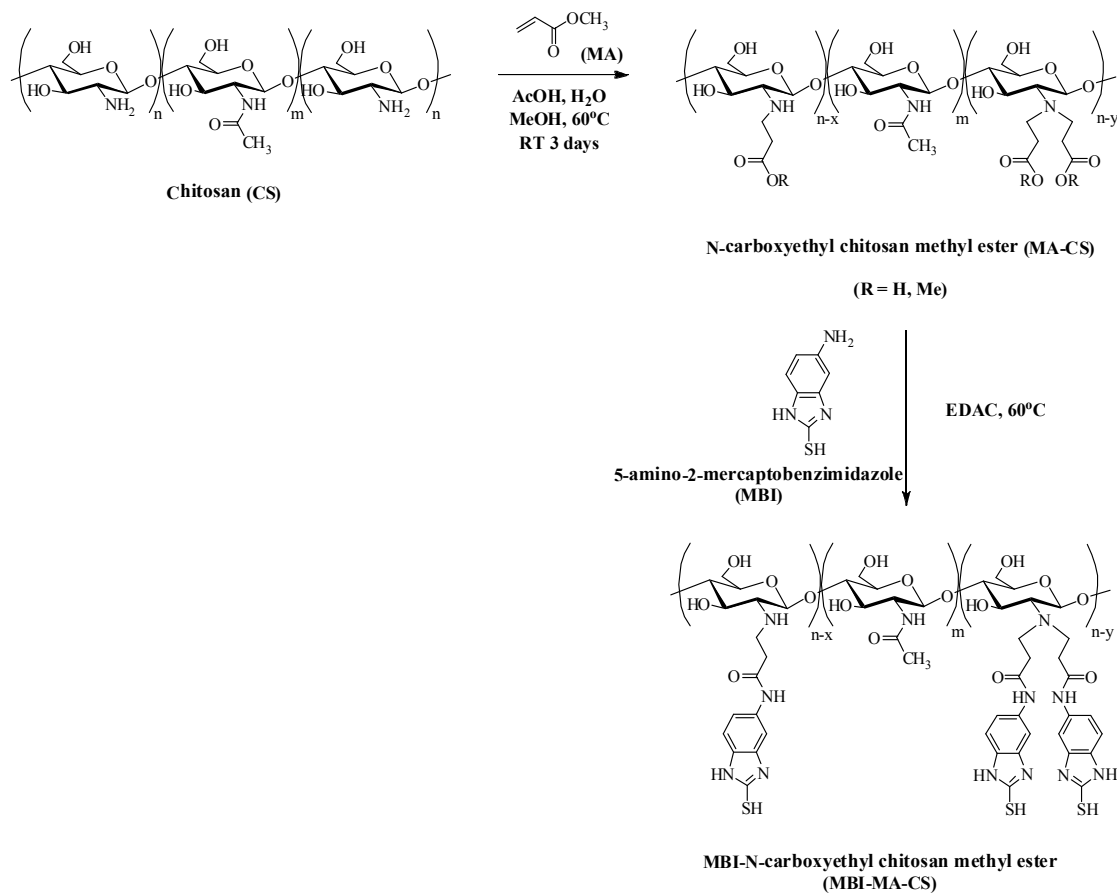
Scheme 1 Synthesis flowchart of *N*-carboxyethyl chitosan methyl ester (MA-CS) and MBI-*N*-carboxyethyl chitosan methyl ester (MBI-MA-CS)

3.3.2 Chemical characterization

3.3.2.1 Fourier transformed infrared spectroscopy (FT-IR)

The CS, MA-CS and MBI-MA-CS were prepared as potassium bromide pellets. FTIR spectra were performed by a Nicolet 6700 Fourier transform infrared (FTIR) spectrometer in the region from 4000 cm^{-1} to 400 cm^{-1}.

3.3.2.2 ^{1}H Nuclear Magnetic Resonance spectroscopy (NMR)

^{1}H NMR spectra were recorded on Bruker NMR spectrometer operated at 400 MHz. D_2O/CF_3CO_2H (1%, v/v) was used to dissolve 5 mg of chitosan and modified chitosan (MA-CS and MBI-MA-CS). The substitution of carboxylic and methyl ester group were determined by ^{1}H NMR spectroscopy according to Eq. (1) as previously described [39].

$$[COOMe+COOH]\ (\%) \quad = \quad \left(\frac{[H8]}{[H3\text{-}H6]} \times \frac{5}{2} \right) \times 100 \quad\text{........ (1)}$$

Here, [H8] is the integral of the methylene proton of MA-CS at the chemical shift 2.32 ppm and [H3-H6] is the integral of the H3, H4, H5 and H6 proton of MA-CS at the chemical shift between 3.6 and 4.2 ppm. (Figure 4.3b)

3.3.2.3 Thermogravimetric analysis (TGA)

The thermal stability of each of the samples was evaluated using TGA analysis. These experiments were performed on a PerKinElmer Pyris Diamond TG/DTA machine under a nitrogen flow at a rate of 30 mL/min. Approximately 5 mg of samples were placed in the alumina pan, sealed and heated at 10°C/min from 25 to 500 ^{o}C.

3.3.2.4 Determination of the thiol group and disulfide bond content

The degrees of thiol group substitution in these modified polymers were determined spectrophotometrically using Ellman's method [30]. This reaction is now widely used for the assay of cholinesterase and the estimation of sulfhydryl groups in tissues [41]. Briefly, a 5 mg of MBI-MA-CS and control (chitosan and MA-CS) were added to 500 µl of 0.5 M phosphate buffer pH 8.0 and then 500 µl of Ellman's reagent (3 mg of DTNB dissolved in 10 ml of 0.5 M phosphate buffer pH 8.0) were added. The samples were incubated for 2 h at room temperature and the absorbance was measured at a wavelength of 450 nm. L-Cysteine hydrochloride standards (10–70 µmol/l) were used to calculate the amount of thiol moieties on MBI-ME-CS.

The amount of disulfide bonds was determined that it was formed due to the oxidation by air/atmosphere during the thiolation step as described by our research group previously [42]. Briefly, 5 mg of the thiolated polymer was hydrated in 1 mL of 50 mM phosphate buffer pH 8.0 for 30 min. 600 µL of 3% sodium-borohydride solution was added to the polymer solution, and the mixture was incubated for 2 h in an oscillating waterbath. 500 µL of 1M HCl were added in order to destroy the remaining sodium-borohydride. After the addition of acetone (100 µL) the mixture was agitated for 5 min. Thereafter, 1 mL of 1M phosphate buffer pH 8.5 and 200 µL of 0.5% (w/v) DTNB dissolved in 0.5M phosphate buffer pH 8.0 were added. After incubation for 15 min at room temperature aliquots of 200 µL were transferred to a 96-well microtitration plate and the free sulfhydryl groups were determined as decribed above. The amount of disulfide bonds was calculated by subtracting the quantity of free thiol groups as determined by the method described above from the total of thiol moieties present on the polymer.

3.3.3 *In vitro* bioadhesion of mucin to chitosan and modified chitosan

(a) Mucus glycoprotein assay

The Periodic Acid Schiff (PAS) colorimetric method is widely used for analysis of mucins, glycoproteins and other polysaccharides in tissues and cells [43]. The PAS colorimetric assay used for the detection of the free mucin concentration for the studies on the adsorption of mucin on CS, MA-CS and MBI-MA-CS. Two reagent were prepared. Schiff reagent contained 1% (w/v) basic fuchsin (pararosaniline) dissolved in DI water. 20 mL of 1 M HCl and 0.1g of Sodium metabisulphite was added to every 6 ml of fuchsin solution. The resulting solution was incubated at 37°C until it became pale yellow. The solution was filtered before use. Periodic acid reagent was freshly prepared by adding 10 µL of 50% (v/v) periodic acid solution to 7 mL of 7% (v/v) acetic acid solution.

Standard calibration curves were prepared from 2 ml of mucin standard solutions (0.025-0.5 mg/mL). After adding 100 µL of periodic acid reagent, the solutions were incubated at 37 ∘C for 2 h. Then, 100 µL of Schiff reagent was added at room temperature for 30 min. 100 µL aliquots of the solution were transferred in triplicate into a 96-well microtiter plate and the absorbance at 555 nm was recorded.

(b) Adsorption of mucin on chitosan and modified chitosan (MA-CS and MBI-MA-CS)

0.05% (w/v) mucin solution in three different of pH, namely the simulated gastrotinal fluid (SGF, pH 1.2 and 4.0) and the simulated intestinal fluid (SIF, pH 6.4) media, were prepared. Chitosan and its derivatives were dispersed (at 5 mg/mL final) in the mucin solutions. These were mixed, vortexed and shaken at 37 ∘C for 2 h. Then the dispersions were centrifuged at 12,000 rpm for 2 min. The supernatant was harvested and used for the measurement of the free mucin content. The mucin concentration was calculated by reference to the calibration curve, and the amount of

mucin adsorbed to the microspheres was calculated as the difference between the total amount of mucin added and the free mucin content in the supernatant.

3.3.4   Swelling study of chitosan and modified chitosan (MA-CS and MBI-MA-CS)

The swelling behaviour of CS, MA-CS and MBI-MA-CS was studied by observing the change of diameter of the film in media of different pHs at room temperature. A 1 g of each polymer was dissolved in 50 mL of 1% (v/v) aqueous acetic acid to yield a 1% (w/v) polymer solution, then the solution poured into the tray (8 ×10 cm) and air dried to obtained the CS, MA-CS and MBI-MA-CS films. The dried films were cut into 5.0 mm diameter circles and each one was immersed in one of SGF (pH 1.2), 0.1 M sodium acetate buffer (pH 4.0) and SIF (pH 6.4) media. The swelling properties were determined by measuring the change in the diameters of each film at various time intervals (0–24 h). The swelling ratio (Sw) for each sample determined at time t was calculated from Eq. (2) as previously reported [44]

$$S_w \quad = \quad \frac{D_t - D_0}{D_t} \quad x\ 100 \ldots\ldots\ldots\ldots\ldots\ldots\ldots\ldots(2)$$

where D_t is the film diameter at time t and D_0 is the initial film diameter.

3.4   Pharmaceutcal applications

In order to study a phamaceutical application potential of modified chitosan as a drug delivery system. The microspheres were prepared by electrospray technique using simvastatin (SV) as a coronary heart drug is the representation model drug for studying the drug delivery system. The properties of drug loaded microspheres, e.g. morphology, particle size, zeta potential, encapsulation effieciency, and drug release profiles were investigated.

3.4.1 Preparation of drugs-loaded polymer microspheres

A 1% (w/v) chitosan and modified chitosan solution (MA-CS and MBI-MA-CS) in 1% (v/v) aqueous acetic acid was prepared. The SV drug (10, 20 and 30mg) was dissolved in EtOH and then Tween80 was added into it. The mixing of chitosan and SV solution to obtain 1:1,2:1 and 3:1% w/w of drug: polymer ratio.

Chitosan and modified chitosan microspheres were prepared by electrospray technique (Figure 3.2). A 5 ml of prepared solution placed onto the syring pump then fed the liquid through silicone tubing and into the needle. The particles generated by a high electric field applied to the solution until able to overcome the surface tension of the droplet solution. The liquid jet was collected into a coagulant bath containing 40 mL of 5% (w/v) sodium tripolyphosphate solution, stirred at 300 rpm. The microspheres were separated by centrifugation at 12,000 for 5 min and washed by DI for 3 times. Control chitosan and modified chitosan microspheres was prepared in the same method as mentioned above without SV.

The preliminary studies of electrospray parameters on the particle sizes that applied voltage was maintained at 20 kV, using a type 26 gauge needle and the working distance between the needle tip, coagulant solution is 8 cm and varying of flow rate are 1.0 ml/hr.
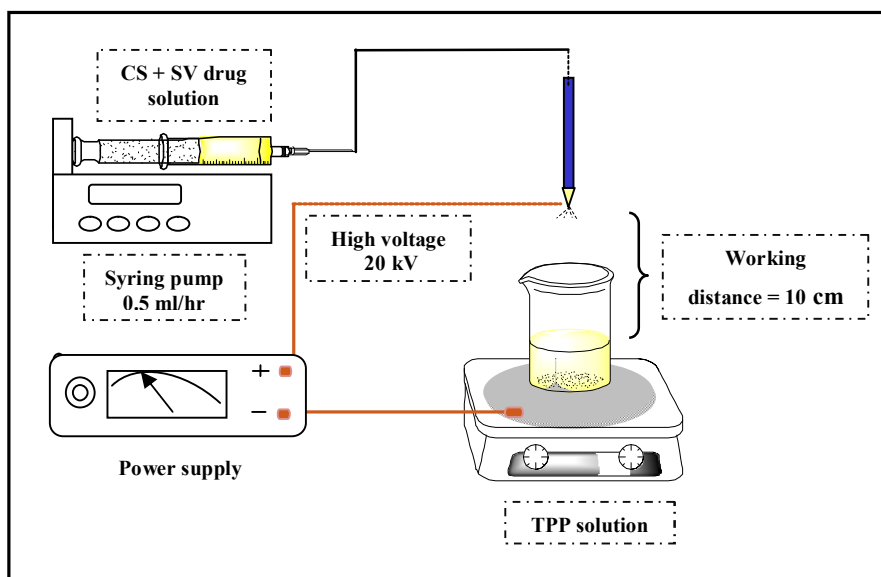
Figure 3.2 Schematic diagram of the electrospray experimental equipment for preparation of SV loaded modified chitosan microspheres.

3.4.2 Characterization of the microspheres

3.4.2.1 Scanning Electron Microscope (SEM)

The surface morphology of sample (before and after the drug loading) were examined by SEM. The samples were mounted onto an aluminum stub using double-sided carbon adhesive tape and coated with gold-palladium. Coating was achieved at 50 mA for 6 min through a sputter coater. The particles were observed via scanning electron microscope under high vacuum at an ambient temperature with a beam voltage of 10-20 kV.

3.4.2.2 Particle size measurement

The particle size and size distribution of microspheres were evaluated with a particle size analyzer (Zetasizer nano series, Malvern instuments). Microspheres are suspended in an aqueous 5% (w/v) sodium tripolyphosphate solution. Size calculation was base on dynamic light scattering (DLS) method as a

software protocol. The scattered light was collected at an angle of 90° through fiber optics and converted to an electrical signal by an avalanche photodiode (APDS). All sample were sonicated and run in triplicate with the number of runs set to 5 and run duration set to 10 seconds.

3.4.2.3 Zeta potential

Zeta potential of the microspheres were determined using particle sizer. The analysis was performed at a scattering angle of 90°. All samples were sonicated and run in triplicate with the number of runs set to 5 and run duration set to 10 seconds.

3.4.2.4 Fourier Transform Infrared (FTIR) Spectroscopy

The FTIR spectra of the pure drug and drug loaded microspheres were examined by using the potassium bromide disk (KBr) method with a Fourier transform infrared (FTIR) spectrometry in the range of 4000-400 cm-1.

3.4.2.3 Thermogravimetric analysis (TGA)

The thermal stability of each of the samples was evaluated using TGA analysis. These experiments were performed on a PerKinElmer Pyris Diamond TG/DTA machine under a nitrogen flow at a rate of 30 mL/min. Approximately 5 mg of samples were placed in the alumina pan, sealed and heated at 10°C/min from 25 to 500 ^{o}C.

3.4.3   Study of the drug behavior of the microspheres

3.4.3.1 Calibration curve of SV

The standard stock SV solution was prepared in 1% (v/v) EtOH. SV 5 mg was accurately weighed and dissolved with 1% (v/v) EtOH into 50 mL volumetric flask and adjusted to volume (100 ppm).

The stock SV solution was diluted to 3, 6, 9, 12, 15 and 18 ppm with 1% (v/v) EtOH in volumetric flask.

The absorbance of standard solution was determined by UV-Vis spectrophotometer at 238 nm. The 1% (v/v) EtOH was used as a reference solution. The absorbance and calibration curve of SV in 1% (v/v) EtOH was shown in appendix 1C

3.4.3.2 Calibration curve of SV in pH 1.2, 4.0 and 6.4

The standard stock SV solution was prepared in 1% (v/v) EtOH in pH 1.2, 4.0 and 6.4. SV 5 mg was accurately weighed and dissolved with 1% (v/v) EtOH into 50 mL volumetric flask and adjusted by various buffers to volume (100 ppm).

The stock SV solution was diluted to 3, 6, 9, 12, 15 and 18 ppm with three different buffers in volumetric flask.

The absorbance of standard solution was determined by UV-Vis Spectrophotometer at 238 nm. The 1% (v/v) EtOH was used as a reference solution. The absorbance and calibration curve of SV in 1% (v/v) EtOH was shown in appendix 2C-4C.

3.4.3.3 Determination of drug loading efficiency (%EE)

The dried SV immobilized onto modified microspheres (2 mg) were immersed in 10 mL of EtOH. The mixture was stirred at room temperature for 30

min.   The supernatant of solution was collected and determined by UV-Vis spectrophotometer at 238 nm.

The actual amount of drug loaded in micrpspheres was calculated from calibration curve of SV in 1% (v/v) EtOH.

The encapsulation efficiency of SV was calculated according to the following equation. All experiments were repeated for three times.

$$\textit{Drug encapsulation efficiency} \quad = \quad \frac{\textit{Actual drug content}}{\textit{Theoretical drug content}} \times 100$$

3.4.3.4 *In vitro* drug release

The SV release from modified microspheres were studied in three difference buffers by dialysis bag diffusion technique.   The accuarate weighted quantities of 10 mg of the spheres were enclosed in a dialysis bag with a molecular weight cut off of 3500 Da and immersed into 50 mL of the appropriate buffer in a flask.   The flask was placed in a shaken water bath at speed of 100 rounds per minutes and incubated $37 \pm 2°C$.

The 3 ml samples were withdrawn at specified time intervals (at 0, 5, 10, 15, 30, 45 minute 1, 2, 3, 4, 5, 6 , 7, 8 and 24 hours, respectively). An equal volume of fresh dissolution medium were placed to maintain the volume constant. The released SV were analyzed by UV-Vis spectrophotometer at 238 nm.

The amount of SV released was calculated by interpolation from a calibration curves containing increasing concentrations of SV. The percentages of cumulative SV release were calculated from this equation.

$$\textit{\% Cumulative release} \quad = \quad \frac{\textit{Amount of SV from release}}{\textit{A mount of SV before release}} \times 100$$

3.4.4 Statistical analysis

All measurement were performed in experiment. Results are presented as mean±SD. Statistical analysis was performed by one-way ANOVA using Microsoft Excel (Microsoft Corporation) with $P<0.05$ considered to indicate statical significance.

CHAPTER IV

RESULTS AND DISCUSSION

4.1   Synthesis of MA-CS and MBI-MA-CS

The firth step, the reaction of CS and MA to form *N*-carboxyethyl chitosan methyl ester (MA-CS) was carried out via micheal addition. The β-carbon in α,β-unsatured-carbonyl compound (MA) was attacked with the amino groups of CS (Sashiwa et al., 2003).The second step, the MBI was covalently reacted at the carboxylic group and methyl ester group of MA-CS via the formation of amide bonds (Fig. 1).
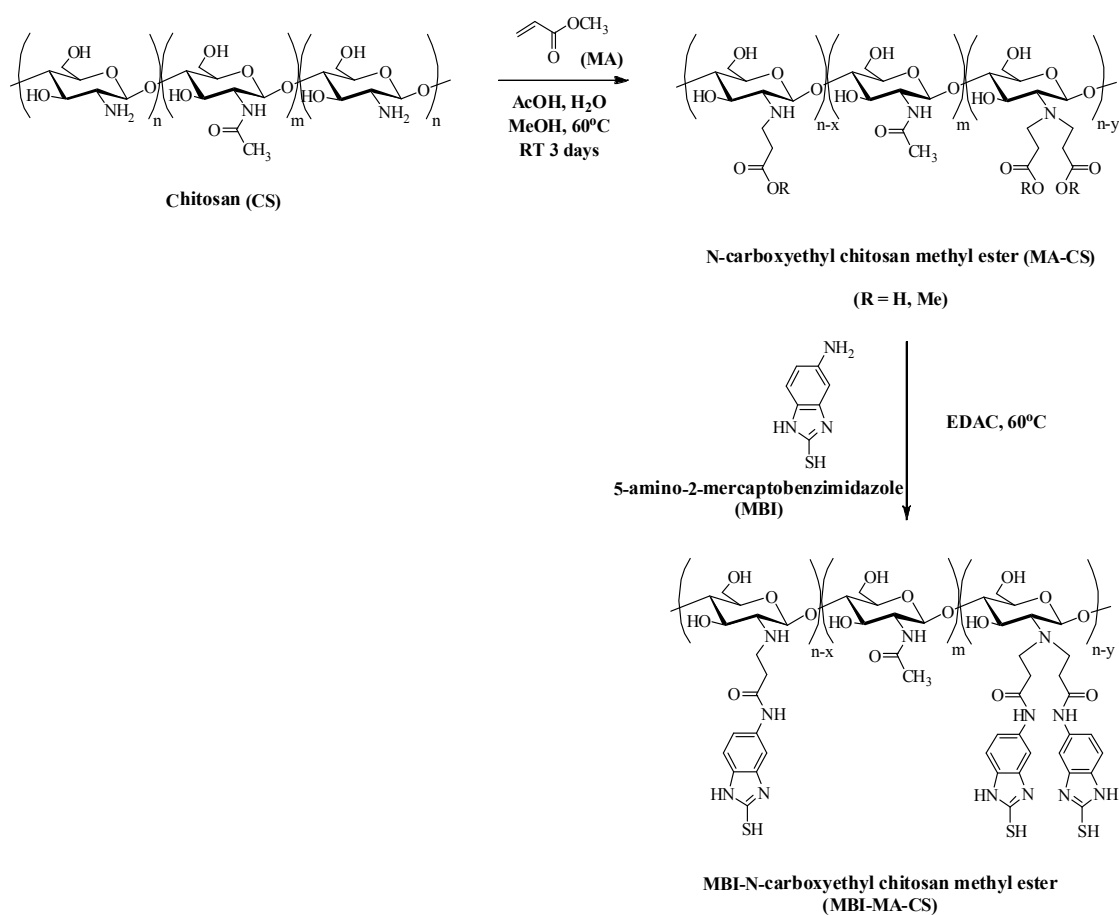
Scheme 1 Synthesis flowchart of *N*-carboxyethyl chitosan methyl ester (MA-CS) and MBI- carboxyethyl chitosan methyl ester (MBI-MA-CS).

4.2   Characterization and physical properties of chitosan and modification of chitosan

4.2.1   Fourier-Transform Infrared Spectroscopy (FT-IR)

The FTIR spectra of CS, MA-CS and MBI-MA-CS are shown in Figure. 2. The FTIR spectrum of CS (Figure. 2a) showed a broad absorption at 3446 cm^{-1} assighed to the stretching vibration of the O-H and N-H bonds. The absorption at 2928 and 2900 cm^{-1} is related to C-H streching. The characteristic CS peak that correspond to the amide C=O streching and the N-H bending (amide I band) were observed at 1645 and 1593 cm^{-1}, respectively. The absorption in the range 1146 to 840 cm^{-1} due to the polysaccharide skeleton, including the symmetric stretching of the glycosidic bonds, C-O-C and involved skeletal vibration of the C-O stretching. After coupling of the MA onto the C2-amine groups of chitosan, the characteristic signal at 1720 cm^{-1} (Figure. 2b), attributed to the stretching vibration of the C=O ester of MA-CS appeared and the peaks of N-H bending was shifted to 1562 cm^{-1} (amide II band). Moreover, the broad overlapping bands and the decreasing of intensity in the 1153 to 848 cm^{-1} range that result from the coupling of the C-N axial stretching and N-H angular deformation range. In addition, the MBI-MA-CS spectra (Figure. 2d) showed a new absorption peak at 1640 and 1615 cm^{-1} were attributed to the amide C=O stretching and secondary amine of MBI-MA-CS, respectively. The absorption band at 1468 cm^{-1} attributed to C=C stretching of aromatic. The peaks at 612 cm^{-1} correspond to the thiol group that confirmed to present of thiol group on MA-CS, indicated that the successful preparation of MA-CS and MBI-MA-CS coupling.
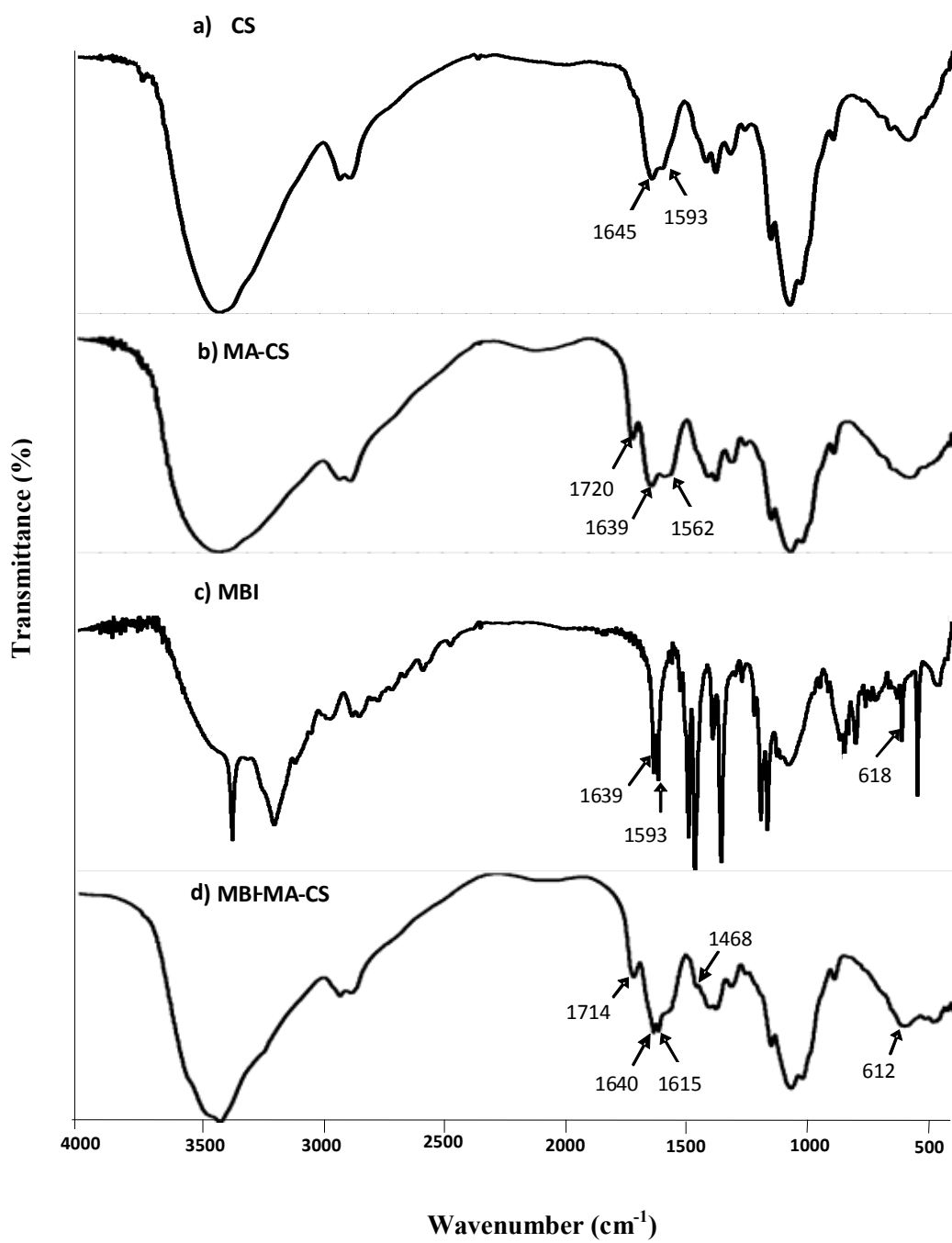
Figure 4.2 Representative FTIR spectra of (a) CS, (b) MA-CS, (c) MBI,

(d) MBI-MA-CS

4.2.2 Nuclear Magnetic Resonance (^{1}H⁻NMR)

The chemical structure of chitosan and modified chitosan (MA-CS and MBI-MA-CS) were characterized by ^{1}H NMR are shown in Figure. 3. The peaks at chemical shifts 4.39, 3.25–3.46, 2.71 and 1.61 ppm were ascribed to the H1(GluN), H3–H6, H2 (GluN) and acetyl (GluNAc) protons in the chitosan skeleton (Figure. 3a), respectively. The appearances of new proton positions from the side chain of MA were observed at 3.1 and 2.7 ppm are assigned to the H7 and H8, respectively (Figure. 3b) that the new proton positions appeared different position when compared to the peak of MA at chemical shifts 6.3(d), 6.1(t) and 5.9(d) ppm attributed to the proton of alkene. The spectra of MBI-MA-CS showed the proton of aromatic ring at chemical shifts between 7.1 and 7.5 ppm are assigned to the H10 and H11 (Figure. 3c) that were shifted from 6.3 and 6.7. (Fig.3d). The ^{1}H-NMR spectrums confirmed that MA-CS and MBI-MA-CS was successfully prepared.
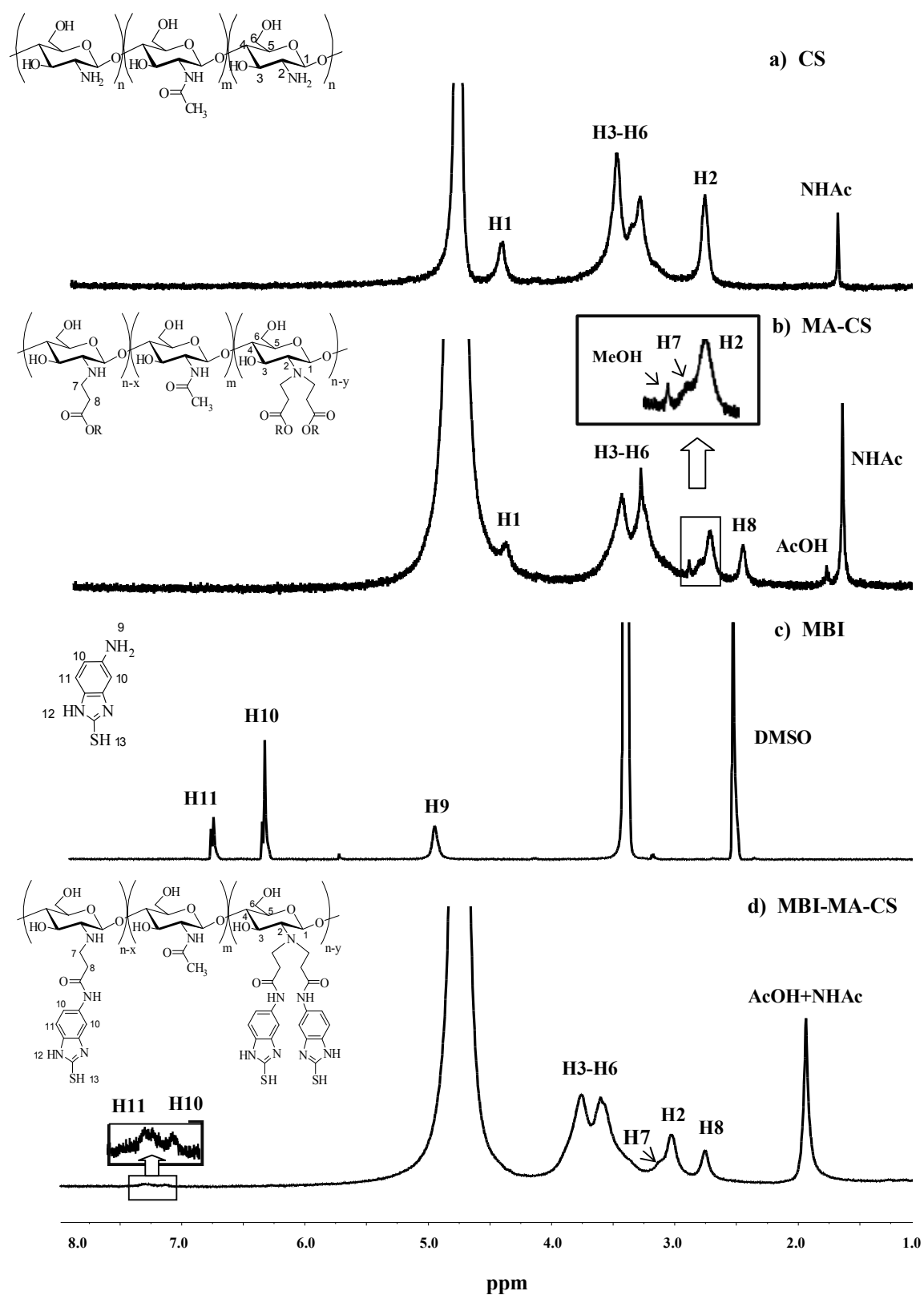
Figure 4.3 Representative ^{1}H NMR spectra of (a) CS, (b) MA-CS and

(c) MBI-MA-CS.

4.2.3 Thermogravimetric analysis (TGA)

The thermal stability and thermal behavior of chitosan and modified chitosan (MA-CS and MBI-MA-CS) were obtained by TGA. The TG and DTG curves of CS are shown in Fig. 4.4

The TG curve of CS showed two stages (Figure. 4.4a) of weight loss, the first being water loss and volatile products (6 % of the total weight) at 50 ^{o}C to 150 ^{o}C, the second stage in temperature range from 325 ^{o}C to 350 ^{o}C with the derivative thermogravimetric (DTG) peak at 326 ^{o}C and weight loss was 45% of the total weight was ascribed to the degradation of CS backbone. In contrast, the MA-CS and MBI-MA-CS showed to degrade at lower temperature than that of CS. For the first stage of MA-CS range between 50-180 ^{o}C (Figure. 4.4b) likely was due to the loss of water 10%, while the second, the thermal decomposition at 290 ^{o}C with 35 % weight loss.

The thermal decomposition of MBI-MA-CS showed two stage (Figure. 4.4c), the first from 50 ^{o}C - 170 ^{o}C being due to the evaporation of water (8% of total weight), followed by the more obvious weight loss (40 % total weight) at 308 ^{o}C that the thermal decomposition. The results was obtained from TGA curve demonstrate the loss of the thermal stability for MA-CS and MBI-MA-CS compare to CS that indicate a decrease of thermal stability by introduction of MA and MBI side chain on CS that change the crystalline structure of CS.
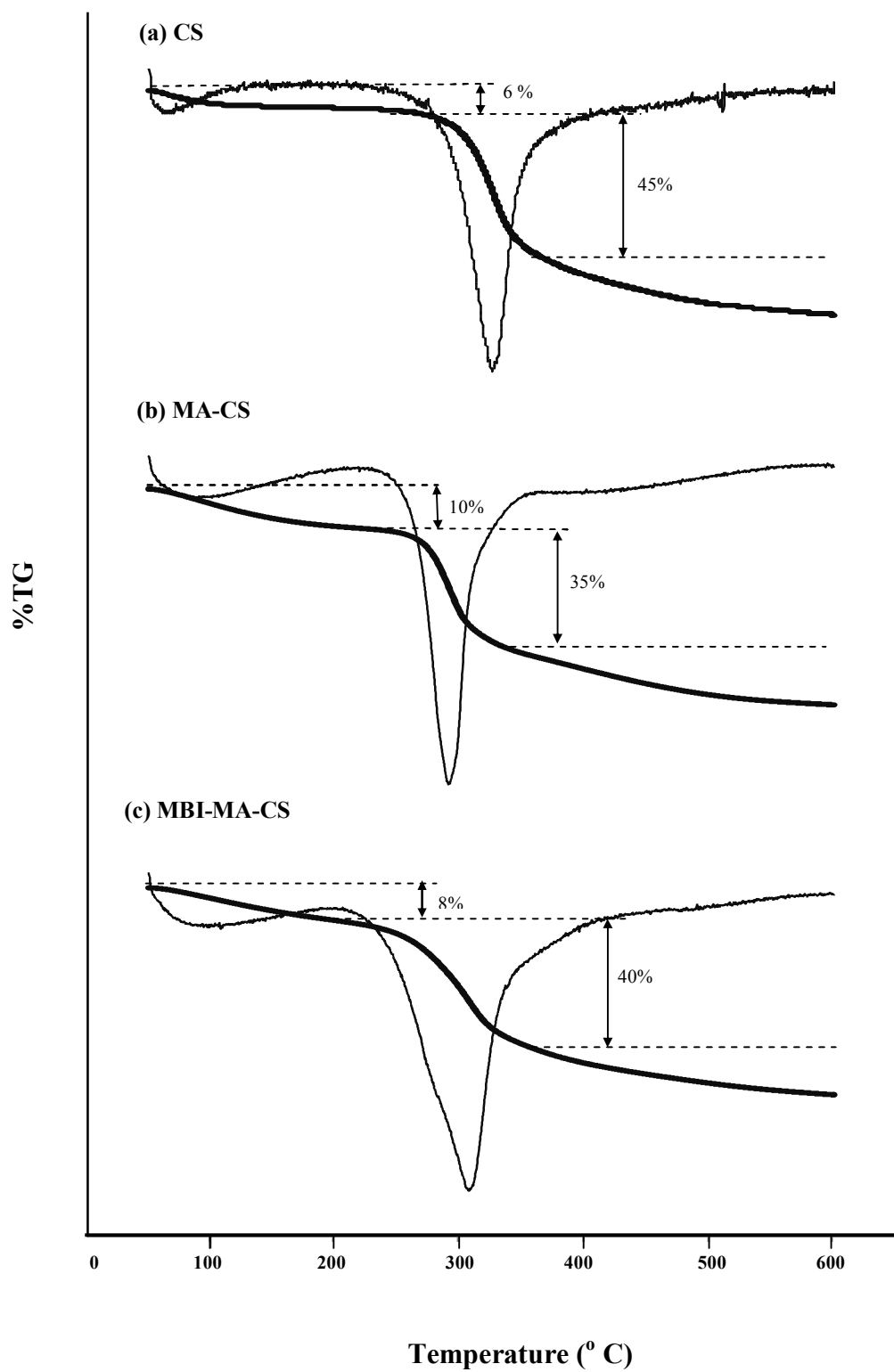
Figure 4.4 Representative TGA thermograms (TG curves) of (a) CS, (b) MA-CS and (C) MBI-MA-CS.

4.2.4 The substitution of MA on CS and quantification of the thiol level on MA-CS

The substitution of MA (COOH+COOMe) on CS was calculated from Eq. (1), was 14.38% (Table 4.1). Decreasing of MA was 12.64% after coupling of MBI on MA-CS.

The amount of free thiol group and disulfide bonds immobilized in the MA-CS derived polymers are summarized in Table 4.1. The MBI-MA-CS polymer derived from a 1:0.1 (w/w) ratio of MBI-MA-CS exhibited of free thiol groups of 11.86 µmol/g and the level of total disulfide groups about 6.54 µmol/g (Appendix A).

Table 4.1 Substitation of MA on MA-CS and the level of free thiol and disulfide groups

Batch	The substitution of MA (%) [COOH+COOMe]	Total thiol Groups (µmol/g) (±SD, n=3)	Total disulfide Groups (µmol/g) (±SD, n=3)
CS	-	-	-
MA-CS	14.38	-	-
MBI-MA-CS	12.64	11.86±0.01	6.54±0.02

4.3 Mucoadhesive properties

4.3.1 Assessment of the mucoadhesive behavior of CS and the modified CS (MA-CS and MBI-MA-CS) by mucus glycoprotein assay

The mechanism of mucoadhesion has been theoretically reported to be based on the six general components of electrostatic, wetting, adsorption, diffusion,

mechanical and fracture theories [30, 35]. Many methods have been employed to evaluate these interactions *in vitro* and *in vivo*.

In this study, porcine mucin type II was selected which is typically used in mucoadhesion assays due to its lower batch-to-batch variability and higher between assay reproducibility [11]. As a strong interaction exists between mucin and CS or its derivatives, mucin should be spontaneously adsorbed onto the surface of the CS or its derivatives.

Periodic acid: Schiff (PAS) colorimetric method was used to qualify mucin-conjugated polymer bioadhesived strength [42, 45] in the simulated gastrointestinal fluid in pH 1.2 (SGF), pH 4.0 and pH 6.4 (SIF) that a strong interaction exists between mucin and CS, modified CS (MA-CS, MBI-MA-CS). The mucin should be spontaneously adsorbed on the surface of the CS and modified CS. The mucoadhesive property of the chitosan and its derivatives was assessed by suspension of mucin in their aqueous solutions (in pH 1.2, 4.0 and 6.4) at room temperature. The linearity range for mucin at the wavelength of detection at 555 nm was obtained as 0.1-0.5 mg/mL. The linear equations obtained by least square method were y = 0.257x-0.021, y = 0.758x+0.020 and y = 1.266x+0.009 in pH 1.2, 4.0 and 6.4, respectively (Appendix B).

4.3.2 Adsorption of mucin on polymer

.   The amount of mucin that was adsorped onto the polymer depend on ionization of sialic acid of the mucus glycoprotein and polymer that is to say the value of p*Ka* and p*I* for sialic acid and mucin are 2.6 and ~3-5, respectively [32]. Therefore the different forms of the glycoprotein will be influenced by the pH value of the environment.

Table 4.2: Comparison of chitosan and modified chitosan to mucoadhesive property

Batch	Absorbed of mucin at pH 1.2 (mg) (±SD, n=3)	Absorbed of mucin at pH 4.0 (mg) (±SD, n=3)	Absorbed of mucin at pH 6.4 (mg) (±SD, n=3)
CS	0.07±0.01	0.33±0.01	0.33±001
MA-CS	0.72±0.01	0.93±0.01	0.40±0.01
MBI-MA-CS	0.77±0.01	0.97±0.02	0.66±0.02

At pH = 1.2, the resulting of the increment of mucoadhesiveness from CS to MA-CS about 10.28 times which is greater than that from CS to MBI-MA-CS with about 11 times (Table 4.2 and see Figure.4.5). The amino groups of CS backbone were protonated to NH_3^+ groups (pKa value of CS are 6.5-6.8) while the less ionization of sialic acid (COOH and SO_3H groups) on the mucin leading to reduce the potential interaction with CS. When the CS was coupled with MA, the aliphatic side chain of MA can further parcipitate hydrophobic interaction with CH_2/CH_3 of mucin side chain (Figure. 4.6). Moreover, the hydroxyl end group of side chain can form hydrogen bonding with –COOH, SO_3H of mucus glycoprotein leading to increase the mucoadhesiveness. For the MBI-MA-CS containing –SH group, it exhibited to stronger mucoadhesiveness than that of CS but showed non-significant increase in the mucin absorption level when compare to MA-CS. This is probably due to the steric effect of aromatic ring that hinder the interaction between the hydrogen bonding of –COOH/-COOCH$_3$ of MA and –COOH/SO$_3$H of mucin. Furthermore, –SH groups on MBI-MA-CS can react with –SH/S-S (cysteine and cystine) on mucin that formed disulfide via only oxidation reaction. The tendency of the increment of mucoadhesiveness is similar in that for pH 4.0. At this pH, the partial amino groups of CS were protonated (NH_3^+), the ionization of sialic acid

(COO- and SO⁻₃ groups) increased leading to the ionic interaction with CS. The results are also consistent with pH 1.2 that the mucoadhesiveness increased from CS to MA-CS about 2.81 times and from CS to MBI-MA-CS greater than about 2.94 times. Therefore, the effect of electrostatic, hydrogen and hydrophobic effects impact on the mucoadhesion of CS, MA-CS and MBI-MA-CS in lower pH range.

At pH 6.4, the amino groups of CS was deprotonated therefore, electrostatic interaction between between the positive charges of the CS backbone (NH^+_3) with either COO^- or SO^-_3 groups on the mucin decreased. Consideration the mucoadhesiveness of MA-CS, the resulting of the increment of mucoadhesiveness from CS to MA-CS about 1.25 times because of the hydrophobic effect, the –CH3 moieties and –CH2 side chain on polymer interact in part with the –CH3 groups on the mucin side chains. Furthermore, MBI-MA-CS found that a significant increase the mucin absorption level that from CS to MBI-MA-CS about 2.06 times. The reactive form of thiolate anions, -S⁻ (pKa ~2.6), this may have lead to a greater extent of the both of oxidation and nucleophilic attack. This can be explained by the formation of covalent disulfide bonds between the thiol group (-SH) on polymer and cysteine-rich (-SH) subdomains of the mucus glycoprotein (Figure. 4.6) [14]. The higher the amount of mucin was bound onto the polymer. Therefore, the effect of hydrogen, hydrophobic and covelent effects impact on the mucoadhesion of CS, MA-CS and MBI-MA-CS in higher pH range.
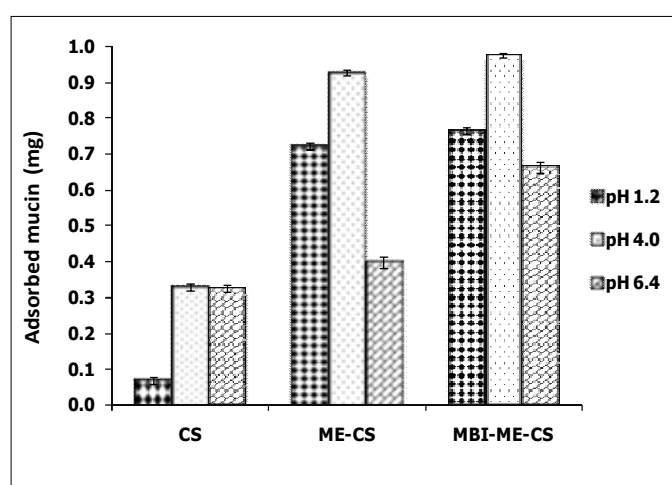
Figure.4.5 Adsorption of mucin on CS and modified CS at pH 1.2, 4.0 and 6.4.

Data are shown as the mean± SD and are derived from three independent repeats.

	CS	MA-CS	MBI-MA-CS
MUCIN			
POLYMER			
pH 1.2	0.07	0.72	0.77
pH 4.0	0.33	0.93	0.97
pH 6.4	0.32	0.40	0.66
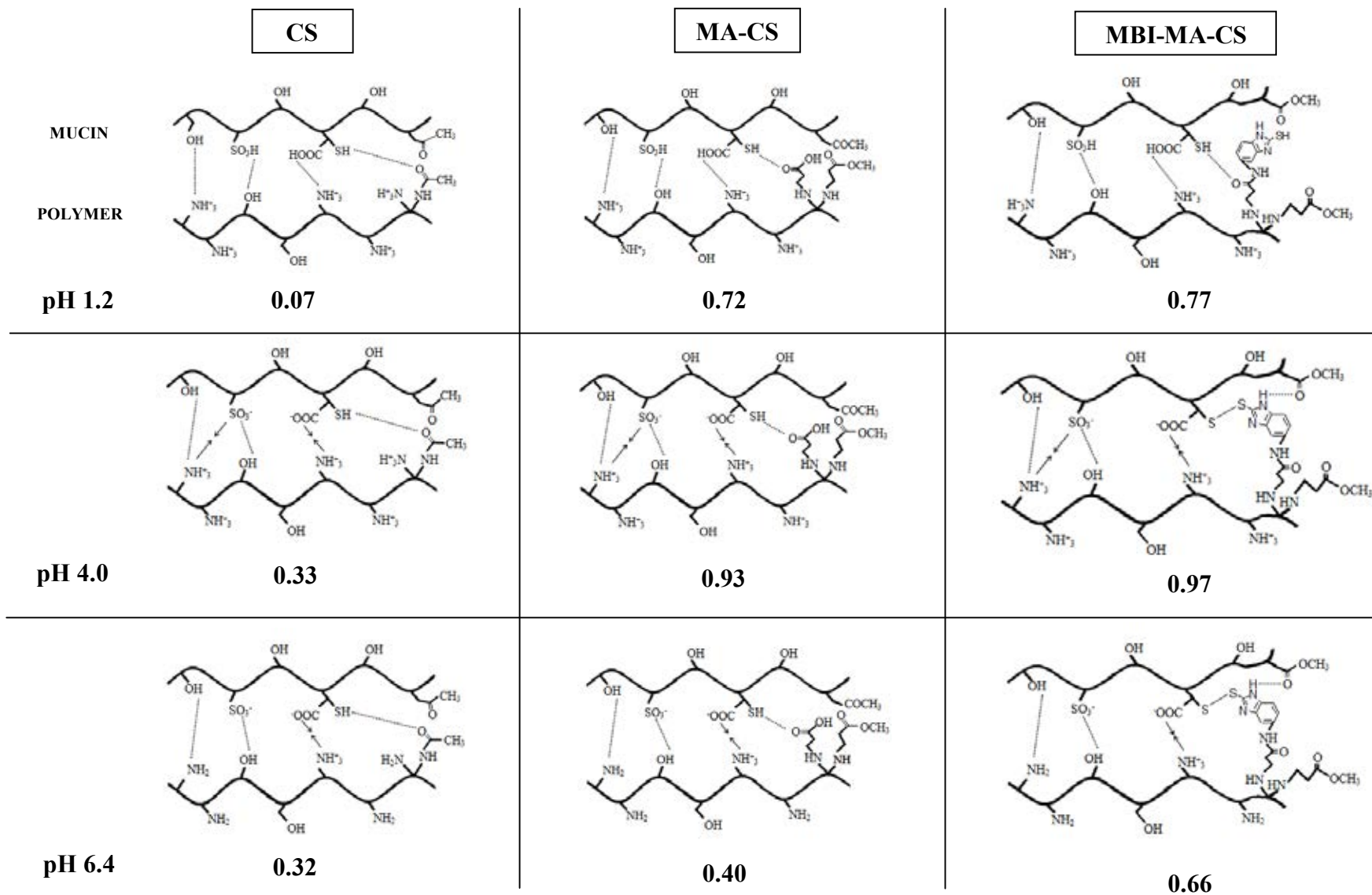
Figure.4.6 Representative mucoadhesive mechanism of the CS and modified CS

4.4 Swelling study

The swelling properties are of paramount importance to consider as it influences the adhesive cohesive properties as well the drug release. However, Most mucoadhesive delivery system are addressed to the small intestine where they reach the mucosal mumbrance in partially hydrated form. Excessive water uptake results in overhydration, loss of cohesive properties and leads to unsuccessful mucoadhesiveness. Therefore, a moderate swelling behavior is indispensable for adequate interdiffusion between polymers chains and mucosa representing the basis for sufficient adhesive [46].

The swelling can be affected by many factors, such as the cross-linking density and the hydrability of the materials, and the ionic strength and pH value of the media [47]. In general, the swelling behavior was measured in three broadly iso-osmotic buffer solutions (the gastrointestinal tract), being SGF (pH 1.2), 0.1 M acetate buffer (pH 4.0) and SIF (pH 6.4) and the swelling ratio was calculated using Eq. (2) as detailed in Section 3.3.5.

The results, as the variation in the swelling ratio with time. The CS, MA-CS and MBI-MA-CS polymers that showed essentially the same pattern (data not shown) are shown in Figure 4.7. As the pH value increased the degree of observed swelling decreased. Indition to, the MA-Chitosan and MBI-MA-Chitosan presenting a lower swelling ratio than that of chitosan in all three different pH media. This may be attributed to the fact that the attactment of MA and MBI on chitosan reduced the overall hydrophilicity, lead to a diminished water uptake compare to chitosan. The reduce swelling behavior as a consequence of the pronounced hydrophobic character of MA-chitosan and MBI-MA-chitosan. Moreover, this could be explained from the pH-dependent charge balance of MBI-MA-Chitosan, MA-Chitosan and chitosan, and so the degree of interaction between these three polymers is modified in accord with their charge balance that showed the mechanism of swelling in Figure 4.8.
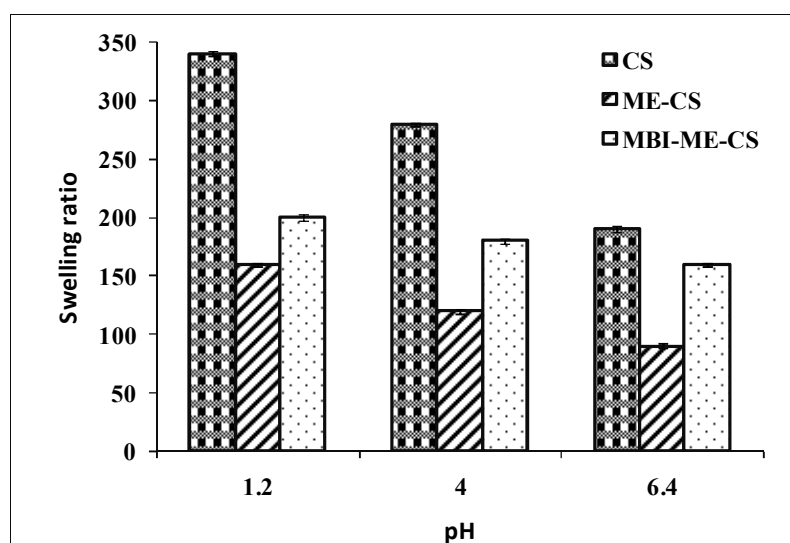
Figure 4.7 Swelling behavior of the CS, MA-CS and the thiolated CS derivatives (MBI-MA-CS). Data are shown at equilibrium (24 hr swelling time) as the mean±1 SD and are derived from three independent repeats.

In strongly acidic medium (pH 1.2), the high swelling behavior can be explained by amino group of chitosan protonated (NH_3^+) and hydrogen bonds were dissociated, inducing the network to become loose and leading to an increase degree of swelling. This cause repulsions in the polymer chains allowing more uptake of water to the polymer. At pH 4.0, the partial amino group of chitosan were protonated (NH_3^+), repulsion in the polymer chains reduced leading to decrease degree of swelling. For MA-Chitosan and MBI-MA-Chitosan polymers that showed essentially the same pattern in the both pH 1.2 and 4.0 are shown in figure 4.7. There is an overall decrease in swelling ratio due to MA-CS was contained of ester groups and carboxylic groups of MA side chain about 14% caused hydrogen bonding between polymer chain resulting that decreased its water absorption. In order to investigate of MBI on MA-Chitosan was more uptake water than MA-Chitosan at pH 4.0 due to, the thiolate groups become charged anionic, S-, which represents the reative oxidation form and thereby lead to electrostatic replustion between the polymer segments. Moreover, the investigate of aromatic thiolated leading to increased steric effect that prevented the intramolecular interations of the CS-NH_2 that increased of swelling when compare to MA-CS.

At a high pH (pH 6.4), amino groups of CS become to the almost complete deprotonization, repulsion in the polymer chains reduced allowing shinking. Furthermore leading to a re-association of the interchain hydrogen bonds and consequently to weaker interactions between the polymer chains and the aqueous media, inducing to decrease its water absorption. For MBI-MA-CS was more uptake water than MA-CS (Figture 4.7) due to the thiolate groups remain charged anionic, S-, which lead to electrostatic replustion between the polymer segments (Figure 4.8) that increased of swelling when compare to MA-CS but swelling decreased when compare to CS because the investigate of aromatic thiolated of MBI-MA-CS caused steric effect that prevented the intramolecular interations of the CS-NH_2. However, the polymers have only a relatively low density of thiol groups compared to that for the amine groups, and so the affects of the amino group are dominant.
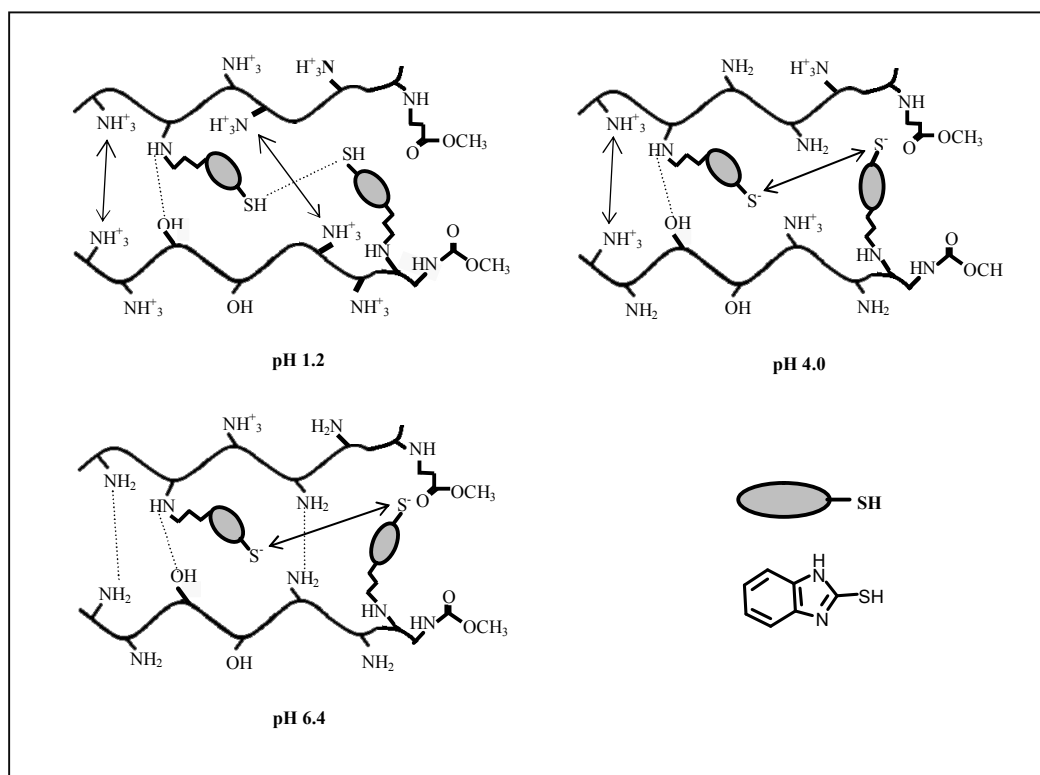
Figure 4.8 Representative swelling mechanism of the MBI-MA-CS in pH 1.2, 4.0 and 6.4

4.5 Morphology

The CS, MA-CS and MBI-MA-CS used in pharmaceutical dosage forms, particularly as a vehicle for controlled drug delivery.

The particles generated by applying a high electric field to the polymer solution until it able to overcome the surface tension of the stream to give continuous stream (drop) and drops into collected beaker containing 5% tripolyphosphate (TPP) as coagulant used to prepare of microparticles by the electrostatic interaction between chitosan and the tripolyphosphate (TPP) polyanion [48].

The microparticle obtained by electrospraying can be controlled by adjusting the operation parameters. In this work, the high voltage power supply was used at about 21 kV that electrostatic repulsions at the liquid level on the Taylor cone so that the droplets became smaller [49].

Next, With this applied voltage, the working distance was increased to higher than 8 cm, leading to increase the travel time from the tip of the needle to the coagulant, therefore, the strength of electrical charge at the droplets will be lost, consequently, increasing in the particle size. Whereas, when decreased the distance lower than 8 cm, the strength of the electric field is increased, but the particle size is larger, because a small distance can impair full solvent evaporation and consequently, wet microspheres impact the collector, leading to collapsing, coalescence and broad size distributions [50]. Therefore, in this work, the distance was selected at 8 cm.

The flow rate, the injection with decreased flow rate leading to reduce the size due to i) The collecting of charge increased on solution and then applied voltage resulting that electrostatic repulsions until the droplets became smaller ii) the evaporation of solvent completed, which is not possible with high flow rates. The effect of gauge has little effect on morphology or size of particles. A smaller gauge (26 G) can produce a narrower size distribution [51].

Therefore, The preliminary studies of electrospray parameters as follows: high voltage power supply at 21 kV, working distance of 8 cm, flow rate, 0.5 ml/h and needle gauge 26 G. The results from studies of CS, MA-CS and MBI-MA-CS microparticles fabrication by the electrospraying technique showed that the successfully prepared.

4.5.1. CS and modified CS (MA-CS and MBI-MA-CS)

The SEM micrographs of CS, MA-CS and MBI-MA-CS microspheres were shown in Figure 4.9.

(1a)

(1b)

(2a)

(2b)

(3a)

(3b)
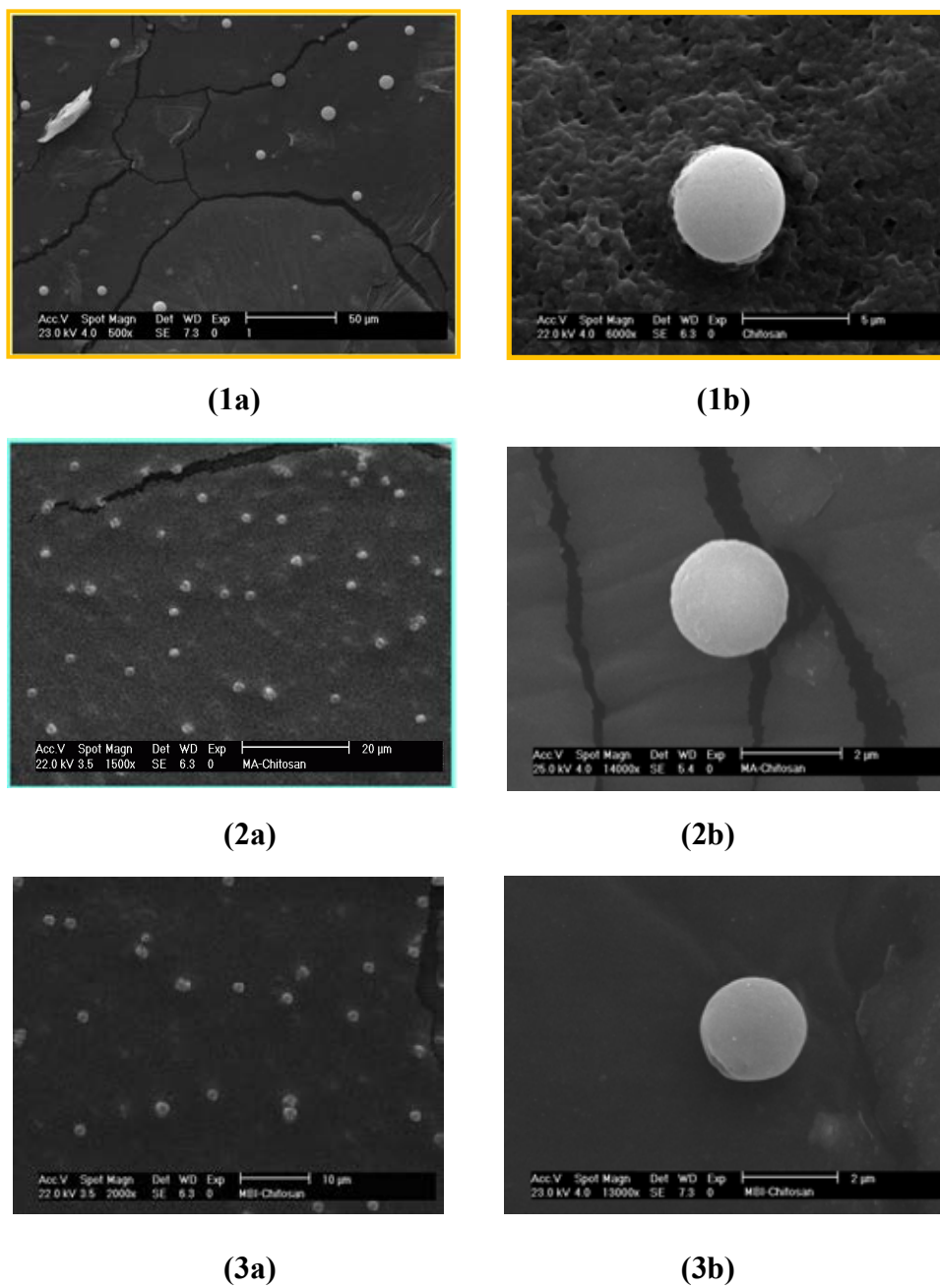
Figure 4.9 Representative SEM images of CS (1a-b), MA-CS (2a-b) and MBI-MA-CS (3a-b) without SV**.**

The surface morphological appearance of CS microspheres was compared with the modified CS (MA-CS and MBI-MA-CS) microspheres that without simvastatin, both of the CS and modified CS microsphere were in a generic spherical shape. Smoothness on the surface could be clearly seen at high magnification and without visible pores. This may be attributed to the fact that modified chitosan successfully fabricated to spherical shapes.

4.5.2. CS and modified CS (MA-CS and MBI-MA-CS) with SV encapsulation

Figure 4.10 showed the morphology of the SV-loaded CS, MA-CS and MBI-MA-CS particles were of an acceptable spherical shape, although slightly flattened, and were smooth surfaced without visible pores.
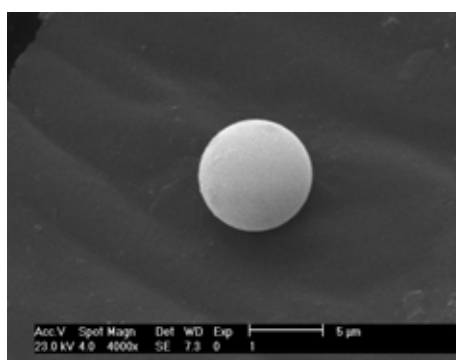
(1a)
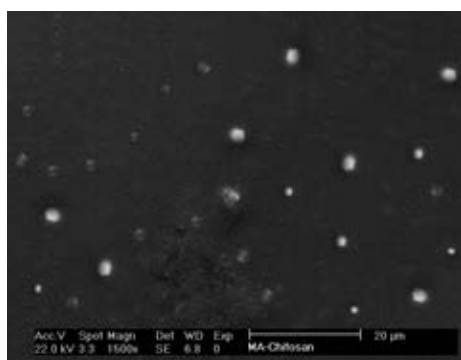
(2a)
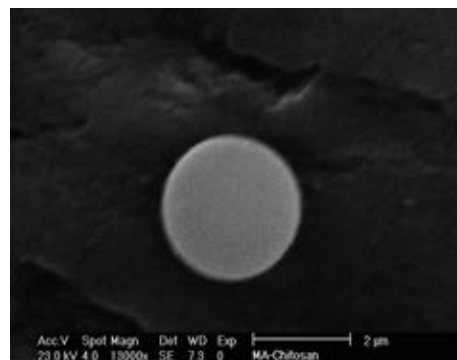
(2b)
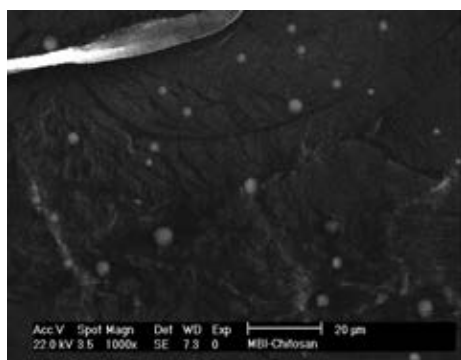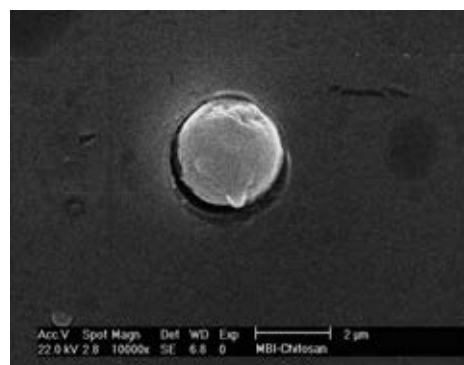
(3a)   (3b)
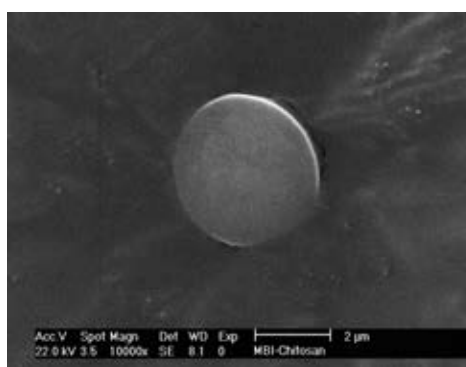
(4a)

Figure 4.10 Representative SEM images of CS (a), MA-CS (2a-b), MBI-MA-CS (3a-b) with 1%SV and MBI-MA-CS (4a) with 4%SV.

4.5.3 Particle size, size distribution

Size distribution and particle size of microspheres (CS, MA-CS and MBI-MA-CS) with and without SV loading were presented in Table 4.3

The size of dried particles measured by SEM showed that CS, MA-CS and MBI-MA-CS without SV were approximately 4.5, 2.0 and 1.7 μm, respectively. After 1%SV loaed into CS, MA-CS and MBI-MA-CS, the particle sizes are larger were approximately 5.4, 2.8 and 2.6 μm, respectively. While, the particle size of MBI-MA-CS with 4%SV loading was of 3.3 μm was larger than that of with 1% loaded SV and without SV, indicating that the particles could encap more drug.

When considering the size paricles and size distribution of the swollen particles measured by particle size analyzer found that CS and modified CS (MA-CS and MBI-MA-CS) without SV particles size was approximately 4.65, 2.3 and 1.98 μm, respectively with PDI approximately 0.73, 0.45 and 0.39, respectively. PDI was used to measure for the width of the particle size distribution (from 0 = monodisperse to 1 = polydisperse).

In case of the size distributions of CS and modified CS (MA-CS and MBI-MA-CS) with SV microspheres showed that they were in the range approximately from 3.53-5.62 μm with PDI from about 0.49 to 0.75. In addition, when SV was loaded onto polymer it results in increasing the mean particle size and size distribution of spheres. Furthermore, The dried and swollen particle sizes were not significantly different, the result of the swollen particle (before and after SV loading) corresponding to particle size was measured by SEM.

4.5.4 Zeta potential (Zp)

Zeta potential measurements will give information about the overall surface charge of the particles and how this is affected by changes in the environment (e.g. pH, presence of counter-ions, adsorption) [51]. When considering the zeta potential, that is surface charge, it can greatly influence particle stability in suspension through the electrostatic repulsion between particles.

The surface of CS microparticles was found to possess negative charge of -15.12 mV and -18.38 for MA-CS because of effect of TPP. The surface negative charge of MBI-MA-CS were increased -21.45 mV (Table 4.3) due to S- anion on surface and effect of TPP.

Zeta potential values are also of interest for the characterization of the microspheres since SV-loaded microspheress display Zp values -13.30, -14.51 and -18.15 mV (1%SV-CS, 1%SV-MA-CS and 1%SV-MBI-MA-CS, respectively) as seen in Table 4.3. Zeta potential data suggest the potential physical stability of microspheres in aqueous dispersion state and confirm the presence of SV on microspheres surface.

Table 4.3 Effect of compositions on morphology of the microsphere**s**

Abbreviations	Shape	Particle size[1] ± SD (µm)	Particle size[2] ± SD (µm)	Zetapotential (mV)	Polydispersity Index (PDI)
Without SV					
CS	Spherical	4.5±0.05	4.65±0.09	-15.12±1.20	0.73±0.10
MA-CS	Spherical	2.0±0.15	2.30±0.15	-18.38±0.87	0.45±0.15
MBI-MA-CS	Spherical	1.7±0.08	1.94±0.13	-21.45±0.68	0.39±0.01
With SV					
1%SV-CS	Spherical	5.4±0.05	5.62±0.08	-13.30±1.33	0.75±0.05
1% SV-MA-CS	Spherical	2.8±0.15	3.12±0.15	-14.51±0.10	0.53±0.05
1% SV-MBI-MA-CS	Spherical	2.6±0.12	2.81±0.20	-18.15±1.43	0.49±0.15
4%SV-MBI-MA-CS	Spherical	3.3±0.05	3.53±0.05	-16.08±0.97	0.67±0.02

[1]Particle size measured by SEM

[2]Particle size measured by particle size analyzer
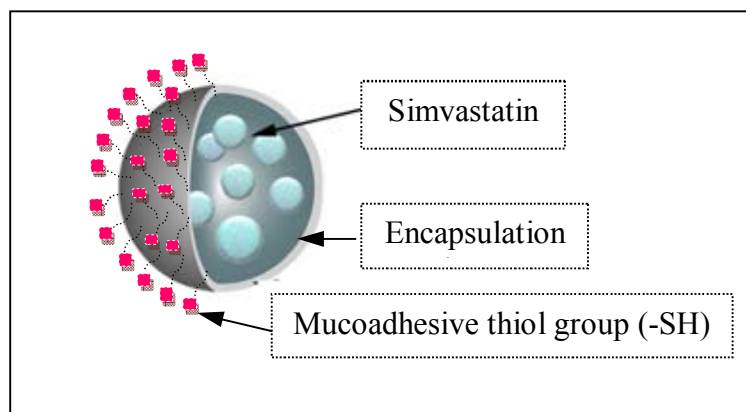
Figure 4.11 Schematic microstructure of SV-loaded CS, MA-CS and MBI-MA-CS microsphere

The microstructure of SV-CSSV-MA-CS and SV-MBI-MA-CS microspheres were speculated as Figure 4.11 to explained the encapsulated SV of polymers. It could be understood by associating the polymer solidification process with the SV loading process. With the soldification process proceeded, the SV was hindered because the structure of microspheres became compact due to the matrix formation between TPP and CS.

Mucoadhesiveness of microspheres

Mucoadhesiveness of microspheres was measured as a way to test their ability to bind to the mucosal surface of the body (mucoadhesiveness). The results of *in vitro* mucoadhesive of the spheres with mucin in three different buffers (pH 1.2, 4.0, and 6.4) are shown in Table 4.4 by PAS method**.**

Table 4.4 Mucoadhesive property of the CS and modified CS microspheres with SV

Abbreviation	Adsorbed of mucin at pH 1.2 (mg) ($\pm$SD, *n*=3)	Adsorbed of mucin at pH 4.0 (mg) ($\pm$SD, *n*=3)	Adsorbed of mucin at pH 6.4 (mg) ($\pm$SD, *n*=3)
SV-CS	0.06±0.01	0.29±0.01	0.27±0.01
SV-MA-CS	0.42±0.01	0.68±0.01	0.29±0.02
SV-MBI-MA-CS	0.44±0.01	0.73±0.01	0.35±0.02

At the low pH (SGF, pH 1.2), the mucoadhesive of the MA-CS and MBI-MA-CS with SV loading exhibited excellent mucoadhesiveness with 7- and 7.33-fold higher than that of the native chitosan. Moreover the MA-CS and MBI-MA-CS loaded SV stronger mucoadhesive property compared to that of the unmodified CS at pH 4.0 and 6.4. At pH 4.0, the SV-MA-CS and SV-MBI-MA-CS microspheres showed mucoadhesiveness about 2.34- and 2.51- fold. For at the pH 6.4, the SV-MA-CS and SV-MBI-MA-CS microspheres showed approximately 1.07- and 1.29- fold, respectively. When considering the mucoadhesiveness of CS and modified CS microspheres displayed a fold strongmucoadhesive property. From these results indicated that the electrostatic effects, indicating that after the CS and modified CS formed polyelectrolyte complex with TPP, the carboxylate groups of TPP were interacted with protonated amino groups of chitosan throught electrostatic interaction, which is likely to be due to the fact that the influence of the positive charge of CS was not enough to increase the mucoadhesion.

4.6 Characterization of microsphere

4.6.1 Fourier transform infrared spectroscopy (FTIR)

FTIR spectroscopy was used to determine the chemical interaction between the drug and the CS and modified CS in the micropheres, samples of 1%SV-CS, 1%SV-MA-CS and 1%SV-MBI-MA-CS were investigated and displayed in Figure 4.12.

The FTIR spectrum of SV (Figure. 4.12a) as can be seen, the -OH stretching absorption band at 3547 cm^{-1}. The absorption band at 3012, 2952, and 2872 cm^{-1} were attributed to the C-H stretching vibrations. The main characteristic peaks of SV at 1721 and 1695 cm^{-1} were due to the stretching bands of ester and lactone carbonyl group. The C-H in-plane bending vibration and skeletal C-C vibrations are observed in the region 1350-950 cm^{-1}. The C-H out-of plane bending modes are usually of weak intensity arises in the region 600-900 cm^{-1}[50].

The FTIR spectrum of 1%SV-CS microspheres are shown in Figure. 4.12b, there were additional absorption peaks at 1711 cm^{-1} corresponding to the ester stretching peaks of SV. The peak at 1225 cm^{-1} was due to the C-H in-plane bending vibration. The peak at 894, 795 and 664 a cm^{-1} correspond to C-H in-plane bending vibrations of SV. These SV characteristic peaks were shifted in the formulations suggesting definite interactions between SV and CS.

For the 1%SV-MA-CS microspheres (Figure. 4.12c), also showed the peak at 1715 cm^{-1} as C=O ester stretching. There were additional absorption peaks at at 2960 cm^{-1} and 2963 cm^{-1} were due to C-H stretching vibrations of SV.

The FTIR spectra of 1%SV-MBI-MA-CS microspheres are shown in Figure 4.12d. As can be seen, the characteristic peak at 2923 cm^{-1} and 1709 cm^{-1} corresponding to the C-H stretching vibrations and ester stretching peaks of SV, respectively. The other peaks of 1%SV-MBI-MA-CS and 1%SV-MA-CS have nearly additional absorption in the position of SV and 1%SV-CS.

When considering SV loaded on CS and modified CS, it was observed that the IR spectra of them have the nearly in the position of the characteristic peak of SV but maybe shifed wave number from pure SV because of effect TPP, The FTIR

spectrum appeared can be confirming the successful loading of SV on CS and modified CS (MBI-MA-CS)microparticle.
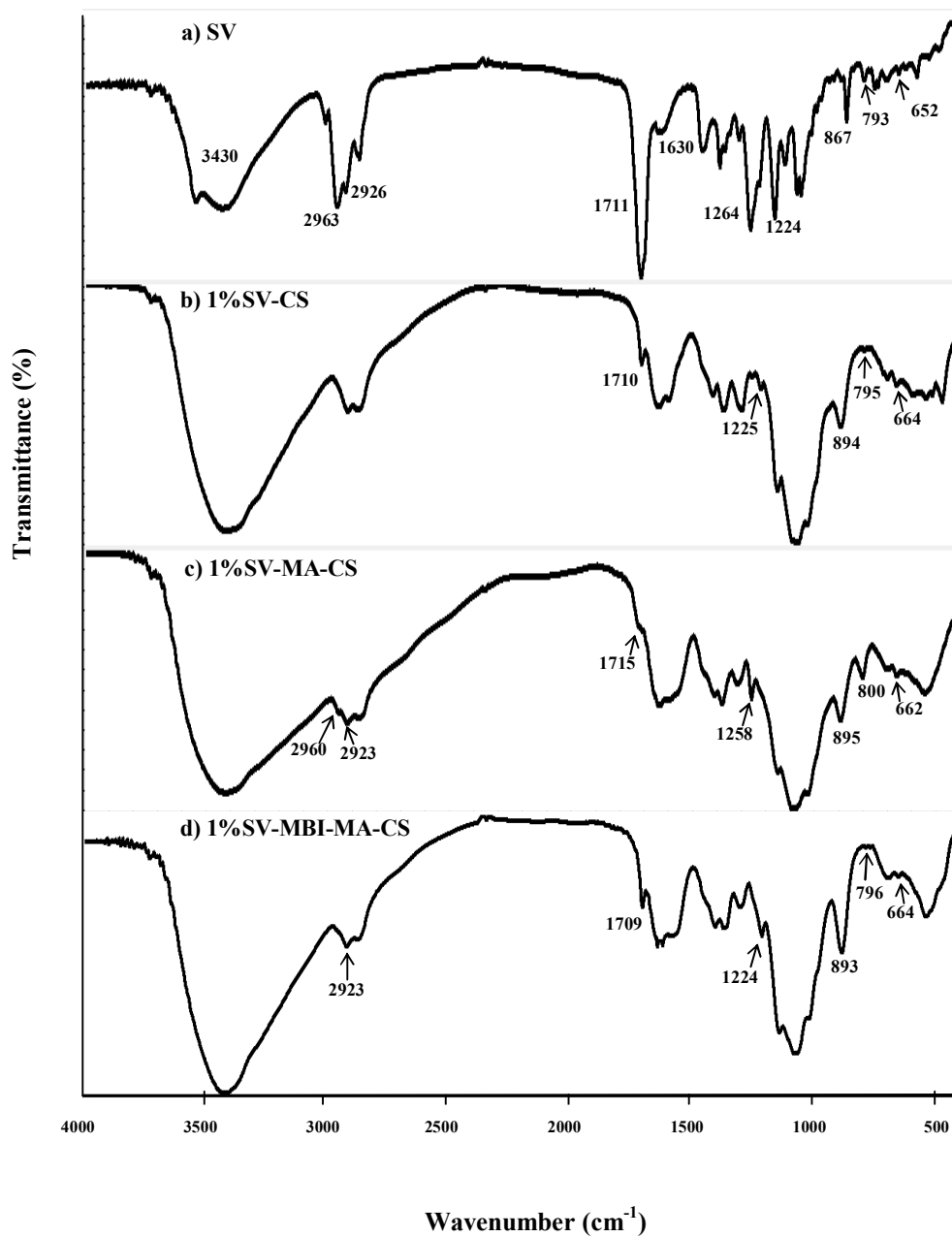
Figure 4.12 FTIR spectra of (a) SV, (b) 1%SV-CS, (c) 1%SV-MA-CS and (d) 1%SV-MBI-MA-CS microspheres.

4.6.2 Thermogravimetric analysis (TGA)

Thermagravimetric analysis (TGA) is a useful technology to characterize the thermal behavior of materials, which is correlated to their structure, and can further the presence of interaction between chitosan and SV. The TGA thermograms of the the CS and modified CS (MA-CS and MBI-MA-CS) microparticles with SV loading were shown in Figure 4.13.

The TGA thermograms for SV loaded CS (Figure. 4.13b) showed the second stages of weight loss. The first decomposition peak, due to water evaporation, was followed by a two-stage, chitosan decomposition occurred in temperature range from 325 ^{o}C to 350 ^{o}C with the derivative thermogravimetric (DTG) peak at 329 ^{o}C (20% of total weight). Furthermore, the DTG peak of SV-CS increased when compared with pure CS. This might be attributed to SV was entrapped by CS.

The thermal decomposition for the SV loaded MA-CS are shown in Figure. 4.13c. The first from 50 ^{o}C - 150 ^{o}C being due to the evaporation of water (5% of total weight). Afterwards, the degradation of MA-CS showed the thermal decomposition at 309 ^{o}C with 25% weight loss. For the TGA curve of SV loaded MBI-MA-CS show the combination of MBI-MA-CS and SV in second stages (Figure. 4.13d). The thermogram was shown a first from 50-150 ^{o}C due to the loss of water. The second stage showed the thermal decomposition (DTG) at 315 ^{o}C corresponding to the degradation of MBI-MA-CS with 35% weight loss. A suggest that the shift of the last decomposition temperature of the SV-MBI-MA-CS to a higher value, compared to that seen with MBI-MA-CS, which the result of inter- and intra-molecular disulfide interactions.

The results were obtained from TGA curve of SV loaded CS, MA-CS and MBI-MA-CS showed a higher polymer thermal stability. It is well established that intramolecular interactions increase the thermal stability of polymers, and so leads to a higher decomposition temperature.
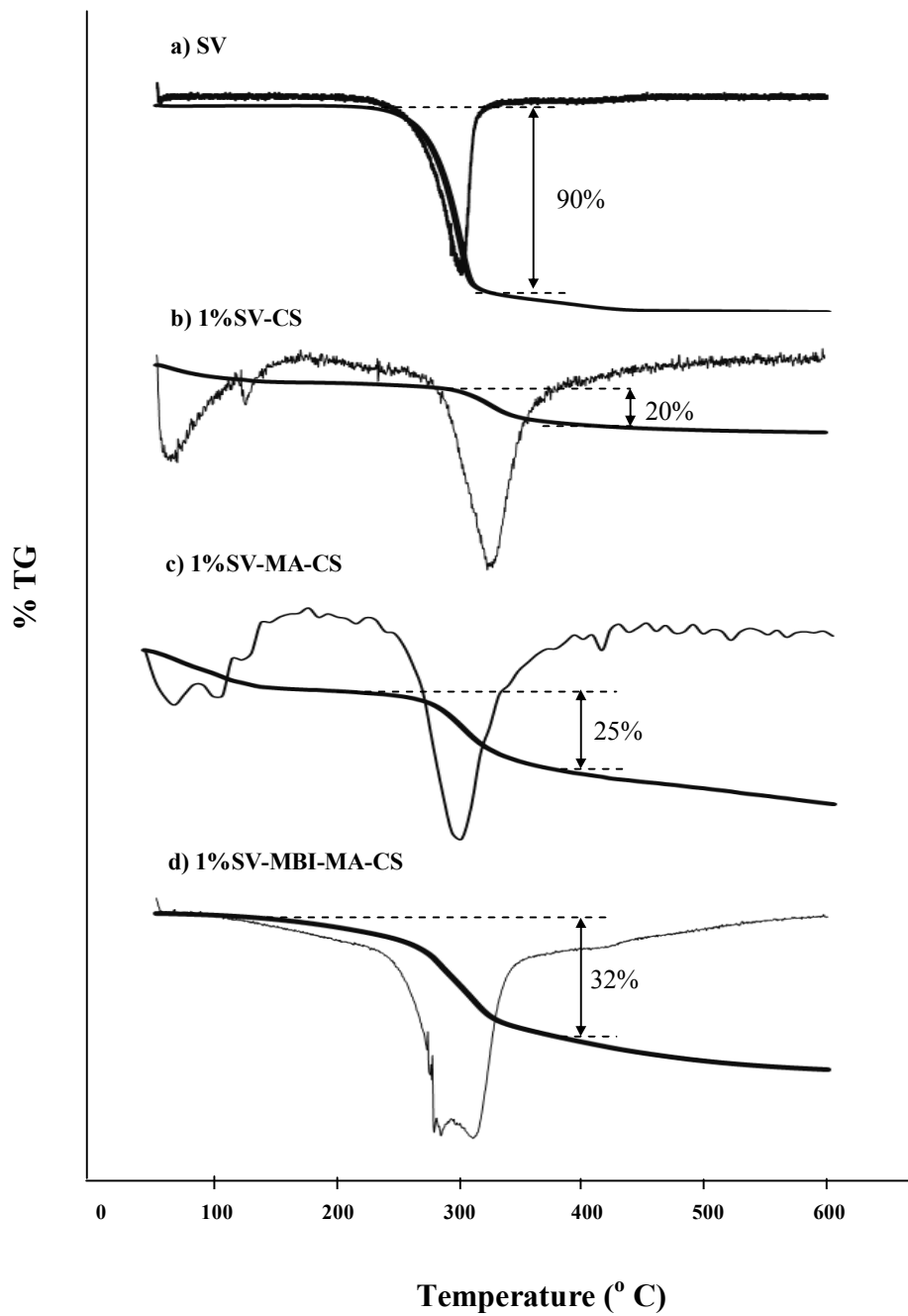
Figure 4.13 TGA thermogram of (a) SV, (b) 1% SV-CS, (c) 1% SV-MA-CS microspheres and (d) 1% SV-MBI-MA-CS microspheres

4.7. Evaluation of drug encapsulation efficiency (%EE)

The percentages of encapsulation efficiency (%EE) of the SV loaded CS, MA-CS and MBI-MA-CS microspheres were given in Table 4.3 that were analyzed using UV/Vis spectroscopy at λ_{max} = 238 nm, with the linear regression equations obtained by the least square method being $y = 0.055x - 0.017$, for the assay in ethanol (Appendix 1C).

In this work, the amount of SV, which is loading on encapsulation efficiency was investigated to achieve the high percentage of encapsulation efficiency. The 1%SV loaded CS, MA-CS and MBI-MA-CS were 53.0%, 70.9% and 64.83% encapsulation efficiency, respectively. The drug entrapment increased for modified CS. This result showed that the compatibility between SV and modified CS were increased. Moreover the increasing of SV loaded MBI-MA-CS from 1% to 2% and 4% found that the increased encapsulation efficiency were 70.45% and 82.10%, respectively. (Table 4.5)

This result explained that the electrospray technique can produce high percentage encapsulation at about 80%.

Table 4.5 Encapsulation of SV loaded polymer microspheres*

Formulations	% Encapsulation
1%SV-CS	53.0±0.03
1%SV-MA-CS	70.90±0.01
1%SV-MBI-MA-CS	64.83±0.01
2%SV-MBI-MA-CS	70.25±0.02
4% SV-MBI-MA-CS	82.10±0.01

* mean ± SD (n=3)

4.8. *In vitro* **SV release profiles**

The release of SV drug from CS and modified CS microspheres were performed at a function of time intervals in buffers pH 1.2, 4.0, and 6.4 (SGF, vaginal fluids, and SIF, respectively) at 37±1°C. The linear equations of SV calibration curve obtained by the least square method being $y = 0.053x – 0.029$, $y = 0.045x – 0.016$ and $y = 0.057x – 0.022$, for the assay in pH 1.2, 4.0 and 6.4, respectively (Appendix 2C-4C) (Figure 4.14-4.17).
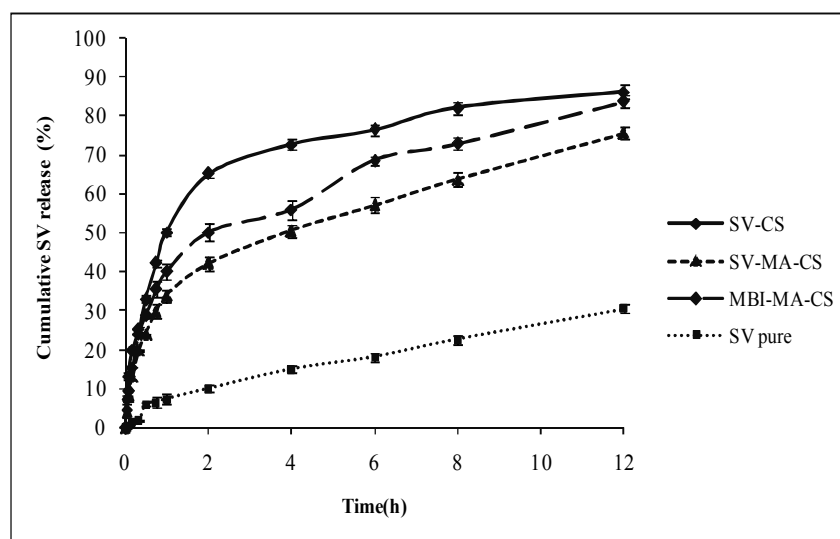
Figure 4.14 Release profiles of 1% simvastatin (from CS, MA-CS and MBI-MA-CS in pH 1.2, 37°C (average± SD, *n*=3).

Figure 4.14-4.16 showed the releasing profiles of SV in three different buffers (pH 1.2. 4.0, and 6.4) from CS and modified CS particles.

The release profiles of the 1%SV loaded CS and modified CS shows the initial burst release in the early stage. The burst release (1 h) was due to the presence of more free drug on the particle surface. The cumulative drug release percentage are approximately 86%, 75% and 83% within hours for CS, MA-CS and MBI-MA-CS in pH 1.2 respectively. The tendency of the cumulative drug release profiles is similar in those for pH 4.0. At the pH 4.0 (Figture 4.15), the cumulative drug release percentages of CS, MA-CS and MBI-MA-CS were about 82%, 62% and 73%,

respectively. Moreover, the release behavior in pH 6.4 (Figure 4.16) was significantly lower than that in pH 1.2 and 4.0. Most of SV released from the spheres in the first 12 h.

Considering the cumulative drug release percentages of MBI-MA-CS were more than those from of MA-CS in all pH medium.indicating that MBI-MA-CS is suitable for sustained released of SV than pure SV and SV loading SV.

The results were due to effect of the swelling of polymer. When considering the cumulative drug release, the MA-CS and MBI-MA-CS microspheres could prolonged release of SV for the all three tested pH within the first 4 hr up to about 40% and SV was still sustained release within 12 h due to the low swelling behavior of polymer in pH 1.2, 4.0 and 6.4 for the both MA-CS and MBI-MA-CS.
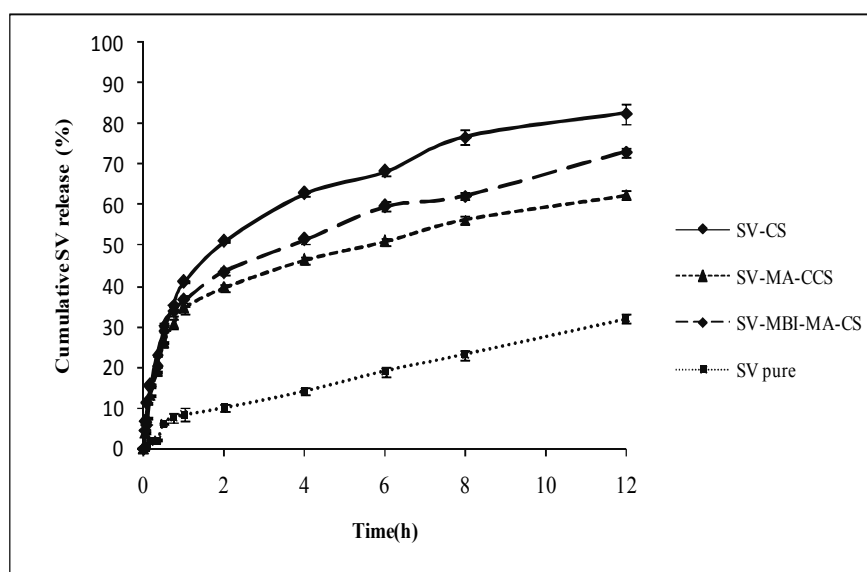
Figure 4.15 Release profiles of simvastatin (1% SV from CS, MA-CS and MBI-MA-CS in pH 4.0, 37°C (average± SD, n=3)
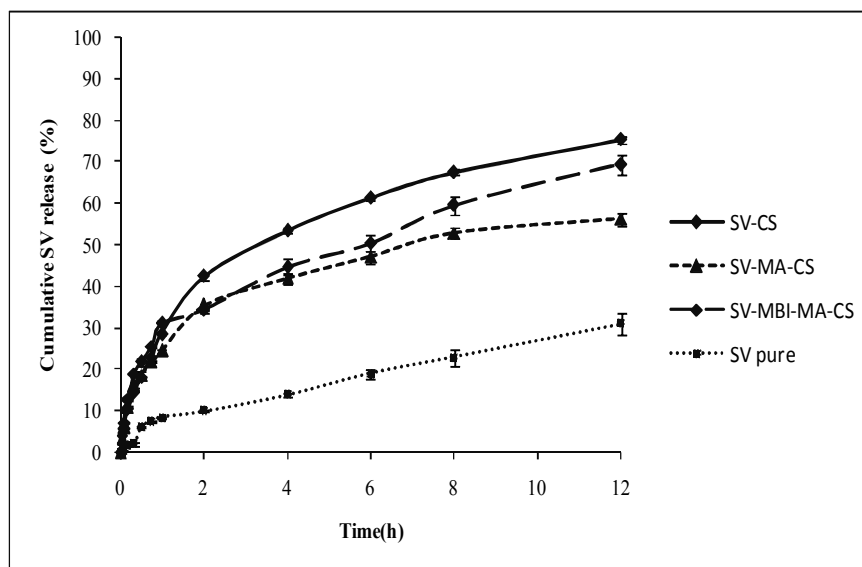
Figure 4.16 Release profiles of simvastatin (1% SV from CS, MA-CS and MBI-MA-CS in pH 6.4, 37°C (average± SD, *n*=3).

As a function of pH, presents the releasing profiles of SV from MBI-MA-CS in three different buffers (pH 1.2. 4.0, and 6.4) were shown on Figure 4.17.
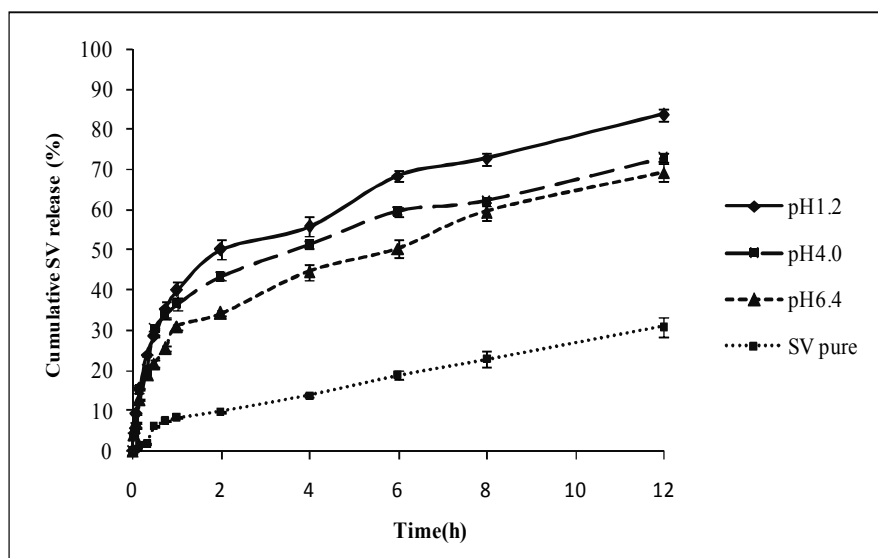
Figure 4.17 Release profiles of simvastatin (SV) from MBI-MA-CS in three different buffers, 37°C (average± SD, n=3)

Regarding the formulation containing thiol group (MBI-MA-chitosan), the results indicated that, after 6 h, 63% of SV (Fig. 4.17) was released from polymer matrices. The presence of thiol moieties led to the formation disulfide bonds within the matrix microspheres. This cross-linking process might provide a tightened three-dimensional polymeric network leading to a more controlled drug release and improved the swelling behavior which is advantage for the diffusion of drug molecules. Additionally, their drug release is reponsible for the swelling ratio of the microsphere with changing pH of the medium (4.0 and 6.4) found that the cumulative SV release shows results in pH 1.2 > pH 4.0 > pH 6.4 (Fig. 7b). This results indicated that the higher swelling ratios of the polymer create larger surface areas to diffuse the drug.

The vitro release profiles of 1% and 4% SV load MBI-MA-CS microspheres were investigated in pH 1.2 for 12 h (Figure 4.18).
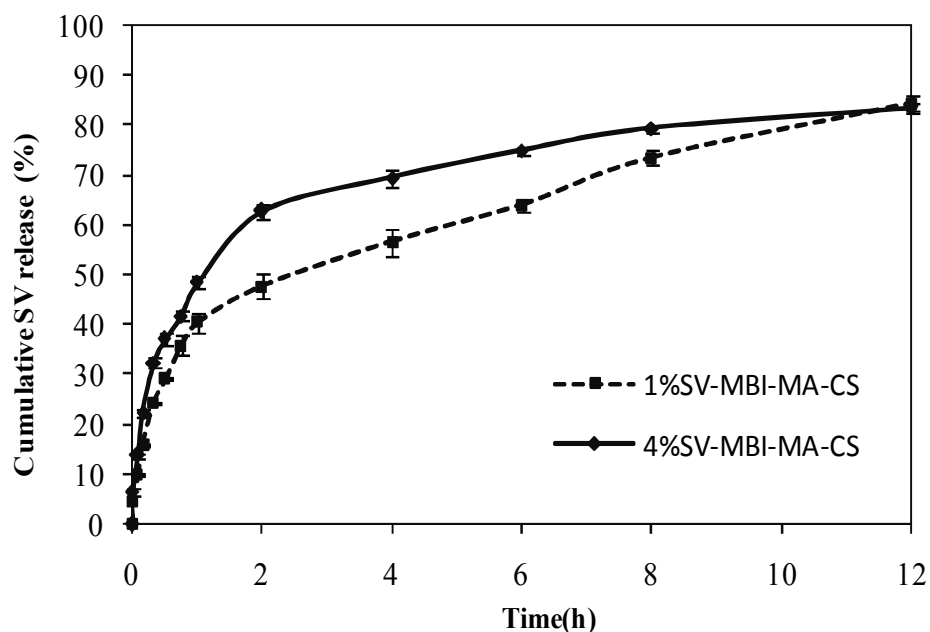
Figure 4.18 Release profiles of 1% and 4% simvastatin (SV) from MBI-MA-CS in pH 1.2 buffers, 37°C (average$\pm$ SD, n=3)

The cumulative release of SV showed that the nanospheres can be prolonged release of SV within the 12 h. The release profiles of the 4%SV load MBI-MA-CS show the initial burst release in firth stage (1 h) with higher than that of 1%SV-MBI-MA-CS. The burst release was considered to be due to the presence of more free drugs on the particle surface and larger diffusion area of the microspheres. Moreover, about 50% of SV was released in 4h and 1 h for 1%SV-MBI-MA-CS and 4%SV-MBI-MA-CS formulation, respectively, and still sustained released within 12 h.

The tendency of cumulative release from 1% and 4% SV-MBI-MA-CS at pH 4.0 and 6.4 is similar pH 1.2 (Figure 4.19-4.20).

Overall, from these results indicated that SV loaded modified CS formulation released the drug slowly than CS.
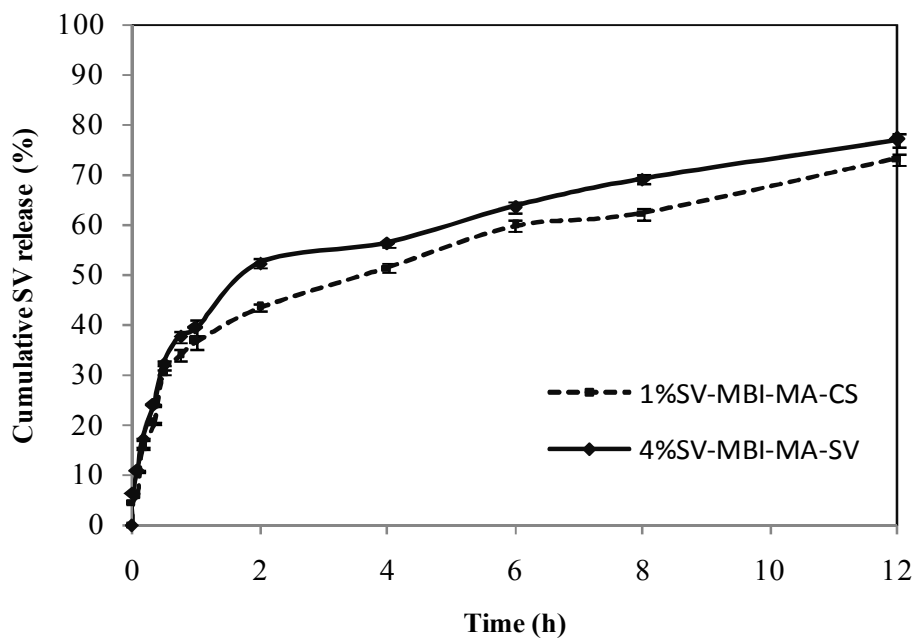
Figure 4.19 Release profiles of 1% and 4% simvastatin (SV) from MBI-MA-CS in pH 4.0 buffers, 37°C (average± SD, *n*=3
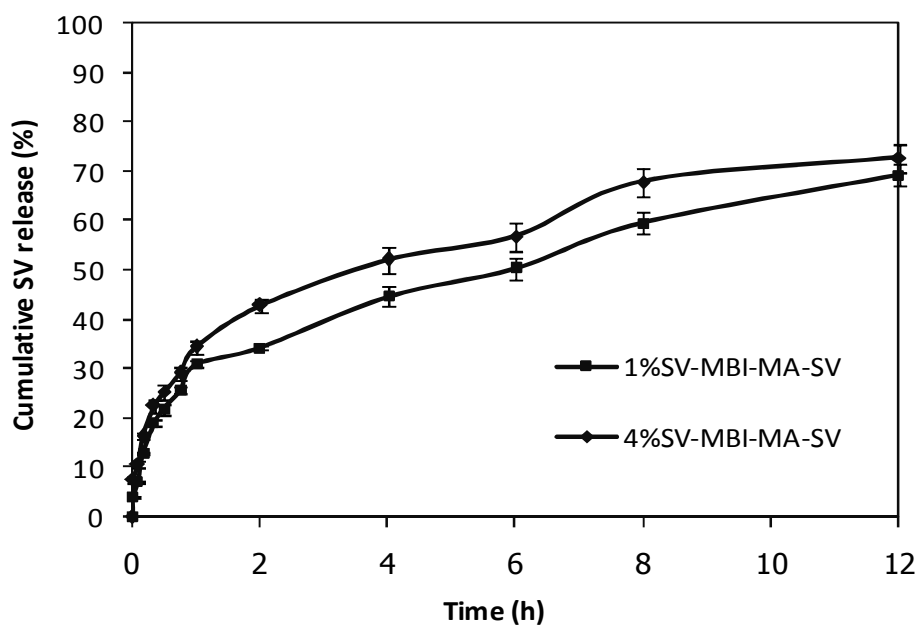
Figure 4.20 Release profiles of 1% and 4% simvastatin (SV) from MBI-MA-CS in pH 6.4 buffers, 37°C (average± SD, *n*=3)

CHAPTER V

CONCLUSION AND SUGGESTION

5.1   Conclusion

In this work, the thiolated CS was synthesized by coupled MA on CS via the micheal addition and then thiolation of MBI was covalently reacted at the carboxylic group and methyl ester group of MA-CS using EDAc as activator. The substitution of MA was calculated about 14.38% by ^{1}H NMR. The amount of thiol groups (MBI) immobilized on MA-CS and disulfide bond were displayed 11.86 and 6.54 μmol thiol groups per gram of polymer, resulted in strongly improved mucoadhesive properties.

The mucoadhesiveness was determined by Periodic acid: schiff (PAS) colorimetric method was used to qualify mucin-conjugated polymer bioadhesived strength in the simulated gastrointestinal fluid (pH 1.2, 4.0 and 6.4) MA-CS and MBI-MA-CS increased 10.28 and 11-fold at pH 1.2, while at pH 4.0 increased ~2.81 and 2.94-fold, at pH 6.4 increased only ~1.25 and 2.06-fold. The data suggests that the lowest pH (1.2) shows the highest mucoadhesive propertive.

Because of these characteristics, the obtained thiolated CS (MBI-MA-CS appear to be promising novel polymers for the development of various drug delivery carriers at mucus sites. The electrospray ionization was used to prepare CS and modified CS microspheres for simvastatin (SV) controlled release.

Microspheres of CS and modified CS can be obtained by fixing, the parameters as follows: working distance of 8 cm, needle gauge of 26 G, flow rate of 0.5 mL/h, stirring rate of 400 rpm and high voltage of 20 kV. The morphology of microspheres was obtained by SEM, showed a good spherical shape that well form. The swollen particle sizes of microspheres were 1-5 μm in the range measured by particizer. The encapsulation of 1%SV loaded CS, MA-CS and MBI-MA-CS

microspheres showed 53, 70 and 64%, respectively. The drug entrapment increased for modified CS. This result showed that the compatibility between SV and modified CS were increased. Moreover, increasing of SV loaded MBI-MA-CS from 1% to 4%SV-polymer (w/w) microspheres found that increased from 64 to 82% drug entrapment. The SV-polymer microspheres can be prolonged release of SV. It was found that the release profiles of simvastatin were greatly improved upon using modified chitosan within 12 hours due to lower swelling of modified CS leading to a more controlled and sustained drug release. Mucoadhesiveness of MA-CS and MBI-MA-CS microspheres with SV were displayed 7- and 7.33-fold at pH 1.2, respectively. Hence, the advantages of the controlled release system based on the mucoadhesive polymer can be improved by using the MA-CS and thiolated chitosan.

5.2   Suggestion

The problem of SV was the poorly absorbed from the gastrointestinal (GI) tract with less than 5%.

We are interested in studying the oral bioavailability of SV and investigating its intestinal absorption. The *in situ* intestinal absorption of SV encapsulated in CS and modified CS will be performed in animal model. The intestinal absorption mechanism should be investigated. The pharmacokinetics will be performed to evaluate the potential of microparticles in the further step as an oral delivery carrier for SV.

REFERENCES

[1]   Carlucci, G., Mazzeo, P., Biordis, L., Bologna, M. Simultaneous determination of simvastatin and itshydroxy acid form in human plasma by highperformance liquid chromatography with UV detection. Journal of Pharmaceutical & Biomedical Analysis 10 (1992): 693-699.

[2]   Margulis-Goshen, K., MSc., Magdassi, S. Formation of simvastatin nanoparticles from microemulsion. Nanomedicine 5 (2009): 274–281.

[3]   Tiwari, R., Pathak, K. Nanostructured lipid carrier versus solid lipid nanoparticles of simvastatin: Comparative analysis of characteristics, pharmacokinetics and tissue uptake. International Journal of Pharmaceutics 7 (2011): 55-62.

[4]   Mishra, S., Kumar, G., Kothiyal, P. Formulation and Evaluation of Buccal Patches of Simvastatin by Using Different Polymers. The Pharma innovation 1 (2012): 87-92.

[5]   Grabovac, V., Guggi, D., Bernkop-Schnurch, A. Comparison of the mucoadhesive properties of various polymers. Advanced Drug Delivery Reviews 57 (2005): 1713–1723.

[6]   Bernkorp-Schnurch, A., Kast, C.E., Guggie, D. Permeation enhanceing polymer in oral delivery of hydrophilic macromolecule: thiomer/GSH system. Journal of Controlled Release 93 (2003): 95-103.

[7]   Patil, S. B., Murthy, R. S. R., Mahajan, H. S., Wagh, R. D., Gattani, S. G. Mucoadhesive polymers: Means of improving drug delivery. International Journal of Pharmaceutics 38 (2007): 102-109.

[8]   Tilloo, S. K., Rasala, T.M., Kale, V. Mucoadhesive microparticulate drug delivery system. International Journal of Pharmaceutical Sciences Review and Research 9 (2011): 52-56.

[9]   Michael L e h r, C. In vitro evaluation of mucoadhesive properties of chitosan and some other natural polymers. <u>International Journal of Pharmaceutics</u> 78 (1992): 43-48.

[10]   Mythri, G. K., Kavith, M., Rupesh Kumar, Sd., Jagadeesh, S. Novel Mucoadhesive Polymers –A Review. <u>Journal of Applied Pharmaceutical Science</u> 01 (2011): 37-42.

[11]   Sinha, V.R. Chitosan microspheres as a potential carrier for drugs. <u>International Journal of Pharmaceutics</u> 274 (2004): 1–33.

[12]   Dodane, V. Pharmaceutical applications of chitosan- A Review. <u>International Journal of Pharmaceutics</u> 1 (1998): 246-251.

[13]   Dash, M., Chiellini F., Ottenbrite, R.M., Chiellini, E. Chitosan- A versatile semi-synthetic polymer in biomedical applications. <u>International Journal of Pharmaceutics</u> 36 (2011): 981–1014

[14]   Bernkop-Schnurch, A. Thiomers: A new generation of mucoadhesive polymers. <u>Advanced Drug Delivery Reviews</u> 57 (2005): 1569–1582.

[15]   Hornof, M. D., Kast, C. E., Bernkop-Schnurch, A. In vitro evaluation of the viscoelastic properties of chitosan–thioglycolic acid conjugates. <u>European Journal of Pharmaceutics and Biopharmaceutics 55</u> (2003): 185–190.

[16]   Schmitz, T., Grabovac, V., Palmberger, T. F., Hoffer, M. K. Bernkop-Schnurch, A, Synthesis and characterization of a chitosan-*N*-acetyl cysteine conjugate. <u>International Journal of Pharmaceutics</u> 347 (2008): 79–85.

[17]   Juntapram, K., Praphairaksit, N., Siraleartmukul, K., Muangsin, N. Synthesis and characterization of chitosan-homocysteine thiolactone as a mucoadhesive polymer. <u>Carbohydrate Polymers</u> 87 (2012): 2399–2408.

[18]   Leitner, V. M., Walker, G. F., Bernkop-Schnurch, A. Thiolated polymers: evidence for the formation of disulphide bonds with mucus glycoproteins. <u>European Journal of Pharmaceutics and Biopharma ceutics</u> 56 (2003): 207–214.

[19]   Prabaharan, M., Gong, S. Novel thiolated carboxymethyl chitosan-g-b-cyclo
        dextrin as mucoadhesive hydrophobic drug delivery carriers.
        Carbohydrate Polymers 73 (2008): 117–125.

[20]   Wang, L. Y., Gu, Y. H., Su, Z. G., Ma, G.H, Preparation and improvement of
        release behavior of chitosan microspheres containing insulin.
        International Journal of Pharmaceutics 311 (2006): 187-195.

[21]   Zhang, S., Kawakami, K. One-step preparation of chitosan solid
        nanoparticles by electrospray deposition. International Journal of
        Pharmaceutics 397 (2010): 211–217.

[22]   Jaworek, A. Micro- and nanoparticle production by electrospraying. Powder
        Technology 176 (2007): 18–35.

[23]   Fukui, Y. Preparation of monodispersed polyelectrolyte microcapsules
        with high encapsulation efficiency by an electrospray technique.
        Colloids and Surfaces A: Physicochem. Eng. Aspects 370 (2010):
        28–34.

[24]   Carlucci, G., Mazzeo, P., Biordis, L., Bologna, M. Simultaneous
        determination of simvastatin and itshydroxy acid form in human
        plasma by highperformance liquid chromatography with UV
        detection. Journal of Pharmaceutical & Biomedical Analysis 10
        (1992): 693-69.

[25]   Ungaro, F., Giovino, Concetta. Use of cyclodextrins as solubilizing
        agents for simvastatin: Effect of hydroxypropyl-β-cyclodextrin on
        lactone/hydroxyacid aqueous equilibrium. International Journal of
        Pharmaceutics 404 (2011): 49–56.

[26]   Huang, X., Brazel, C.S. On the importance and mechanisms of burst release
        in matrix-controlled drug delivery systems. Journal of Controlled
        Release 73 (2001): 121–136.

[27]   Uhrich, K. E., Cannizzaro, S. M., Langer, R. S., Shakesheff, K. M. Polymeric
        Systems for Controlled Drug Release. Chem. Rev 99 (1999):
        3181-3198.

[28]   Ganji, F. Hydrogels in Controlled Drug Delivery Systems. Iranian Polymer
        Journal 18 (2009): 63-88.

[29]   Leong, K.W., Langer, R. Polymeric controlled drug delivery. Advanced Drug
        Delivery Reviews 1 (1988): 199-233.

[30]   Mythri, G. K., Kavitha, M. Novel mucoadhesive polymer- A Review.
        Journal of Applied Pharmaceutical Science 08 (2011): 37-42.

[31]   Tilloo, S.K., Rasala, T. M., Kale, V.V. Mucoadhesive microparticulate drug
        delivery system. Journal of Pharmaceutics and Biopharmaceutics 9
        (2011): 52-56.

[32]   Smart, J.D. The basics and underlying mechanisms of mucoadhesion.
        Advanced Drug Delivery Reviews 57 (2005): 1556-1568.

[33]   Peppas, N.A., Sahlin, J.J. Hydrogels as mucoadhesive and bioadhesive
        materials: a review. Biomaterials 17 (1996): 1553-1561.

[34]   Andrews, G.P., Laverty, T.P., Jones, D.S. Mucoadhesive polymeric
        platforms for controlled drug delivery. European Journal of
        Pharmaceutics and Biopharmaceutics 71 (2009): 505-518.

[35]   Wang, Y.W., Gu, Y. H., Su, Z. G., Ma, G. H. Preparation and
        improvement of release behavior of chitosan microspheres containing
        insulin. International Journal of Pharmaceutics 311 (2006): 187–
        195.

[36]   Ko, J.A., Park, H.J. Preparation and characterization of chitosan
        microparticles intended for controlled drug delivery. International
        Journal of Pharmaceutics 249 (2002): 165–174.

[37]   Bock, N., Dargaville, T.R., Woodruff, M. Electrospraying of polymers
        with therapeutic molecules: State of the art. Progress in Polymer
        Science 37 (2012):1510– 1551.

[38]   Bohr, A., Kristensen, J., Stride, E., Dyas, M. Preparation of microspheres
        containing low solubility drug compound by electrohydrodynamic
        spraying. International Journal of Pharmaceutics 412 (2011):
        59–67.

[39]   Sashiwa, H. Chemical modification of chitosan. Part 15: Synthesis of
        novel chitosan derivatives by substitution of hydrophilic amine using

N-carboxyethylchitosan ethyl ester as an intermediate. Carbohydrate Research 338 (2003): 557–561.

[40] Osuna, B., Teutonico, D., Arpicco, S., Vauthier, C., Ponchel, G. Characterization of chitosan thiolation and application to thiol quantification onto nanoparticle surface. International Journal of Pharmaceutics 340 (2007): 173–181.

[41] Dietza, A., Rubinstein, H. M. Laboratory note standardization of the ellman reaction. Clin. Biochem 35 (1972): 36-138.

[42] Anitha, A., Deepa, N., Chennazhi, K.P., Nair, S.V., Tamura, H., Jayakumar, R. Development of mucoadhesive thiolated chitosan nanoparticles for biomedical applications. Carbohydrate Polymers 83 (2011): 66-73.

[43] Kilcoyne, M., Gerlach, J.Q. Periodic acid–Schiff's reagent assay for carbohydrates in a microtiter plate format. Analytical Biochemistry 416 (2011): 18–26.

[44] Dung, P.l. Water soluble derivatives obtained by controlled chemical modifications of chitosan. Carbohydrate Polymers 24 (1994): 209-214.

[45] Majeti, N.V., Kumar, R. A review of chitin and chitosan applications. Reactive & Functional Polymers 46 (2000): 1–27.

[46] Colinet, I., Dulong, V., Mocanu, G., Picton, L., Le Cerf, D. Effect of chitosan coating on the swelling and controlled release of a poorly water soluble drug from an amphiphilic and pH-sensitive hydrogel. International Journal of Biological Macromolecules 47 (2010): 120–125.

[47] Khalid, M.N., Agnely, F., Yagoubi, N., Grossiord J.L. Water state characterization, swelling behavior, thermal and mechanical properties of chitosan based networks. European Journal of Pharmaceutical Sciences 15 (2002): 425–432.

[48] Quan, G., Wang, T., Cochrane, C., McCarron, P. Modulation of surface charge, particle size and morphological properties of chitosan–TPP

nanoparticles intended for gene delivery. <u>Colloids and Surfaces B: Biointerfaces</u> 44 (2005) :65–73.

[49]   Fukui, Y., Maruyama, T., Iwamatsu, Y., Fujii, A., Tanaka, T. Preparation of monodispersed polyelectrolyte microcapsules with high encapsulation efficiency by an electrospray technique. <u>Colloids and Surfaces A: Physicochemical and Engineering Aspects</u> 370 (2010): 28-34.

[50]   Bock, N., Dargaville, T.R., Woodruff, M.A. Electrospraying of polymers with therapeutic molecules: State of the art. <u>Progress in Polymer Science</u> 37 (2012): 1510-1551.

[51]   Ambike, A., Mahadik, K. R., Paradkar, A. Spray-Dried Amorphous Solid Dispersions of Simvastatin, a Low T_g Drug: In Vitro and in Vivo Evaluations. <u>Pharmaceutical Research</u> 22 (2005): 990-998.

[52]   Sharipova, A., Aidarovaa, S., Cernoch, P., Millerb, R. Effect of surfactant hydrophobicity on the interfacial properties of polyallylamine hydrochloride/sodium alkylsulphate at water/hexane interface. <u>Colloids and Surfaces A: Physicochem</u> 30 (2012): 235-243.

APPENDIX

APPENDIX A

Standard curve of *L*-cysteine Hydrochloride

The concentration versus peak absorbance of *L*-cysteine. are presented in Table 1A. The plot of calibration curve of L-cysteine hydrochloride is illustrated in Figure 1A.

Table 1A Absorbance of various concentrations of *L*-cysteine Hydrochloride by UV Spectrometer.
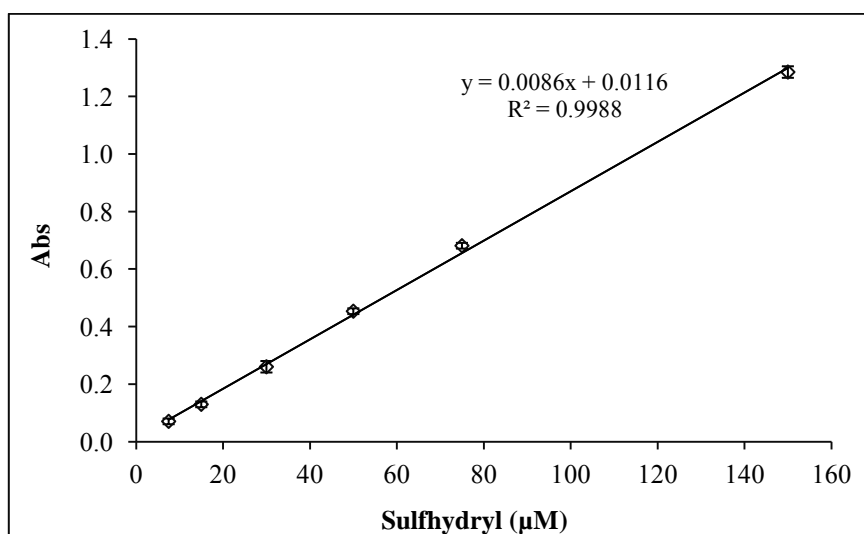
Figure 1A Standard cureve of *L*-cysteine Hydrochloride by UV spectrometer

Table 2A Absorbance thiol groups of MBI-MA-CS by UV spectrometer.

Batch	Abs.	Abs.	Abs.	thiol (μM)	Thiol(μmol/g)
MBI-MA-CS	0.490	0.483	0.487	59.3	11.86

Table 3A Absorbance disulfide groups of MBI-MA-CS by UV spectrometer**.**

Batch	Abs.	Abs.	Abs.	Total thiol (μM)	disulfide (μM)	disulfide (μmol/g)
MBI-MA-CS	0.987	0.990	1.08	124.7	32.25	6.54

APPENDIX B

Calibration curve of mucin (type II)

The concentration versus peak absorbance mucin glycoprotein (type II) determined by UV as the same condition described in chapter III is presented in Table 1B. The plot of calibration curve of mucin is illustrated in Figure 1B

Table 1B Absorbance of various concentrations of mucin (type II) at pH 1.2, 4.0, and 6.4 UV spectrophotomer

Concentration (mg/2mL)	Absorbance		
	HCl (pH 1.2)	Acetate buffer (pH 4.0)	PBS (pH 6.4)
0.2	0.063	0.159	0.260
0.4	0.131	0.324	0.527
0.6	0.184	0.498	0.766
0.8	0.224	0.635	1.000
1.0	0.275	0.762	1.290
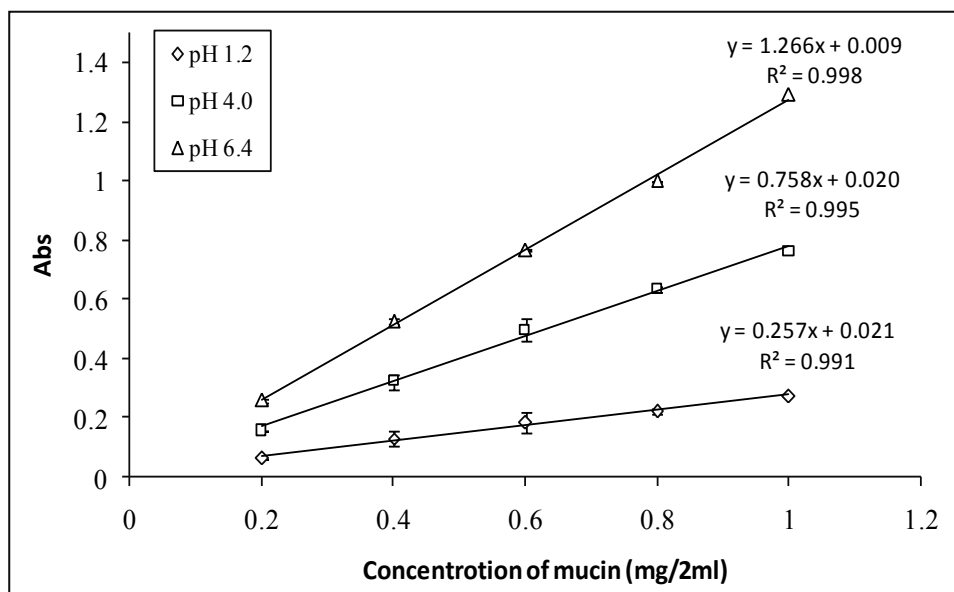
Figure 1B Standard curve of mucin at pH 1.2, 4.0, and 6.4

Table 2B Absorbance of free and adsorpbed mucin CS, MA-CS and MBI-MA-CS in pH 1.2 by UV spectrophotomer.

Batch	Abs.	Abs.	Abs.	Free mucin (mg)	Absorbed mucin (mg)	SD
CS	0.320	0.325	0.336	0.930	0.070	0.011
MA-CS	0.089	0.088	0.100	0.278	0.722	0.009
MBI-MA-CS	0.085	0.078	0.081	0.235	0.765	0.009

Table 3B Absorbance of free and adsorpbed mucin CS, MA-CS and MBI-MA-CS in pH 4.0 by UV spectrophotomer.

Batch	Abs.	Abs.	Abs.	Free mucin (mg)	Absorbed mucin (mg)	SD
CS	0.537	0.542	0.519	0.670	0.330	0.009
MA-CS	0.075	0.074	0.078	0.073	0.927	0.008
MBI-MA-CS	0.036	0.046	0.036	0.026	0.974	0.006

Table 4B Absorbance of free and adsorpbed mucin CS, MA-CS and MBI-MA-CS in pH 6.4 by UV spectrophotomer.

Batch	Abs.	Abs.	Abs.	Free mucin (mg)	Absorbed mucin (mg)	SD
CS	0.980	0.989	0.985	0.674	0.326	0.010
MA-CS	0.713	0.779	0.820	0.602	0.398	0.015
MBI-MA-CS	0.434	0.211	0.426	0.336	0.664	0.016

APPENDIX C

Calibration curve of SV

Table 1C Absorbance of simvastatin drug in 80 (%v/v) EtOH determined in 238 nm**.**

Concentration (ppm)	Abs	Abs	Abs	AVG	SD
3	0.179	0.183	0.184	0.182	0.001
6	0.397	0.370	0.374	0.380	0.014
9	0.519	0.529	0.530	0.526	0.006
12	0.687	0.669	0.669	0.695	0.004
15	0.836	0.848	0.849	0.844	0.007
18	1.014	1.021	1.023	1.019	0.004

$$y = 0.055x + 0.017$$
$$R^2 = 0.999$$
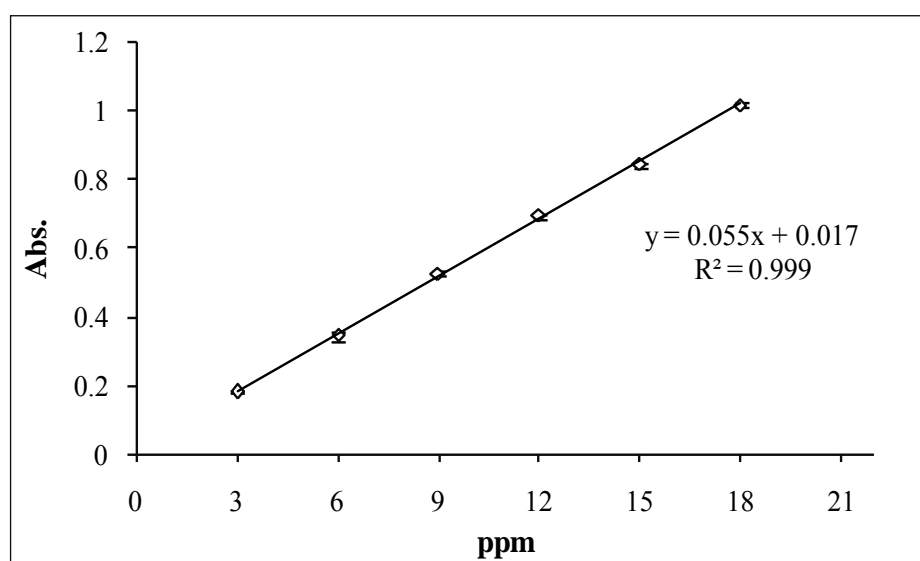
Figure 1C Calibration curve of simvastatin in 80% (v/v) EtOH
determined in 238 nm

Table 2C Absorbance of simvastatin drug in pH 1.2 determined in 238 nm

Concentration (ppm)	Abs	Abs	Abs	AVG	SD
3	0.139	0.132	0.138	0.316	0.003
6	0.297	0.289	0.289	0.291	0.004
9	0.454	0.452	0.446	0.450	0.004
12	0.619	0.609	0.606	0.611	0.006
15	0.780	0.778	0.779	0.799	0.001
18	0.928	0.958	0.938	0.941	0.015

$y = 0.045x + 0.016$
$R^2 = 0.999$
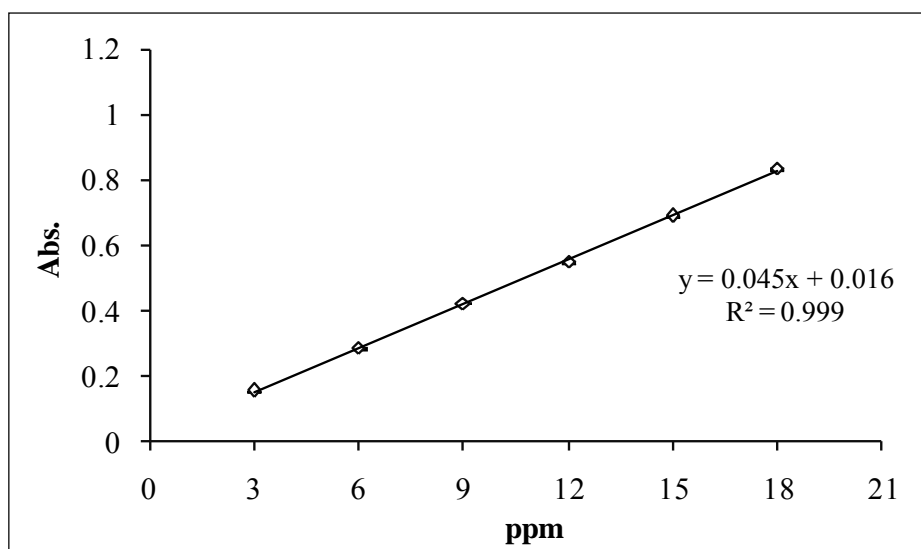
Figure 2C Calibration curve of simvastatin in pH 1.2

determined in 238 nm

Table 3C Absorbance of simvastatin drug in pH 4.0 determined in 238 nm

Concentration (ppm)	Abs	Abs	Abs	AVG	SD
3	0.155	0.156	0.156	0.155	0.000
6	0.280	0.289	0.291	0.286	0.005
9	0.426	0.425	0.425	0.425	0.000
12	0.550	0.551	0.553	0.551	0.001
15	0.691	0.693	0.691	0.691	0.001
18	0.835	0.837	0.837	0.836	0.001

$y = 0.053x - 0.029$
$R^2 = 0.999$
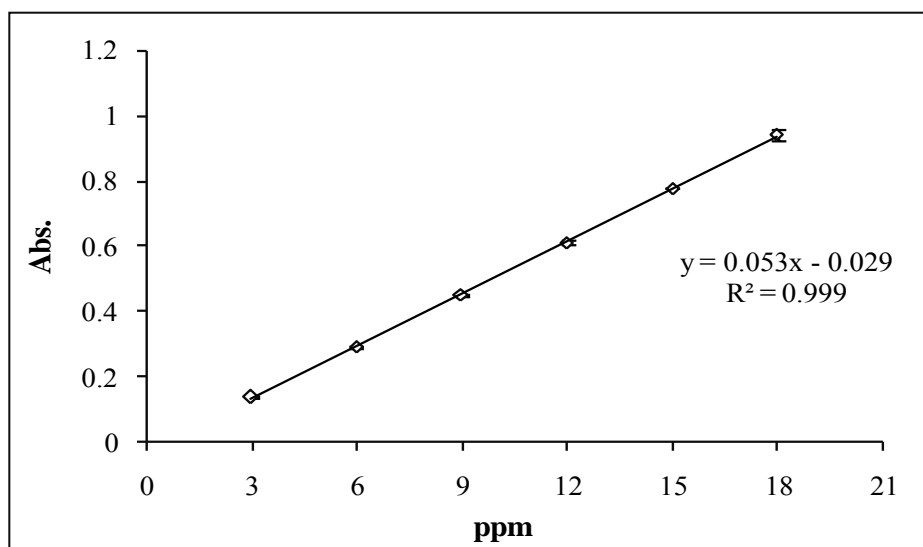
Figure 3C Calibration curve of simvastatin in pH 4.0

determined in 238 nm

Table 4C Absorbance of simvastatin drug in pH 6.4 determined in 238 nm

Concentration (ppm)	Abs	Abs	Abs	AVG	SD
3	0.18	0.2	0.201	0.193	0.011
6	0.366	0.368	0.367	0.367	0.001
9	0.535	0.536	0.534	0.535	0.001
12	0.724	0.720	0.721	0.721	0.002
15	0.875	0.874	0.873	0.874	0.001
18	1.059	1.060	1.050	1.056	0.005

$y = 0.057x + 0.022$
$R^2 = 0.999$
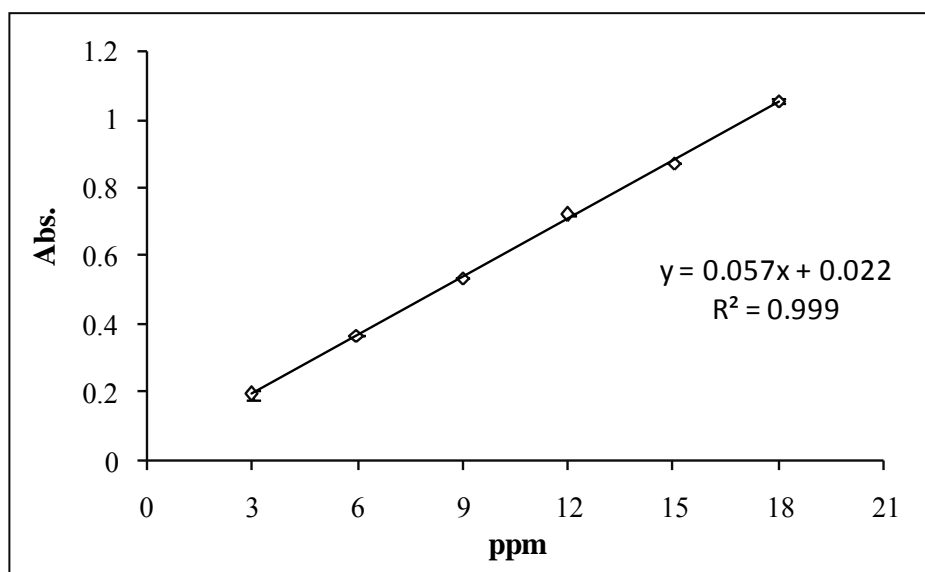
Figure 4C Calibration curve of simvastatin in pH 6.4
determined in 238 nm

APPENDIX D

Encapsulation

and

Cumulative Drug Release

Table 1D Encapsulation (%EE) from CS and modified CS microspheres in Ethanol

Formulation	Abs.	Abs.	Abs.	Conc.(ppm)	% EE
1%SV-CS	0.075	0.077	0.072	1.100	53.0
1%SV-MA-CS	0.097	0.098	0.100	1.418	70.9
1%SV-MBI-MA-CS	0.089	0.085	0.900	1.296	64.83
2%SV-MBI-MA-CS	0.095	0.091	0.097	1.404	70.21
4%SV-MBI-MA-CS	0.101	0.12	0.101	1.642	82.10

Table 2D Cumulative SV release from CS microspheres in pH 1.2

Time (min)	Amount of SV release				
	1	2	3	Mean	SD
0	0	0	0	0	0
10	5.9177	8.3190	7.5472	7.2613	1.225945
20	12.4357	13.9794	13.2933	13.2361	0.773456
30	19.2110	20.8405	20.0686	20.0400	0.815127
40	24.3568	25.9091	25.2230	25.1630	0.777897
50	31.9897	33.8851	33.0274	32.9674	0.949109
60	38.3362	40.0600	39.2882	42.2281	0.863488
120	49.2281	51.1235	50.0086	50.1201	0.95259
240	60.2916	62.1870	61.0720	65.1835	0.95259
300	69.6398	72.2213	71.1921	72.6741	1.299543
360	76.4151	78.9966	78.1389	76.5066	1.314736
480	81.5609	84.8370	83.8851	82.0840	1.685294
720	85.7633	89.0395	88.0875	86.2864	1.685294

Table 3D Cumulative SV release from CS microspheres in pH 4.0

Time (min)	Amount of SV release				
	1	2	3	Mean	SD
0	0	0	0	0	0
10	6.4646	6.5657	6.5152	6.5152	0.050505
20	10.9091	11.1111	11.1616	11.0606	0.133624
30	18.0808	17.5758	17.8283	17.8283	0.252525
40	25.5556	25.0505	25.3030	25.3030	0.252525
50	31.0101	30.6061	30.9596	30.8586	0.220146
60	37.7778	37.3030	37.5556	37.5455	0.237535
120	43.2323	42.8586	43.3131	43.1347	0.242494
240	50.2020	49.8283	50.2323	50.0875	0.225036
300	59.6970	60.3333	59.7273	59.9192	0.358977
360	67.1717	68.6162	69.2222	68.3367	1.053431
480	76.6667	80.1313	79.7273	78.8418	1.89448
720	81.6162	86.0404	85.7374	84.4646	2.471509

Table 4D Cumulative SV release from CS microspheres in pH 6.4

Time (min)	Amount of SV release				
	1	2	3	Mean	SD
0	0	0	0	0	0
10	2.2329	2.3126	2.6396	2.3950	0.215508
20	5.2632	5.4226	6.3078	5.6645	0.562771
30	10.2871	10.4785	10.5821	10.4492	0.149685
40	14.1946	14.4657	14.4099	14.3567	0.143171
50	18.0223	18.3732	18.3573	18.2509	0.198136
60	22.8868	23.1180	23.1419	23.0489	0.140933
120	28.3892	28.6603	28.7241	28.5912	0.177839
240	34.6093	35.6778	35.9011	35.3961	0.690488
300	48.8038	48.2775	49.2982	48.7932	0.51045
360	61.4035	60.9569	62.1372	61.4992	0.595902
480	67.6236	67.1770	68.3573	67.7193	0.595902
720	75.4386	74.1946	76.1722	75.2685	0.999751

Table 5D Cumulative SV release from MA-CS microspheres in pH 1.2

Time (min)	Amount of SV release				
	1	2	3	Mean	SD
0	0	0	0	0	0
10	3.9918	4.0583	4.0184	4.0229	0.033486
20	8.0102	8.1566	8.1433	8.1034	0.080937
30	13.1996	13.3459	13.3326	13.2927	0.080937
40	19.7195	19.9989	20.2517	19.9901	0.266231
50	23.7246	23.9774	24.2702	23.9907	0.273017
60	27.7830	30.7635	30.9232	29.8232	1.768715
120	31.7881	34.7686	34.9283	33.8283	1.768715
240	36.3121	39.1596	39.1862	42.2193	1.651733
300	42.6990	45.4134	45.4400	50.5175	1.574913
360	47.8883	50.8689	51.5608	57.1060	1.951468
420	55.7389	58.7194	58.7460	63.7348	1.728553
720	69.0449	71.7593	71.6529	75.6375	1.537367

Table 6D Cumulative SV release from MA-CS microspheres in pH 4.0

Time (min)	Amount of SV release				
	1	2	3	Mean	SD
0	0	0	0	0	0
10	3.7612	3.9179	3.8395	3.8395	0.078358
20	7.5223	7.8358	7.6007	7.6529	0.163114
30	12.8507	13.1641	13.2424	13.0857	0.207315
40	18.9625	18.8058	19.1976	18.9887	0.197196
50	25.8580	25.8580	26.4065	26.0409	0.316679
60	30.0893	29.9796	31.9386	30.6692	1.100695
120	33.8505	33.8975	36.1699	34.6393	1.325734
240	39.1788	39.2258	40.7146	39.7064	0.873444
300	45.9176	45.9959	47.4690	46.4608	0.874007
360	50.7757	50.2272	52.0138	51.0056	0.915187
480	52.9698	52.4213	54.2078	53.1996	0.915187
720	62.2160	61.5891	63.5324	62.4458	0.991815

Table 7D Cumulative SV release from MA-CS microspheres in pH 6.4

Time (min)	Amount of SV release				
	1	2	3	Mean	SD
0	0	0	0	0	0
10	3.5880	3.4890	3.5038	3.5269	0.053378
20	6.4336	6.1490	6.0401	6.2076	0.203151
30	11.1350	10.9742	10.9890	11.0328	0.088885
40	15.8365	16.2943	16.8040	16.3116	0.483988
50	18.0635	18.6450	19.4022	18.7036	0.671258
60	21.5277	22.1092	22.2478	21.9616	0.382063
120	26.1055	26.7117	26.8379	24.5517	0.391561
240	29.1985	29.3099	29.6835	35.3973	0.254042
300	35.1372	36.4858	37.9729	41.9444	1.418425
360	41.6945	42.9812	44.5921	47.0893	1.45181
480	49.4890	50.7139	52.4485	52.8838	1.48702
720	57.9022	59.1270	60.7379	56.2557	1.422233

Table 8D Cumulative SV release from MBI-MA-CS microspheres in pH 1.2

Time (min)	Amount of SV release				
	1	2	3	Mean	SD
0	0	0	0	0	0
10	4.6473	4.7247	4.6714	4.6811	0.03964
20	9.3255	9.4959	9.4664	9.4293	0.091071
30	15.3670	15.5374	15.4990	15.4678	0.089383
40	23.7321	23.9025	24.3158	23.9834	0.300156
50	28.3948	28.5343	28.9871	28.6387	0.30966
60	33.1196	36.4346	36.7211	35.4251	2.001795
120	37.7823	41.0974	41.3770	40.0856	1.999571
240	44.5983	48.5330	48.6470	47.2594	2.305308
300	52.9634	57.3628	57.6185	55.9816	2.616928
360	62.1030	63.7141	64.7338	63.5170	1.326399
480	71.2427	73.0086	74.3240	72.8584	1.546127
720	81.9314	84.4719	84.6876	83.6970	1.532812

**Table 9D** Cumulative SV release from MBI-MA-CS microspheres in pH 4.0

Time (min)	Amount of SV release				
	1	2	3	Mean	SD
0	0	0	0	0	0
10	4.4444	4.5612	4.4700	4.4919	0.061385
20	8.8889	9.1224	8.8488	8.9534	0.147787
30	15.1852	15.3257	15.4169	15.3093	0.116724
40	22.4074	21.8938	22.3499	22.2171	0.281403
50	30.5556	30.1040	30.7426	30.4674	0.328291
60	35.5556	34.9024	37.1830	35.8803	1.174475
120	40.0000	39.4636	42.1091	40.5242	1.398495
240	46.2963	45.6668	47.4001	46.4544	0.877382
300	54.2593	53.5486	55.2636	54.3572	0.86169
360	60.0000	58.4747	60.5546	59.6765	1.077042
480	62.5926	61.0290	63.1089	62.2435	1.083007
720	73.5185	71.7022	73.9646	73.0618	1.198341

**Table 10D** Cumulative SV release from MBI-MA-CS microspheres in pH 6.4

| Time (min)	Amount of SV release				
	1	2	3	Mean	SD
0	0	0	0	0	0
10	4.1771	4.0619	4.1404	4.1264	0.05886
20	7.4900	7.1587	7.1374	7.2620	0.197697
30	12.9634	12.7762	12.9854	12.9083	0.114966
40	18.4369	18.9698	19.8567	19.0878	0.717229
50	21.0296	21.7066	22.9269	21.8877	0.961537
60	25.0627	25.7396	26.2895	25.6973	0.614506
120	30.3921	31.0979	31.7135	31.0678	0.661202
240	33.9930	34.1227	35.0760	34.3972	0.591408
300	40.9069	42.4769	44.8713	42.7517	1.996476
360	48.5409	50.0389	52.6930	50.4243	2.102699
480	57.6153	59.0413	61.9766	59.5444	2.223756
720	67.4099	68.8359	71.7719	69.3392	2.22415

APPENDIX E
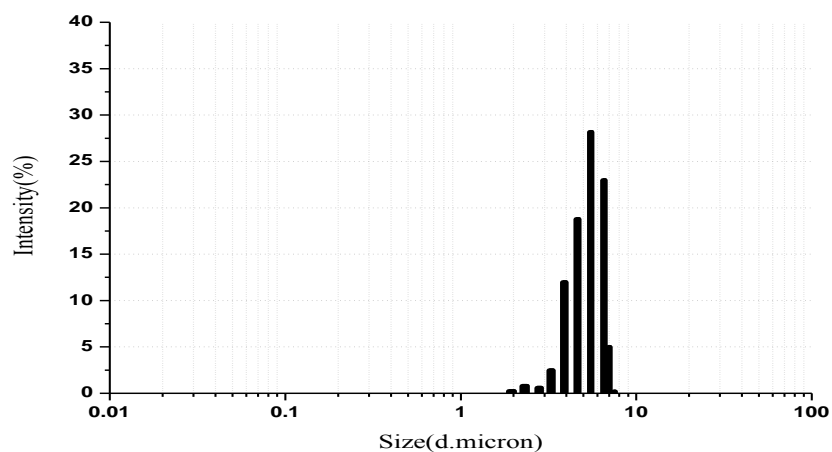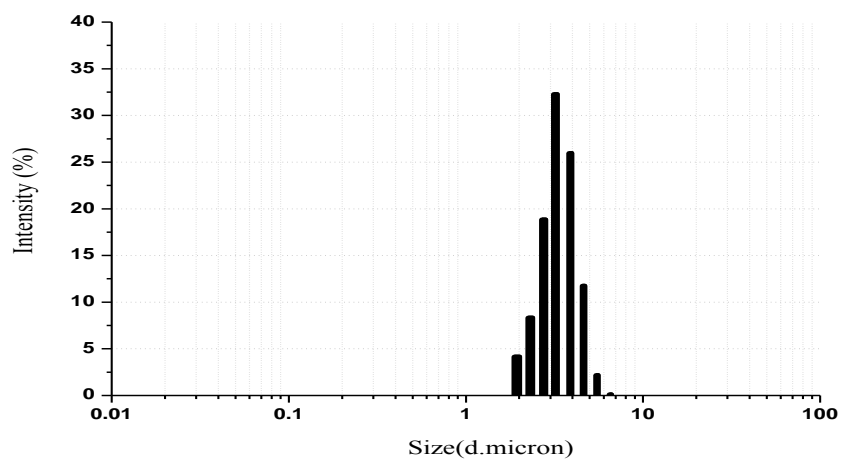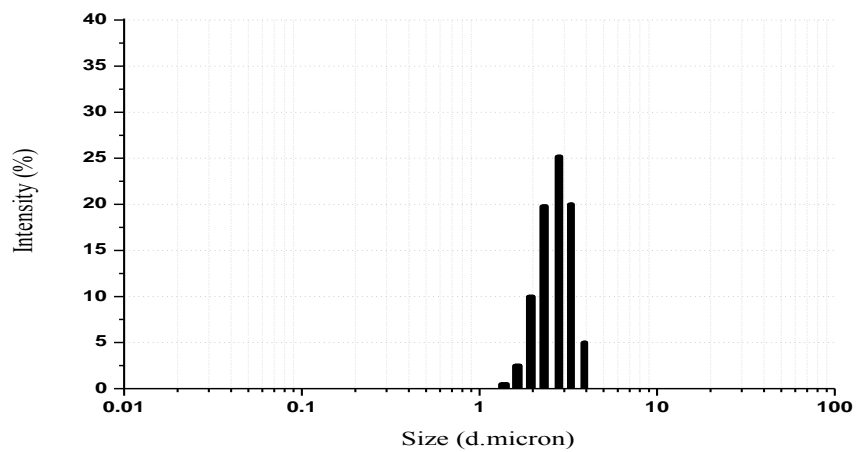
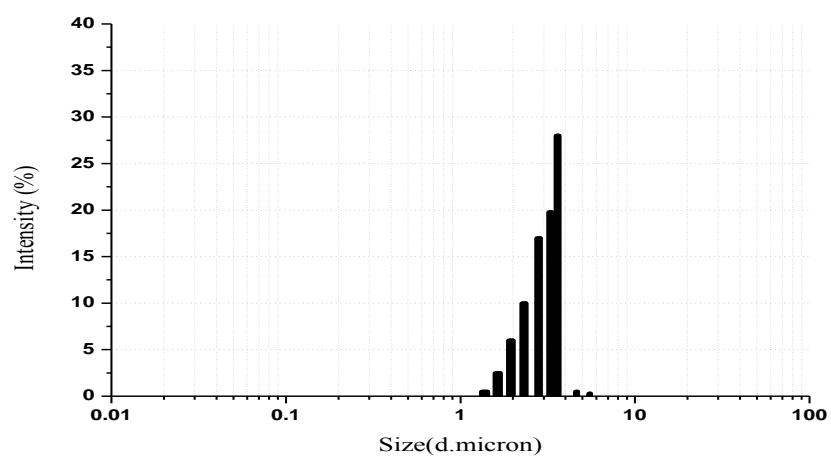**Particle size of**

microspheres
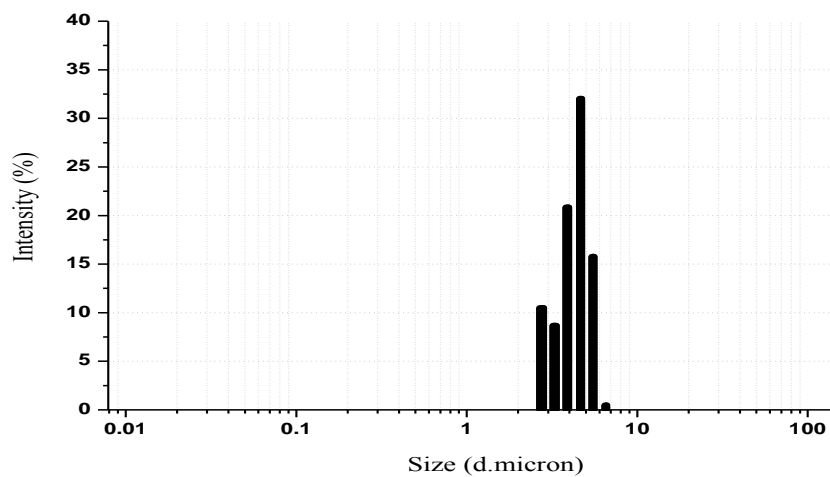
Figure 1E Particle size of CS particle without SV.
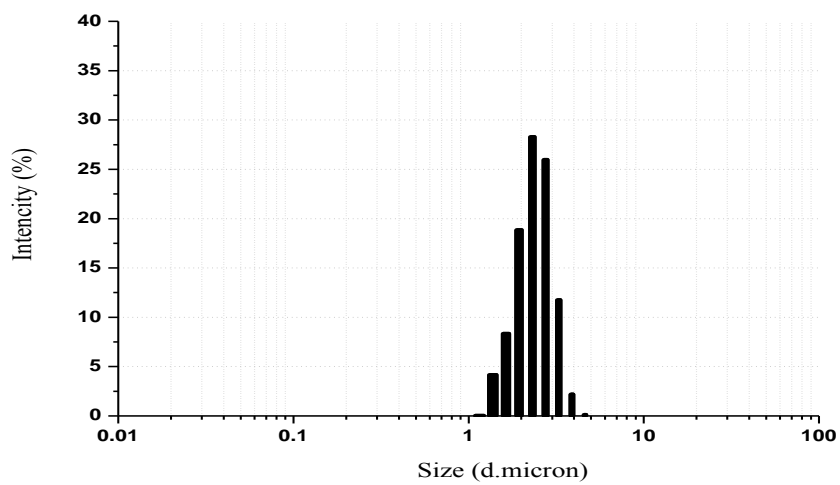
Figure 2E Particle size of MA-CS particle without SV.
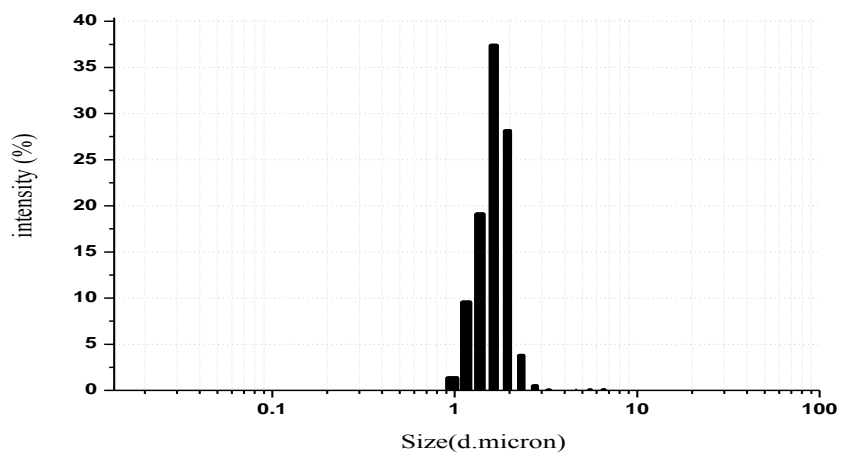
Figure 3E Particle size of MBI-MA-CS particle without SV.

Figure 4E Particle size of MA-CS particle with 1%SV.

Figure 5E Particle size of MA-CS particle with 1%SV.

Figure 6E Particle size of MBI-MA-CS particle with 1%SV

Figure 7E Particle size of MBI-MA-CS particle with 4%SV

VITAE

Name	:	Miss. Mullika kongsong
Date of birth	:	April 28, 1988
Nationality	:	Thai
Address	:	15/2 Moo 4, Nathamtai District, Muang Trang, 92190

University Education : Bacherlor's Degree from Department of Industrail Chemistry, Faculty of Applied Science, King Mongkut's University of Technology North Bangkok, 2006-2009

Master's Degree from Program of Petrochemistry and Polymer Science, Faculty of Science, Chulalongkorn University, 2010-2012

Conference attendance: Poster presentation "Synthesis and properties of mucoadhesive chitosan-5-amino-2-mercaptobenzimi

dazole for hydrophobic drug delivery system" The 9th SPSJ International Polymer Conference (IPC 2012) "Progress and Future of Polymer Science and Technology"